Universidad de Huelva

Departamento de Ingeniería Química, Química Física y Ciencias de los Materiales

Tribological investigation of the structural degradation of lubricating greases from an energy point of view

Memoria para optar al grado de doctor
presentada por:

Leif Ahme

Fecha de lectura: 12 de septiembre de 2024

Bajo la dirección de los doctores:

Miguel Ángel Delgado Canto

Erik Kuhn

Huelva, 2024

Universidad de Huelva

Department of Chemical Engineering,
Physical Chemistry and Materials Science

Doctoral Thesis:

TRIBOLOGICAL INVESTIGATION OF THE STRUCTURAL DEGRADATION OF LUBRICATING GREASES FROM AN ENERGY POINT OF VIEW

LEIF AHME

Doctoral Program in Industrial and Environmental Science and Technology

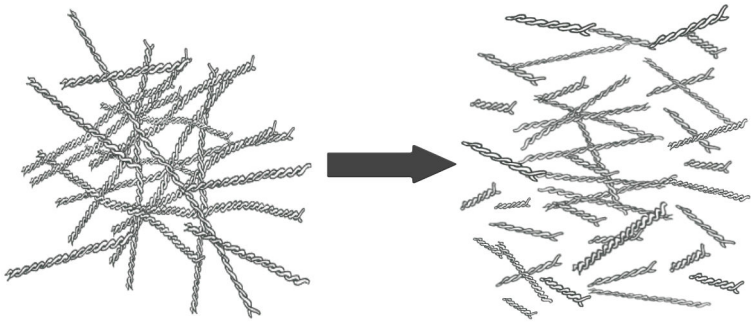

2024

Supervisors: Prof. Dr. Miguel Ángel Delgado Canto, Prof. Dr.-Ing. Erik Kuhn

TRIBOLOGICAL INVESTIGATION OF THE STRUCTURAL DEGRADATION OF LUBRICATING GREASES FROM AN ENERGY POINT OF VIEW

Research memory presented by Leif Ahme to apply for a doctoral degree at the University of Huelva.

The present dissertation has been performed at the Department of Chemical Engineering, Physical Chemistry and Materials Science of the University of Huelva, in cooperation with the Hamburg University of Applied Sciences (HAW-Hamburg) at the Department of Mechanical Engineering and Production Management (Hamburg, Germany), under the supervision of Prof. Dr. Miguel Ángel Delgado Canto and Prof. Dr.-Ing. Erik Kuhn, who approves its defence:

Prof. Dr. Miguel Ángel Delgado Canto

Prof. Dr-Ing. Erik Kuhn

Huelva, April 2024

Abstract

Studying lubricating greases encompasses various aspects essential for understanding their behaviour and performance. Lubricating greases, such as viscoelastic lubricants, are subject to shear-induced structural degradation, defined in this thesis as "grease wear" when subjected to mechanical stress during friction. The barely understood mechanisms underlying this phenomenon are the focus of this thesis. This research work aims to achieve a quantifiable differentiation of the grease wear behaviour of pure biogenic and non-biogenic model greases to investigate, model and analytically describe these mechanisms. Various greases were investigated, including lithium, calcium, and polyurea greases, which had different base oils and viscosities.

A key element of this tribological study is the energetic consideration of the friction process, which is particularly relevant for lubricating greases. Thus, one part of this thesis deals with the expended energy during the friction process regarding the shear-induced structural rearrangement of the three-dimensional network of thickeners in the base oil. In this context, a grease wear parameter (R_{tee}) was developed. It provided decisive insights into the structural degradation of lubricating greases due to mechanical stress. The higher the parameter value, the lower the structural degradation of the stressed grease. Consequently, greases with a higher thickener content had lower R_{tee}-values, which indicates more significant structural degradation in the stressed lubricating grease.

Another part analyses the mechanical structural degradation induced by shear stress in rheological tests, considering the influence of thickener type, thickener composition and base oil properties. Different optical measurements were used to quantify further the structural degradation caused by the internal friction process of lubricating greases. By analysing eleven model greases under stressed and unstressed conditions using transmitted light microscopy, SEM and AFM, images showed significant differences in the structure of the lubricating greases due to the shear-induced frictional energy compared to unstressed samples. Furthermore, it was found that the type of thickener exerted a significant influence on the internal frictional energy. Lithium and

calcium greases exhibited lower mechanical energy dissipation during shearing than polyurea or isolated pure biogenic greases. The differences were due to the distribution of agglomerates based on thickener particles, the size of which depended on both the thickener content and the base oil viscosity.

The last part of this thesis investigates the internal friction-dependent temperature changes in the bulk of all greases studied under controlled environmental conditions with high shear stress using two measurement setups. A conventional rheometer-measuring cell and a newly developed temperature-measuring cell (Calidus) were used. At the same time, the temperature changes were linked to the lubricating grease components and the structural degradation. In particular, greases formulated with lithium and calcium soaps show the highest internal temperature profiles and drastic temperature drops with time, indicating significant shear-induced structural degradation. In contrast, a grease with a lower base oil viscosity shows the lowest maximum internal friction-dependent temperature changes and a moderate variation during the test. Within the group of pure biogenic greases, the biogenic grease B3 shows the slightest temperature changes.

In summary, this thesis contributes to a comprehensive understanding of the frictional behaviour of lubricating greases, covering aspects such as grease wear behaviour, shear-induced microstructural changes, mechanical structural degradation, and internal friction-dependent temperature changes. The investigations aimed to provide insight into the frictional behaviour of different types of lubricating greases under different conditions, including comparing biogenic and non-biogenic compositions.

Resumen

El estudio de las grasas lubricantes abarca diversos aspectos importantes para comprender su comportamiento y rendimiento. Las grasas lubricantes, entendida como un lubricante con comportamiento viscoelástico, están sujetas a una degradación estructural inducida por la acción de la cizalla durante el proceso de fricción. En esta tesis dicha degradación estructural de la grasa se ha denominado "grease wear" y el trabajo de investigación desarrollado se centra en los mecanismos poco conocidos que subyacen a este fenómeno. El objetivo de este trabajo de investigación es lograr una diferenciación cuantificable de dicha degradación estructural con el fin de investigar, modelar y describir analíticamente estos mecanismos. Se ha investigado un conjunto de grasas modelos, con formulaciones amigables con el medioambiente o tradicionales (grasas de litio, calcio y poliurea) con diferentes aceites base y viscosidades.

Un elemento esencial de esta investigación, desde el punto de vista de la Tribología, es el estudio energético del proceso de fricción, que es particularmente relevante cuando se lubrica con grasas lubricantes. Así, parte de este trabajo trata de la energía disipada durante el proceso de fricción debida a la reorganización de la estructura 3-D del espesante en el seno de un aceite base inducida por la cizalla. En este contexto, se ha definido un parámetro que trata de cuantificar la degradación estructural inducida por la cizalla (R_{tee}). Este parámetro proporcionó información decisiva sobre el deterioro estructural de las grasas lubricantes debido a la cizalla. Tal que, cuanto mayor era el valor de Rtee, menor fue la degradación estructural de la grasa lubricante sometida a esfuerzos cortantes. En consecuencia, las grasas con un mayor contenido de espesante mostraron valores más bajos de R_{tee}, lo que indica una mayor degradación estructural en la grasa lubricante sometida a tales esfuerzos.

Desde un punto de vista reológico, dicha degradación estructural inducida por la cizalla se ha analizado mediante ensayos en un reómetro rotacional, teniendo en cuenta la influencia del tipo y contenido de espesante, así como la naturaleza (tipo y viscosidad) del aceite base. Se han realizado medidas con equipos de microscopía para observar directamente las degradaciones de la estructura de las once grasas lubricantes causada por el proceso de fricción

interna. Todas las grasas se analizaron en condiciones de reposo y tras ser sometida a la acción de la cizalla, mediante diversas técnicas de microscopía, de luz transmitida, de barrido electrónico (SEM) y de fuerza atómica (AFM). Las imágenes obtenidas revelaron diferencias significativas en la estructura de las grasas debidas a la energía de fricción inducida por la cizalla en comparación con las muestras en reposo. Además, se observó que el tipo de espesante influía significativamente en la energía de fricción interna. Las grasas de litio y calcio mostraron disipación de energía mecánica durante la cizalla menor que la grasas de poliurea o las grasas biodegradables. Estas diferencias se debían principalmente a la distribución de aglomerados de partículas de espesante, cuyo tamaño dependía tanto del contenido de espesante como de la viscosidad del aceite base.

En la última parte de este trabajo, se analizan los cambios de temperatura en el seno de las grasas lubricantes estudiadas debidos al proceso de la fricción interna inducido por la cizalla. Se ha tenido especial precaución en en controlar las condiciones ambientales, para que éstas no interfieran en las medidas de temperaturas. Se ha usado hasta dos configuraciones distintas para medir in-situ la temperatura del interior de la grasa durante su cizallamiento: una célula de medición reométrica convencional y una célula de medición de temperatura de nuevo desarrollo (Calidus). Los cambios de temperatura observado se han relacionado con los componentes de las grasas lubricantes estudiadas y el parámetro de degradación estructural definido en esta tesis. En particular, las grasas formuladas con jabones de litio y calcio han mostrado perfiles de temperatura interna más acusados, con caídas drásticas de la temperatura con el tiempo, lo que indica una importante degradación estructural inducida por la cizalla. Por el contrario, una grasa formulada con un aceite de baja viscosidad mostraba el menor aumento de temperatura interna, así como las menores variaciones durante su cizallamiento. Dentro del grupo de grasas amigables con el medioambiente, la grasa B3 ha mostrado los cambios de temperatura más bajos.

En resumen, este trabajo de tesis contribuye a una comprensión global del comportamiento de fricción de las grasas lubricantes, tanto con formulaciones biodegradables como tradicionales, abarcando aspectos como la degradación estructural inducida por la acción de la cizalla durante el proceso de fricción, la disipación energética debida esta degradación estructural, y los cambios de temperatura dependientes de la fricción interna. Con el propósito de tratar de poner en valor las formulaciones de grasas lubricantes a partir de recursos sostenibles, no tóxicos y biodegradables.

Kurzzusammenfassung

Die Untersuchung von Schmierfetten umfasst verschiedene Aspekte, die für das Verständnis ihres Verhaltens und ihrer Leistung wichtig sind. Schmierfette, wie z.B. viskoelastische Schmierstoffe, unterliegen bei mechanischer Beanspruchung während der Reibung einem scherungsinduzierten Strukturabbau, der in dieser Arbeit als "Schmierfettverschleiß" bezeichnet wird. Die kaum verstandenen Mechanismen, die diesem Phänomen zugrunde liegen, stehen im Mittelpunkt der vorliegenden Arbeit. Ziel dieser Forschungsarbeit ist es, eine quantifizierbare Differenzierung des Fettverschleißverhaltens von rein biogenen und nicht-biogenen Modellfetten zu erreichen, um diese Mechanismen zu untersuchen, zu modellieren und analytisch zu beschreiben. Es wurden verschiedene Fette, darunter Lithium-, Calcium- und Polyharnstofffette mit unterschiedlichen Grundölen und Viskositäten, untersucht.

Ein wesentliches Element dieser tribologischen Untersuchung ist die energetische Betrachtung des Reibungsprozesses, welches für Schmierfette besonders relevant ist. So befasst sich ein Teil dieser Arbeit mit der aufgewendeten Energie während des Reibungsprozesses in Bezug auf die scherinduzierte strukturelle Umlagerung des dreidimensionalen Netzwerks von Verdickern im Grundöl. In diesem Zusammenhang wurde ein Schmierfettverschleißparameter (R_{tee}) entwickelt. Dieser lieferte entscheidende Erkenntnisse über die strukturelle Verschlechterung von Schmierfetten durch mechanische Belastung. Je größer der Wert des Parameters, desto geringer ist der Strukturabbau des beanspruchten Schmierfetts. Folglich wiesen Fette mit einem höheren Verdickergehalt niedrigere R_{tee}-Werte auf, was auf einen stärkeren Strukturabbau im beanspruchten Schmierfett hinweist.

In einem weiteren Teil wird die durch Scherbeanspruchung induzierte mechanische Strukturdegradation in rheologischen Tests unter Berücksichtigung des Einflusses von Verdickertyp, Verdickerzusammensetzung und Grundöleigenschaften analysiert. Verschiedene optische Messungen wurden eingesetzt, um die durch den inneren Reibungsprozess von Schmierfetten verursachte strukturelle Verschlechterung, weiter zu quantifizieren. Durch die Analyse von elf Modellfetten unter belasteten und unbelasteten Bedingungen mittels Durch-

lichtmikroskopie, REM und AFM zeigten die Bilder signifikante Unterschiede in der Struktur der Schmierfette aufgrund der scherinduzierten Reibungsenergie im Vergleich zu unbelasteten Proben. Darüber hinaus wurde festgestellt, dass die Art des Verdickers einen signifikanten Einfluss auf die innere Reibungsenergie ausübt. Lithium- und Calciumfette wiesen beim Scheren eine geringere mechanische Energiedissipation auf als Polyharnstoff oder isolierte rein biogene Fette. Die Unterschiede sind auf die Verteilung von Agglomeraten auf Basis von Verdickerpartikeln zurückzuführen, deren Größe sowohl vom Verdickergehalt als auch von der Grundölviskosität abhängt.

Im letzten Teil dieser Arbeit werden die von der inneren Reibung abhängigen Temperaturänderungen im inneren der Fettmasse, aller untersuchten Schmierfette, unter kontrollierten Umgebungsbedingungen mit hoher Scherbeanspruchung anhand von zwei Messaufbauten untersucht. Zum Einsatz kamen eine konventionelle Rheometer-Messzelle und eine neu entwickelte Temperatur-Messzelle (Calidus). Gleichzeitig wurden die Temperaturveränderungen mit den Schmierfettkomponenten und dem Strukturabbau in Verbindung gebracht. Insbesondere Fette, die mit Lithium- und Kalziumseifen formuliert sind, zeigen die höchsten internen Temperaturprofile und drastische Temperaturabfälle mit der Zeit, was auf einen signifikanten scherungsinduzierten Strukturabbau hinweist. Im Gegensatz dazu zeigt ein Fett mit einer niedrigeren Grundölviskosität die geringsten maximalen internen reibungsabhängigen Temperaturänderungen und eine moderate Variation während des Tests. Innerhalb der Gruppe der rein biogenen Fette weist das biogene Fett B3 die geringsten Temperaturänderungen auf.

Zusammenfassend trägt diese Arbeit zu einem umfassenden Verständnis des Reibungsverhaltens von Schmierfetten bei, dass Aspekte wie Fettverschleißverhalten, scherinduzierte mikrostrukturelle Veränderungen, mechanische Strukturdegradation und innere reibungsabhängige Temperaturänderungen umfasst. Die Untersuchungen zielten darauf ab, einen Einblick in das Reibungsverhalten verschiedener Schmierfettarten unter unterschiedlichen Bedingungen zu erhalten und dabei auch biogene und nicht-biogene Zusammensetzungen zu vergleichen.

Acknowledgements

This thesis represents not only my individual efforts but also many people's thoughts, suggestions, support, and contributions. It fills me with joy to express my gratitude to some of them in no particular order.

Firstly, I would like to thank my supervisors, Prof. Dr. Miguel Angel Delgado Canto and Prof. Dr.-Ing. Erik Kuhn, for their tireless guidance and ongoing support throughout the process of this thesis. They have always taken the time to discuss my questions and concerns related to my research. Their extensive expertise in research and academia was invaluable to me, and their assistance enabled the successful completion of this thesis.

Furthermore, I would also like to thank the scientific staff of the Tribology Research Centre (TREC) at the Hamburg University of Applied Sciences (HAW Hamburg), Dipl.-Ing. Thomas Rieling and Dipl.-Ing. Niels Eiben for their helpful advice, excellent support and the enjoyable time we spent together in the laboratory. I would also like to thank Mrs. Vera Liedtke-Scheffler from the Institute of Materials Science and Welding Technology for her support at the SEM.

In addition to my research at the HAW, I was also able to conduct investigations as part of a co-operation with the University of Hamburg at the Institute of Physical Chemistry. I want to thank members of various working groups who welcomed me as one of their own and gave me the best possible support with all the measuring equipment used. I especially want to thank Dr. Hauke Heller, Mr. Clemens Schröter and Mr. Martin Kehden.

At the same time, I have had the pleasure of getting to know many people at the HAW with whom I have worked over the years. Their efforts, time, thoughts and willingness to engage in countless discussions with me were and are of great importance to me. Even though our time together was brief, I want to emphasise my former colleague, Mr. Felix Gellert.

No less than thanks go to my partner, who motivated me tirelessly, always had an ear for me and put an incredible amount of time, heart, and soul into reviewing my work. This unconditional help, whether in talking through ideas or simply with words of encouragement, has made a decisive contribu-

tion to the completion of this thesis. I overcame many crises through her understanding, patience, and encouraging presence.

Last but not least, I would like to thank my family for providing me with the framework to complete this thesis to this extent and, of course, for the financial support during the years of my university education.

I am eternally grateful for the opportunity to write this thesis and for the support I received during the process. I hope that the results of my work will benefit science and society.

Thank you again to everyone who has supported me.

Hamburg, April 2024 Leif Ahme

Contents

List of Figures

List of Tables

List of Abbreviations

3D	Three-dimensional
A.C.	Before Christ
AFM	Atomic Force Microscope
API	American Petroleum Institute
Au	Gold
CO2	Carbon dioxide
BC	Before Christ
BMBF	Federal Ministry of Education and Research
Ca	Calcium
CP	Cone-and-Plate (measuring geometry)
CSR, CR	Controlled Shear Rate
CSS, CS	Controlled Shear Stress
DIN	German Institute for Standardisation
DSC	Differential Scanning Calorimeter
e.g.	Exempli gratia (that is)
et al.	Et alia (and others)
EU	European Union
HAW	Hamburg University of Applied Sciences
HDR	High Dynamic Range

HOSO	High Oleic Sunflower Oil
i.e.	Id est (for example)
ISO	International Organization for Standardization
Li	Lithium
LVE	Linear Viscoelastic
MCT	Medium-Chain Triglycerides
Mech.	Mechanical
NLGI	National Lubricating Grease Institute
PAG	Polyglycol
PAO	Poly-Alpha-Olefin
Pd	Palladium
PHA	Polyhydroxyalkanoates
PP	Parallel-Plate (measuring geometry)
PTD	Peltier Temperature Device
Pu	Polyurea
REACH	Registration, Evaluation, Authorisation and Restriction of Chemicals
SAOS	Small Amplitude Oscillation Tests
SEM	Scanning Electron Microscope
TREC	Tribology Research Centre
UV	Ultraviolet
wt.	Weight

List of Symbols

Symbol	Unit	Description
c_p	J/(g·K)	specific heat capacity
C_{SR}	[s^{-1}/min^{-1}]	conversion factor shear rate
d	[mm]	diameter
E_R	[J]	friction energy
F_L	[N]	load (e.g. compressive force in tribology)
F_N	[N]	normal force (acting vertical on the reference plane)
F_R	[N]	friction force
G'	[Pa]	storage modulus
G''	[Pa]	loss modulus
G*	[Pa]	complex shear modulus
h	[mm]	gap dimension, layer thickness, fluid level
i	[-]	(individual) counting number (e.g.; i = 1 to k)
$\widehat{i}$	[-]	peak value

Symbol	Unit	Description
$\left\lvert\bar{i}\right\rvert$	[-]	rectified value
lg		logarithm (to the basis 10)
m	[g]	mass
m	[-]	total number of segments (sum equation)
M_d	[Nm]	measured torque
$\widehat{M_d}$	[Nm]	peak measured torque
$\left\lvert\overline{M_d}\right\rvert$	[Nm]	rectified measured torque
M_R	[Nm]	frictional torque
n	[min^{-1}]	rotational velocity
P	[W]	power
P_R	[W]	frictional power
Q_{12}	[J]	quantity of energy supplied to the system as heat
R	[mm]	radius
R^2	[-]	goodness-of-fit of simple linear regression
R_{tee}	[-]	ratio of the total expended energy
R_Z	[-]	average surface roughness
s_R	[mm]	friction path
T	[°C], [K]	temperature

Symbol	Unit	Description
T_0	[K]	starting temperature value
t	[s]	time
U_1-U_2	[J]	change in the internal energy of a closed system
V	[cm^3]	volume
v	[m^2/s]	kinematic viscosity
v_s	[m/s]	sliding speed (tribology)
W_{12}	[J]	amount of thermodynamic work done by the system
W_R	[J]	friction work
γ	[%],[1]	deformation or strain
γ_{max}	[%],[1]	maximum deformation
γ_f	[%]	crossing point / yield point
γ_y	[%]	critical point
$\dot{\gamma}$	[s^{-1}]	shear rate
$\hat{\dot{\gamma}}$	[s^{-1}]	shear rate peak
$\lvert\overline{\dot{\gamma}}\rvert$	[s^{-1}]	rectified shear rate
δ	[°]	phase shift angle, loss angle
ΔT	[K]	temperature change
Δt	[s]	segment of time

Symbol	Unit	Description
η	[Pas]	(shear) viscosity
π	[-]	circle constant ($\pi = 3.141592$)
ρ	[g/cm³]	density
σ_{max}	[Pa]	maximum tensile or compressive stress
τ	[Pa]	shear stress
φ	[rad], [°]	deflection or displacement angle
ω	[rad/s], [s^{-1}]	angular velocity (rotation), angular frequency (oscillation)
f, μ	[-]	coefficient of friction
Σ		summation sign (“sigma”)

"Great things are done by a series of small things brought together."

Vincent van Gogh; 1853 - 1890

1 Introduction

The global climate crisis affects all sectors of human coexistence and industry. There is evidence of increasing industrialisation combined with further increases in energy requirements. As a result of the climate crisis, there is an increasing focus on sustainability and energy efficiency. At the same time, humankind has been concerned with saving energy since the beginning. In this context, Tribology, as the science of wear, friction and lubrication, is decisive in optimising and extending the service life of machines and systems [1]. There is potential for pursuing sustainability goals, especially for reducing CO_2 emissions, as lubricants are mainly designed to minimise friction and wear [2]. Around 23 % of global primary energy losses are due to friction, corresponding to around 119 exajoules and estimated at around 2.54 trillion € [3]. In addition, Woydt [4] predicts that a 30 % reduction in friction losses could save 2.27 to 4.55 gigatonnes of CO_2 emissions worldwide. Furthermore, the longer service life of components can reduce the material footprint and thus conserve resources.

The use of lubricating greases to reduce friction and wear in various industrial applications is ubiquitous. Over one million tonnes of lubricants reduce friction and wear losses in Germany [5]. Lubricating greases are viscoelastic lubricants subject to structural changes over time during friction due to temperature, shear stress and chemical environmental conditions [6]. According to the concept of wear defined by Kuhn [7]: *"Wear is the dissipation of frictional energy (energy introduced into a tribological system)."* Thus, the shear-induced structural changes in the grease can be expressed as "grease wear". It significantly impacts their use and performance, leading to increased energy consumption, maintenance requirements and ultimately, an increase in the ecological footprint. Typically, grease wear is a natural occurrence characterised by the general properties of structural degradation in greases, and the specific material pairing does not influence it [7].

Regarding the ecological footprint, developing competitive biogenic lubricants is becoming increasingly important. Bongardt and König [5] state that about 50 % of the conventionally used lubricating greases end up in the envir-

onment and thus lead to a long-term burden on nature, as they are difficult to degrade [5]. Since 2007, the European Chemicals Regulation REACH has imposed high protection for human health and the environment on all manufacturers, importers and users. It promotes the free movement of chemicals on the internal market and strengthens competitiveness and innovation [8]. The growing number and importance of ecolabels in technical use favour the switch to biogenic ingredients to produce lubricating greases. In addition, as oil reserves diminish and petroleum products become more expensive and uncertain, there is an urgent need to conserve finite resources [9, 10]. The aim is to reduce dependence on non-renewable resources and use biodegradable and renewable raw materials. It promotes sustainability and reduces the environmental impact of conventional lubricating greases, often based on fossil resources.

However, the production of biogenic lubricants requires considerable experience and knowledge. Developing lubricating greases is time-consuming, as an optimised manufacturing process and suitable ingredients are crucial. It is known that the rheological and tribological behaviour of lubricating greases is strongly dependent on the manufacturing process and composition, as these have a significant influence on the microstructure and the associated physical properties of these biogenic greases [9, 10].

1.1 Justification and Novelty of the Thesis

Considering that grease wear is directly related to the dissipation of energy by the grease entering the tribological system, it is crucial to investigate the structural degradation of lubricating greases in more detail from an energy point of view. These achievements will help find sustainable and energy-efficient solutions which contribute to reducing fuel consumption and, therefore, greenhouse gas emissions. For this purpose, this research work has analysed the rheological properties, the shear-induced structural degradation, and the internal friction-dependent temperature changes of a significant number of lubricating greases. Structural degradation can be subdivided into chemical and physical degradation [11, 12]. This thesis focuses on physical degradation, which includes the destruction of the thickener structure by mechanical stress, known as mechanical grease degradation [11–13]. Mechanical degradation usually occurs at high speeds (shear rates) and low operating temperatures [11, 13, 14]. This research aims to extend the understanding of the wear behaviour of

lubricating greases and offers a novel perspective on this important topic.

Lubricating greases are of high industrial relevance as they play a crucial role in almost all mechanical systems, whether in the automotive industry, aviation, heavy industry or wind power generation [6, 15]. The results of this work can contribute to improving the efficiency and service life of these mechanical systems, which has a significant economic impact. Furthermore, the wear of lubricating greases is a complex phenomenon influenced by various factors such as material composition, temperature, pressure, speed and environmental influences. This thesis examines some of these factors to understand grease wear behaviour better. In addition, innovative test and analysis methods are applied in this research work to simulate and evaluate the wear behaviour of lubricating greases. The knowledge gained can be used to optimise lubricating grease formulation to achieve a longer service life. This work also contributes to the existing knowledge base in Tribology. It expands the understanding of the interaction of lubricating greases with the environment, opening up new research opportunities.

This thesis is, therefore, of great importance in terms of its industrial relevance and innovative approach. It contributes to improving the performance of lubricating greases in a wide range of applications and can potentially change how we understand and control the dissipated energy in mechanical systems. Since the underlying mechanisms of the structural and mechanical degradation of lubricating greases are still insufficiently understood and cannot be described analytically, this thesis pursues researching, modelling and presenting them in an analytical form.

1.2 Aim of the Thesis

This thesis aims to develop a comprehensive understanding of the underlying mechanisms of the structural degradation of lubricating greases and simultaneously assess its effects on frictional energy, i.e., energy dissipation during friction. Furthermore, by integrating sustainability aspects into tribological research, solutions will be developed to improve the performance of lubricating greases and minimise resource consumption and environmental impact. The main aims of this thesis are listed below:

- Study the structural skeleton details of lubricating greases on the micro- and nanoscale using optical light microscopy, scanning electron microscopy (SEM), and atomic force microscopy (AFM) and identify changes

in the structural skeleton (fracture, entanglement or realignment of the fibres) of several lubricating greases due to shear stress, and to analyse them from an energetic point of view.

- Simulate the mechanical structural degradation of lubricating greases using different rheological tests and analyse the influence of the thickener, both type and composition and the base oil on it.
- Analyses internal friction-dependent temperature changes on the bulk of lubricating greases under mechanical stress. For this purpose, the heat dissipation during the friction process in a grease volume is to be observed and analysed as a function of the composition of the base oil and the thickener.
- Develop a method to evaluate the interactions (van der Walls or H-bonds) between the fibres or the base oil and the capillary forces of selected model greases.

All these objectives have been developed by analysing the influence of the thickener, both type and composition, and the base oil on the microstructure, mechanical structural degradation, and internal friction-dependent temperature changes, respectively. In addition, the greases studied were divided into pure biogenic lubricating greases and non-biogenic model greases traditional, i.e., traditional greases. The aim is to examine how sustainable lubricant formulations, optimised lubrication strategies, and innovative friction reduction concepts can influence the structural degradation of lubricating greases.

The results of this thesis provide valuable insights that can contribute to developing more environmentally friendly and energy-efficient lubricating greases and lubrication strategies. Thus, the knowledge gained from this thesis will contribute to the further development of tribological models and create a basis for future research in sustainable Tribology. It will enable companies to lower their operating costs, reduce energy consumption, and at the same time promote environmental protection.

1.3 Thesis Outline

In addition to the introduction, the thesis is divided into four further chapters and the appendix:
In line with a cumulative thesis, the second chapter explains the state of

the art in a broad outline to provide a basis for the theoretical principles. The aim is to give the reader an insight into lubricating greases and their unique features. The contents of Tribology and Rheology expand the basics of lubricating greases. Finally, a precise literary analysis is carried out regarding the main focus of research in order to define it conscientiously.

Chapter 3: "Materials and Test Methods" describes the number of lubricating greases studied according to their composition. Later, the test methods are explained based on the measuring devices used. In addition, the respective test procedures are described by outlining the measures to be prepared and the test parameters explicitly used in this work.

The fourth chapter, "Results and Discussion", contains summaries of the test results of the three scientific journal articles produced during this thesis. In addition, further test results obtained in this research work are briefly analysed.

The final chapter, "Conclusions and Outlook", briefly summarises all relevant and innovative findings. In the outlook, further testing and evaluation possibilities for future research projects in the subject area of this thesis are shown.

The annexe of this thesis contains all three scientific journal articles with the respective names and affiliations of the authors, as well as the complete reference and the impact factor of the journal or publisher.

2 State of the Art

This chapter is intended to provide the reader with a basic understanding of the theory of this thesis. For this purpose, a detailed introduction to the field of knowledge of lubricating greases and their unique features is given. Subsequently, the field of Tribology knowledge is presented with the respective components of friction and wear. This part of the thesis is completed with the basics of the Rheology of lubricating greases. The final part is the energetic interpretation of the structural degradation of greases, which is related to the rheological behaviour of the lubricating greases.

2.1 Fundamentals of lubricating greases

Lubrication became indispensable when people started using tools with moving parts. A lubricant was needed to reduce effort, for example, when moving blocks of stone to build pyramids or using a wheeled cart to transport goods. It can be assumed that the first practical application of lubricants was an accidental discovery rather than a direct innovation [16]. According to historical reports, grease-like substances, oil and water were used as lubricants in pre-Christian times to minimise friction. Figure 2.1 shows a wall relief from an Egyptian pharaoh's tomb, dated around 2400 BC. It depicts a worker using a lubricant - in this case, water - to move statues [17]. From the 19th century onwards, lubricants played a central role in technical applications, especially in gears and gearwheels. In the initial stages, lubricants primarily relied on natural and animal ingredients until the advent of petroleum and the development of mineral oil processing techniques, which eventually supplanted them [18].

The selection of a lubricant depends on the stress profile within a friction pairing. It intends to optimise movement between solid, stressed surfaces while maintaining geometric shapes, thus minimising abrasion and wear, increasing service life and economic efficiency [19, 20]. Other tasks of lubricants are to ensure heat dissipation, sealing and corrosion protection. Mineral or synthetic

oils are mainly used as the basis for lubricants. In order to subdivide lubricants better, they are assessed according to consistency and aggregate state, which is why differentiation between lubricating oils and lubricating greases is helpful [19, 20]. Consistency is the degree of uniformity, stability, or reliability in the lubricant's quality behaviour or performance over time. It can apply the thickness or texture of the lubricant [21, 22].

Figure 2.1: Egyptian worker pouring biogenic lubricant for moving statues [17]

Lubricating oil is a liquid used to reduce friction, dissipate heat, remove particles from the friction pairs, and minimize the wear between mechanical components in contact [23]. In Tribology, lubricating oils are used owing to their low viscosity and liquid characteristics; unlike lubricating grease, they react more efficiently in tribosystems with high speeds and accelerations [19, 24]. It is a liquid that cannot be mixed with water and has a higher condensation point than water. Generally, it is a technically advanced product composed of a complex mixture of hydrocarbons, which can be divided into mineral or synthetic oil. Other rapidly biodegradable base oils are being developed [25, as cited in 7].

In scenarios where lubricating oils are technically or economically disadvantageous or impossible, lubricating greases are the alternative. A lubricating grease can be described as a lubricating oil augmented with a thickening agent, primarily characterized by its consistency. Lubricating greases are used in mechanisms that require less frequent lubrication and where oil lubrication would not stay in place. In addition, lubricating greases also act as sealants to prevent the entrance of water, powder, or other external contaminants. Examples are cases where lubricating oils drip or flow away, and a permanent supply on the friction pairs would not be possible. The great advantage of lubricating greases is that they cannot flow away at the friction point, e.g., in a rolling bearing. It means that taking constructive sealing measures is unnecessary and saves costs. In addition, lubricating greases retain their shape under everyday shear stress and temperature, preventing contamination (penetration of water and dirt particles). However, greases cannot guarantee a

cooling or cleaning effect, unlike lubricating oils. Instead, they are used for some components as lifetime lubrication and, in these cases, are not changed or refilled. In addition, they can better absorb shock stresses on bearings and show more favourable lubrication characteristics than lubricating oils in mixed and boundary friction areas [7, 20, 26].

2.1.1 Definition of lubricating greases

According to DIN 51825, lubricating greases are *"consistent lubricants composed of mineral oil and/or synthetic oil and a thickener. They may contain additives and/or solid lubricants"* [27]. Kuhn has developed the following definition for lubricating greases from several different definitions: *"Lubricating greases are colloidal disperse systems. They consist of a base oil and a solid. Lubricating greases have distinct viscoelastic characteristics"* [7]. Delgado demonstrated that lubricating greases are inherently complicated due to their non-Newtonian flow behaviour [28, 29]. It means that the flow behaviour of a grease is not proportional to the applied stress. Thus, unlike oils, lubricating greases have a very high initial viscosity that decreases under shear stress, allowing them to function as an oil-lubricated bearing with approximately the same viscosity as the base oil used in the grease formulation [2, 7, 26, 28, 29].

2.1.2 Composition of greases

The composition of a grease depends on the respective requirements of its application. The composition is usually indicated by the percentage of the three essential elements. Conventional grease comprises 65 to 95 wt.% base oil, 5 to 35 wt.% thickener and 0 to 10 wt.% additives [2, 20, 30]. For most greases, metal soaps are used as thickeners and added additives to achieve the grease's unique characteristics. Lubricating greases obtain their particular viscoelastic behaviour through the formation of a three-dimensional (3D) network of the thickener, which is characterised by physical bonds such as H-bridge or Van der Waals forces and steric impediments among thickener particles, also surrounded by the base oil [30–32]. Moreover, increasing the consistency of greases by the thickener prevents the loss of lubricant under operating conditions. However, this leads to considerable resistance to the flow and pumping.

The base oil has a decisive role in the lubrication features of lubricating greases. It is intended to prevent metallic contact with the tribo-pair com-

ponents, ensuring lubrication by building up a layer of oil. The thickness of the oil layer is directly related to the viscosity of the base oil, which is strongly dependent on temperature. Accordingly, a decisive factor for the choice of grease is the viscosity-temperature de]pendence, which can be described using the viscosity index. Base oils with a viscosity of 100-220 mm^2/s at a temperature of 40 °C are mainly used for standard greases [26, 33]. The most used base oils for grease are mineral oils, although, in particular or demanding cases, synthetic or vegetable oils are also used [19, 33, 34]. The most essential base oil types are briefly described below. In addition, many requirements are placed on base oil, such as good lubricating characteristics, good oxidation stability, good thermal resistance, sufficient flow characteristics and low chemical reactivity. However, these characteristics can be improved by adding additives.

Mineral oils are obtained by distillation of petroleum and partly also from coal. It is a mixture of numerous hydrocarbons with different molecular structures and sizes [35, 36]. Mineral oils are classified according to the characteristics of the original crude oil as aromatic, naphthenic and paraffinic [37, as cited in 7]. According to the API standard, mineral oils are classified into group I (with less than 90 % saturates, greater than 0.03 % sulfur and with a viscosity-index range of 80 to 120), group II (with more than 90 % saturates, less than 0.03 % sulfur and with a viscosity index of 80 to 120), and group III (greater than 90 % saturates, less than 0.03 % sulfur and have a viscosity index above 120) [38, 39]. Synthetic oils result from chemically defined base elements. They are often produced to have excellent viscosity-temperature behaviour, a viscosity index higher than 120, and a low tendency to coke [40, as cited in 7, 36]. They are classified by API standard into groups IV (for polyalphaolefins (PAOs)) and group V (for the rest of the synthetic oils) [38, 39]. In contrast to mineral oils, synthetic oils are used less frequently because their price is relatively high [40, as cited in 7, 36]. However, it is highly demanded in high-performance applications like engine oils. Classification of synthetic oils can be made into synthetic hydrocarbons like polyalphaolefins (PAOs), carboxylic acid esters (di-ester oils), polyglycols (PAGs), aromatic polyether oils, phosphoric acid esters (phosphate esters), silicone oils, silicic acid esters (silicate esters) and chlorofluorocarbon oils [41]. Due to the increasing demand for rapidly biodegradable and, thus, more environmentally friendly lubricating oils, biological base oils are now available on the market. These include vegetable oils (rapeseed, sunflower, castor oil), synthetic esters, and low-viscosity polyglycols (water-soluble types). However, using such biological base oils is

not without problems, as the temperature behaviour, UV radiation stability and ageing behaviour, especially with native oils, often still show weaknesses. It limits the range of application due to the weaker characteristics compared to other base oils [42, as cited in 7].

The thickener is about 5-35 % of the total weight in a typical grease composition. The thickener agent in lubricating grease is crucial in determining the final product's physical properties. Thickeners are molecules, polymers, or particles partially soluble in the base oil; metal soaps are often used as thickeners in lubricating greases. They arrange to impart a semi-solid consistency to the grease by forming a relatively stable spatial network. The thickener acts like a sponge that holds the base oil and additives [2, 7, 26, 29, 43]. It enables the formulated grease to meet a desired level of consistency or hardness and other performance requirements. The grease consistency is mainly due to the amount of thickener in the product. Generally, the more thickener is present, the more solid the grease will be. It is essential because it allows the grease to stay in place in applications with intermittent operation, reduces leakage, and can be used to suspend solid additives [2, 20, 26].

Thickeners can be divided into three main groups: Metal soaps, complex soaps and non-soap thickeners (organic or inorganic). Some of the most essential thickener types are listed in the following table 2.1 [19, 33]. The characteristics of lubricating greases depend significantly on the type and concentration of the thickener agent. These include temperature resistance, speed behaviour, load-carrying capacity, oil release characteristics, dropping point, rheological behaviour, water and acid resistance, and mechanical-dynamic stability [33].

Table 2.1: Some of the most essential types of thickeners for lubricating greases [19, 26]

Simple Metal soaps	**Complex Metal soaps**	**Non-soaps**	
		Organic	**Inorganic**
lithium soaps, calcium soaps, aluminium soaps, sodium soaps, lead soaps, zinc soaps	lithium complex soaps, calcium complex soaps, aluminium complex soaps, sodium complex soaps, barium complex soaps	ureas, polyamides, polyimides, organic pigments (e.g. phthalocyanine, polyethylene, polypropylene)	bentonite, pyrogenic silica, metal stain, graphite

Additives are chemical compounds. They are used in lubricating greases to improve the base oils' existing characteristics significantly or to give them new qualities. Additives enable characteristics that cannot be achieved even by elaborate grease processing to be attained. Additives can be divided into two categories concerning their solubility and characteristics. Insoluble additives, such as graphite, molybdenum disulphide, talcum or mica, improve the friction behaviour of metallic surfaces and are used in high-pressure applications. Soluble additives are antioxidants, rust and corrosion inhibitors. Characteristics that improve the base oil are differentiated into physical, chemical, or chemical and physical properties [2, 21, 22].

Finally, it should be noted that producing lubricating greases is highly time-consuming. An optimal manufacturing process and suitable components are essential, as they strongly influence the three-dimensional structure of lubricating greases and, consequently, its rheological and tribological behaviour [9, 10]. The research of Delgado et al. [29] has shown that the structural skeleton of the lubricating greases (size and shape of the dispersed phase particles) strongly depends on the processing conditions and the grease composition, especially on the thickener contents and the base oil viscosity.

2.1.3 Classification of greases

There are various criteria for classifying lubricating greases. They are classified according to the NLGI consistency classes. In addition, lubricating greases can also be classified according to the type of base oil (mineral, synthetic or biological), the composition (depending on the type of thickener, e.g. lithium grease, calcium grease), the characteristics (fluid grease, block grease), the area of application (rolling bearings, plain bearings, open gears) or the service temperature (low, standard or high-temperature greases) [2, 7, 34].

Often, lubricating greases are divided into consistency classes. Although the consistency description is a very rough way of looking at it, the advantage is the efficient evaluation. Similar to the viscosity of oils, they are categorised as "firm" or "soft". Consistency refers to the resistance of a grease to the penetration of a piezo-cone in free fall. DIN 51818:1981-12 [44] divides greases into nine NLGI classes, shown in table 2.2 [7, 43].

Penetration is, as seen from the table below, a measure of the consistency of a grease in mm (millimetre). The value is determined by a penetration test on the penetrometer as specified in DIN ISO 2137. In such a test, the penetration depth of a standardised cone into a grease sample is determined

after five seconds. A high penetration depth subsequently describes a softer grease [43].

Table 2.2: Consistency classes of lubricants (NLGI classes) [44, as cited in 45]

NLGI-Classes	Fulling penetration in 0.1 mm	Appearance	Application
000	445 … 475	fluid	Gearbox greases, central lubrication systems
00	400 … 430	semi-fluid	Gearbox greases, central lubrication systems
0	355 … 385	very soft	Gearbox greases, rolling bearing greases, central lubrication systems
1	310 … 340	soft	Rolling bearing greases
2	265 … 295	medium firm	Rolling bearing greases, plain bearing greases
3	220 … 250	firm	Rolling bearing greases, plain bearing greases, water pump greases
4	175 … 205	very firm	Rolling bearing greases, water pump greases
5	130 … 160	hard	Water pump greases, block greases
6	85 … 115	very hard	Block greases

2.1.4 Types of lubricating grease

As described in the previous section, the various lubricating greases are often classified according to NLGI classes or thickeners. In the following section, the different greases and the types of thickeners are explained in more detail. Among them, a distinction can be made between metal soap greases, non-soap greases and pure biogenic greases. Metal soap greases have a simple metal soap, a complex metal soap or a mixed soap as a thickener. Non-soap greases include modified clays (bentonites), polyurea compounds or pigments as thickeners [6, 7, 43]. Pure biogenic lubricating greases are those in which, in addition to the biological base oil, biological substances are also used as thickeners. The most significant proportion of thickeners used in lubricating greases is metal soap greases (approx. 75 %), 70 % of which are lithium soap greases [33].

The most common greases include conventional greases consisting of simple soap greases (such as lithium, calcium, sodium, aluminium and barium soap greases), mixed base soap greases (lithium and calcium soap grease) and complex soap greases (lithium, calcium, sodium, and aluminium complex soap greases) [2, 6, 7]. Biogenic greases are divided into partially biogenic and pure biogenic greases. Partially biogenic greases contain conventional thickeners,

such as metal soaps, and biogenic base oils, such as vegetable oil. In the development of pure biogenic greases, the thickener also consists of biological substances, such as lignocellulose fibres, corncob grist or lignin sulphonate [7].

2.1.5 Pure biogenic greases

About 40-50 % of the 5 million tonnes of lubricants used each year in Europe are estimated to be released into the environment due to operational losses, spills during refilling, leaks or accidental damages [46]. The resulting environmental damages have increased interest in renewable and biodegradable lubricants. Thus, developing pure biogenic greases is highly demanded by society as their use in various industrial applications can help avoid direct and indirect environmental pollution. A policy framework has been created to support shifting towards a low-cost, resource-efficient economy and low carbon emission, e.g., the EU ecolabel or European regulation REACH (Registration, Evaluation and Authorisation of Chemicals) [47–49].

According to the EU ecolabel guarantees, lubricating greases have a limited impact on the aquatic environment, contain a restricted quantity of hazardous substances, and perform as well as or better than a conventional lubricant available on the market. However, it does not necessarily have to be composed of entirely biodegradable substances. However, lubricating greases are defined as pure biogenic if produced from bio-based raw materials. Conventional base oils such as mineral oil are replaced by vegetable oil, animal fats or other environmentally compatible hydrocarbons. Traditionally used thickeners such as metal soaps are trying to be replaced by biogenic thickeners such as biopolymers. Pure biogenic greases are rapidly biodegradable and non-toxic to humans and the environment [7, 50]. Microorganism degradation of the substance's chemical structures is used to measure biodegradability [51]. Biodegradability is assessed individually for each lubricant component and divided into three categories: mildly biodegradable substances, inherently biodegradable substances and non-biodegradable substances [52–54].

Currently, researchers at the University of Huelva (Spain) are particularly pushing the development of pure biogenic greases [7]. In research works [55–63], various grease compositions were investigated that are based on biogenic thickeners such as lignocellulosic derivatives, chitin, glycerol stearates or sorbitan stearates as well as castor or high oleic sunflower oil as biodegradable base oil. These compositions were analysed rheologically and tribologically and compared with conventional lubricating greases, thickened using lithium-12-

hydroxysteate. The results of the investigations show that some of the newly developed lubricating greases have comparable or even better thermal, rheological and mechanical characteristics than conventional lubricating greases. Some tribological tests also found that the friction coefficients of the completely biogenic lubricating greases investigated were lower than those of the reference greases at specific working conditions [57]. In addition, the work of Acar [64] within the TriBioGen research project should also be mentioned in this context. The overall objective of this project was to reduce the amount of conventionally used grease thickeners in the long run towards conventionally applicable pure biogenic greases. For this purpose, some newly developed pure biogenic lubricating greases with innovative biogenic thickener ingredients were investigated with rheological and tribological measurements [65]. In addition, two selected model lubricating greases were compared with each other through tests on a rolling bearing test bench concerning their friction and wear behaviour [66].

2.1.6 The lubricating greases' microstructure

In order to examine the tribological grease behaviour, it is worth taking a closer look at the grease structure. As Kuhn [7] points out, it is essential to note that the term structure is used differently. Since this thesis work deals with the structural degradation of greases, the focus was on the network formed by the thickener. The thickener forms a three-dimensional network of structural units such as fibres, fibre agglomerates and rods in greases. This microstructure of the grease is formed by the crystallisation of the thickener particles in the lubricating oil during the manufacturing process [9]. The type of structural unit will depend on the type of thickener agent. Farrington [67] conducted an exciting size comparison study between individual soap fibres and various viruses and bacteria. Figure 2.2 shows the typical structures of individual metallic soaps and their lengths from this study. Moreover, the grease microstructure depends on the concentration of the thickener, the type and viscosity of the base oil and the manufacturing process condition (mixing speed, crystallization rate, homogenization step intensity and others) [29, 68–71]. In this sense, Delgado et al. [29] have shown that low concentrations of thickener in lithium grease lead to large platelets. In contrast, higher concentrations lead to a higher density of physical entanglements between the fibres. Moreover, lithium greases made with a high-viscosity base oil have longer fibres and larger inter-fibre cavities in which the base oil is entrapped

compared to those made with a low-viscosity base oil, which developed a more entangled structure [29]. As discussed in this thesis, the grease microstructure will affect its ability to dissipate energy and, therefore, its interaction with the tribological system [72].

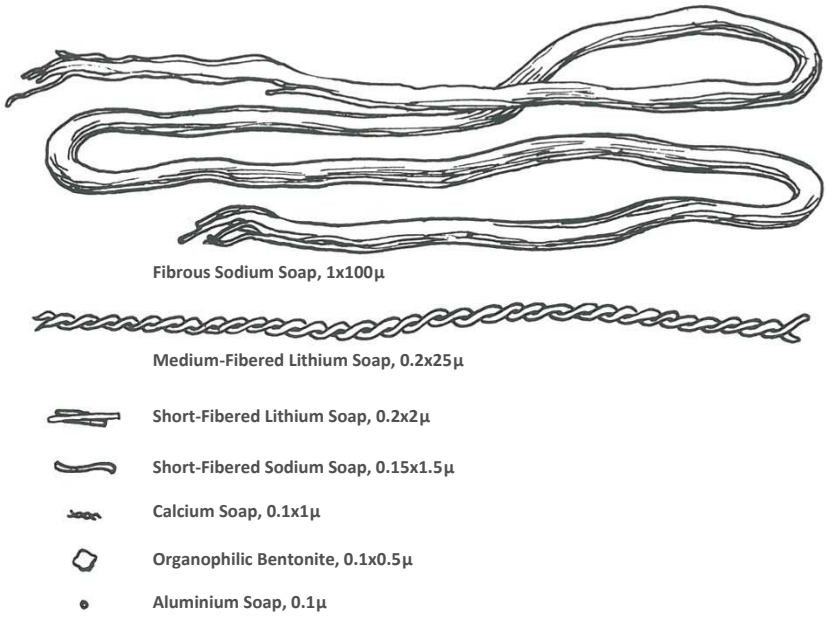

Figure 2.2: Size comparison between individual metal soap fibres according to Farrington [67]

Microscopic images help to show the arrangement of the fibres' structure or the formation of a network to document the differences between the types of thickener agents studied [7]. In this context, the macrostructures of lubricating greases (mainly agglomerates of particles) can be visualised very well with an optical microscope. Numerous papers in the literature have addressed grease structure through the use and analysis of optical imaging methods [22, 68, 71, 73–89]. In contrast, more in-depth details on the microstructural structures are visualised most effectively by both scanning electron microscopy (SEM) and atomic force microscopy (AFM) techniques [73]. A significant difference between the SEM and AFM techniques is that the SEM technique operates

in a vacuum, which means that the lubricating oil must be extracted or its volatility reduced prior to the experiments. A delicate treatment of the grease sample is required to remove the oil without altering the structure of the grease before it can be measured. In contrast, tests in the AFM technique can be carried out under atmospheric pressure, whereby the grease sample is not exposed to any extraction pretreatment. Prior to initiating the scan sequence, it is essential to have a uniformly smooth upper surface on the sample to guarantee high-quality AFM images [68, 86].

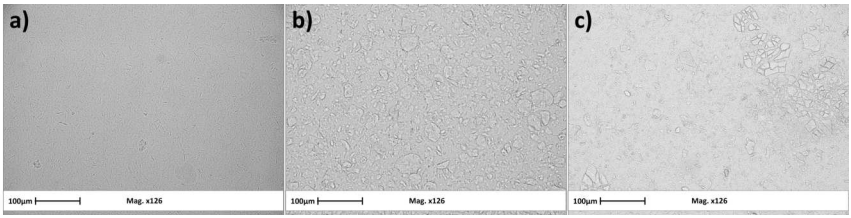

Figure 2.3: Optical microscope images of a) lithium grease (C2); b) calcium grease (C6); c) polyurea grease (C7)

Figure 2.3 shows the structure of three optical microscope images of lithium, calcium and polyurethane grease. As can be appreciated, different agglomerate arrangements are visible. In the case of lithium grease (figure 2.3a), hardly any agglomerate structures can be seen; the structure is relatively homogeneous and is characterised by a fibre structure. In contrast, the calcium and polyurea grease agglomerates are much more visible by a simple optical microscope with 126x magnification (figure 2.3b and 2.3c). Even differences in shape can be observed.

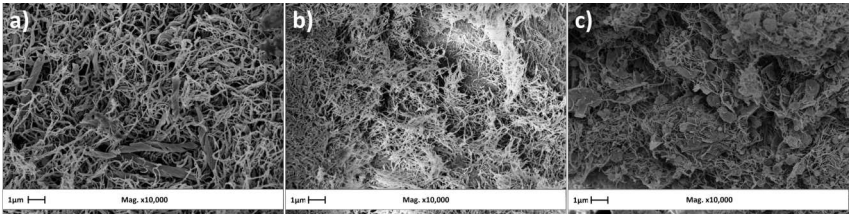

Figure 2.4: SEM images of a) lithium grease (C2); b) calcium grease (C6); c) polyurea grease (C7)

Figures 2.4 and 2.5 illustrate SEM and AFM images, respectively, for lithium, calcium and polyurethane greases. In contrast to the optical microscope images, SEM and AFM clearly observe each thickener agent's comparatively long and entangled fibre structures. In addition, the twists of the lithium soap fibres can also be recognised. On the one hand, the SEM and AFM analysis showed that the microstructure of the lithium grease has significantly broader and larger fibres than the calcium grease. On the other hand, the polyurea grease shows thickening particles in the form of platelets connected with some fibres. It is worth pointing out that SEM measurements provide an image of the structural network with better resolution than AFM. However, the latter allows the thickener particles to be observed as they are dispersed in the oil. Combining the three optical microscopy techniques allows a clear image of the lubricating greases' microstructure to be obtained.

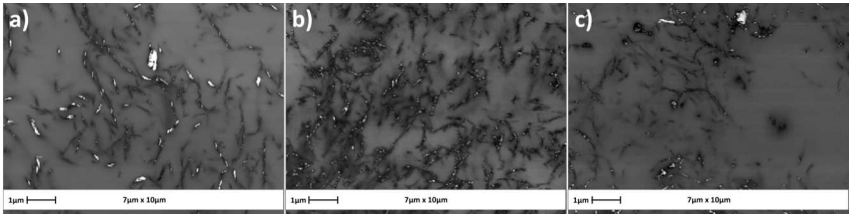

Figure 2.5: AFM images of a) lithium grease (C2); b) calcium grease (C6); c) polyurea grease (C7)

2.2 Basic of Tribology

This section explains the meaning and objectives of Tribology. The term tribology is derived from the Greek word combination tribein (τρίβειν, in English: rub, wear) and lógos (λόγος, in English: theory) and thus means "friction science". Tribology is thus the science of friction and the phenomena associated with it. It includes, for example, solid body wear, which can be reduced by lubrication. Tribology is, therefore, considered a technical term that includes the relationships between friction (term to define the loss of mechanical energy during a relative movement of contacting surfaces), wear (term to define the loss of material from the surface of a solid body caused by mechanical causes) and lubricants (the intermediate material to minimize the direct contact between the mating surfaces) [90].

Figure 2.6: Fragment of a rotating wooden platform with bronze balls from ships [18]

Peter Jost delivered a fundamental definition of Tribology in 1966. However, humankind had already been dealing with friction long before Christ. On the one hand, they tried to minimise friction when transporting heavy loads by placing wooden logs underneath them, and on the other hand, they tried to use friction to generate fire [33]. Particularly remarkable are the early attempts to build roller bearings. From around 50 A.C., fragments (figure 2.6) show bronze balls with guide pins on a ship's platform. These balls could not rotate freely but only around the pivots [18].

2.2.1 What is Tribology?

To understand the term Tribology, the definition of DIN standard 50323-1 [91] is given below:

> *Tribology is the science and technology of surfaces acting on each other in relative motion. It covers the entire field of friction and wear, including lubrication, and includes corresponding boundary film surface interactions between solids and between solids and liquids or gases.*

As mentioned in the previous section, it was Peter Jost in 1966 who provided the basic definition for the "artificial word" Tribology in the Jost Report. He said: *"Tribology is the science and technology of interacting surfaces in relative motion and of related subjects and practices."* [92, as cited in 7]. Kuhn [7] extends the concept further and defines the scientific discipline of Tribology as: *"...the endeavour of energetically stressed tribological systems that have been brought out of thermodynamic equilibrium to regain a stable situation (stationary non-equilibrium)"*.

2.2.2 The tribology system

A tribological system (tribosystem) is the model that contains the tribo-pair, the lubricant and the environmental conditions involved in the tribology studies. It includes the properties of each component and the resulting changes and the processes and variables characteristic of the stress [93]. The function of a tribological system is to convert the input variables into technically usable

output variables. The resulting loss variable due to friction (loss of mechanical energy) and wear (loss of material) is regarded as a further output variable. The input variables also include disturbance variables that influence both the output and loss variables [43, 94]. Figure 2.7 shows the schematic of a tribosystem. The tribological components (base body, mating surface, lubricant as intermediate material and ambient medium) are called the tribosystem structure. At the same time, the input variables (including movement, stress, and temperature) are considered the stress collective [20, 93].

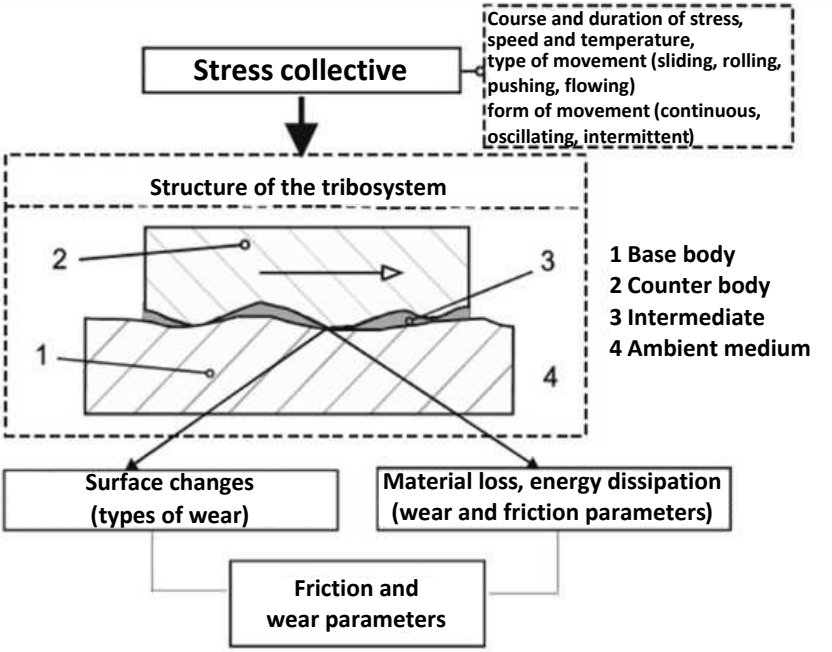

Figure 2.7: Schematic of a tribological system according to Gesellschaft für Tribologie [93]

2.2.3 Friction

The term friction is defined in the seventh worksheet of the Society for Tribology as follows [93]:

Friction is an interaction between touching material areas of bodies. It coun-

teracts a relative movement. In the case of external friction, the areas of material in contact belong to different bodies; in the case of internal friction, they belong to the same body.

Kuhn has developed the following definition for friction: *"Friction is the supply of mechanical energy to a tribological system"* [7]. Fleischer provides another helpful and comprehensible definition, stating that friction is: *" the loss of mechanical energy during the running, starting or ending of a relative movement of contacting surfaces"* [95]. The effect of friction can be perceived in the form of forces (friction force, F_R), moments (friction moments, M_R), power (frictional power, P_R), or as a process in which mechanical work (friction work, W_R or friction energy, E_R) is primarily converted into other forms of energy [95]. According to DIN 50281, friction can be measured in force and energy [43, 96].

2.2.3.1 Types of friction according to movement

Two types of frictional forces act between two surfaces: static friction and kinematic friction. Static friction occurs when the surfaces are at rest, while kinetic friction occurs when relative motion exists between the surfaces. Thus, when the solid body begins to move, the force of static friction has reached its maximum value. In the tribological field of application, friction is subdivided according to the type of movement. Accordingly, three main types of friction can be distinguished, depending on the type of relative movement of the contact partners [20, 43, 94, 97]:

- Sliding friction
- Rolling friction
- Drilling friction

Sliding friction describes friction between bodies whose velocities in the contact surface differ in magnitude and direction (figure 2.8). Rolling friction describes friction between bodies in point or linear contact, where the velocities in the contact surface are equal in magnitude and direction, and at least one body performs a rotational movement about an axis currently located in the contact surface (figure 2.8). A sliding component is superimposed in a particular type of rolling friction. Drilling friction (figure 2.8) is the friction between bodies in point contact (idealised) whose velocities in the contact

surface differ in amount and direction. In this case, at least one body performs a rotational movement about an axis perpendicular to the centre of the contact surface [93].

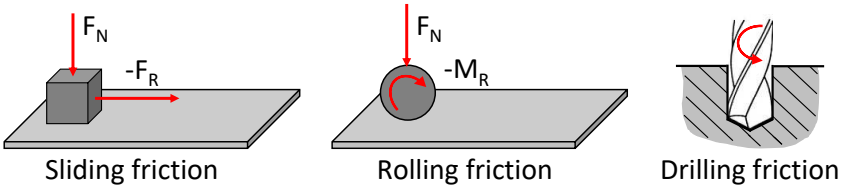

Figure 2.8: Sliding friction, rolling friction according to Kuhn [98] and drilling friction

2.2.3.2 States of friction according to the friction surface

According to DIN 50323-3 [99], the aggregate state of the intermediate material in the tribosystem is a criterion for classifying friction into friction states, i.e., solid, liquid, and gas. The last two can be combined as fluid. In addition, types of friction can occur combined, of which mixed friction is the best known [7, 43, 94, 97].

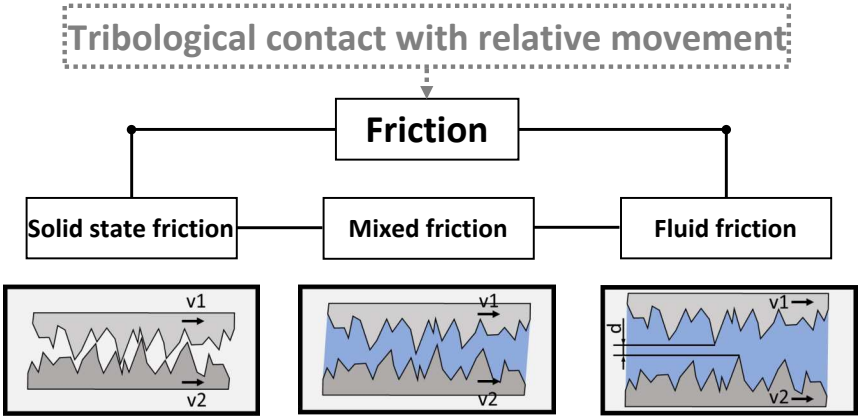

Figure 2.9: The three types of friction - solid friction, mixed friction, and fluid friction according to Kuhn [98]

In the case of solid friction, frictional forces occur when solid bodies are in

direct contact with each other (figure 2.9). Fluid friction is defined as friction occurring in the intermediate material area with fluid properties (liquid or gas). This state of friction is also valid for a hydrostatically or hydrodynamically generated fluid layer of matter that completely separates solids (figure 2.9). This condition is also valid for gases if a gapless separating gaseous film can be generated aerostatically or aerodynamically. Mixed friction is any mixed-form friction state, mainly that of solid and fluid friction (figure 2.9) [43, 93].

2.2.3.3 Friction mechanisms

When technical surfaces come into contact, locally and temporally stochastically distributed micro-contacts occur in the contact area, referred to as friction mechanisms. These elementary processes of friction inhibit movement and dissipate energy. If one assumes that each micro-contact represents a significant resistance to movement, then according to Czichos and Habig [43], the macroscopic friction force (F_R) can be approximately assigned to the number of micro-contacts, which in turn increases approximately linearly with the normal force F_N : $F_R \sim$ number of micro-contacts $\sim F_N$.

The friction mechanisms can be simplified into the following types (figure 2.10):

- Adhesion and shearing
- Plastic deformation
- Ploughing
- Elastic hysteresis and damping

Adhesion is an atomic or molecular friction mechanism based on the energy loss caused by the atomic or molecular conditions built up on the contact surfaces during relative motions. The most common cause of this adhesion is Van der Waals bonding or Van der Waals adhesion [43, 97, 100]. When tangential relative motion occurs between bodies, plastic deformation may occur caused by contact deformations. It can result in energy losses due to such dissipative processes [43, 97, 100]. When two bodies with different hardnesses are in contact, furrowing might occur. The more rigid surface roughness hills penetrate the softer opposing body in this process. When tangential displacement occurs, a friction component is produced by the material's resistance to the furrowing from the more rigid mating body. Furrowing can significantly affect

the friction component [43, 97, 100]. Elastic hysteresis and damping represent energy-dissipative friction processes in which mechanical motion energies are converted into other forms of energy. Most converted energy is released as heat [43, 97, 100]. As a rule, the various friction mechanisms are present at the same time, whereby the respective types and characteristics depend on the friction condition [97].

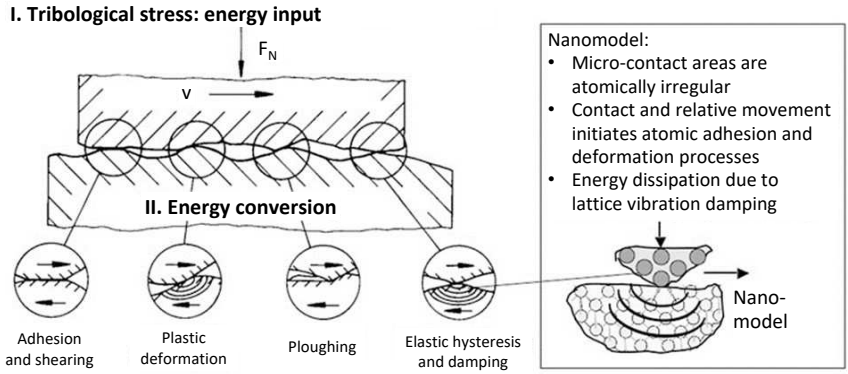

Figure 2.10: Friction mechanisms according to Czichos and Habig [43]

2.2.3.4 Friction measurement variables

Friction measurement variables are critical factors in understanding and assessing the interactions between surfaces in contact. These variables encompass parameters like frictional force (F_R), frictional torque (M_R), coefficient of friction (f or μ), and friction angle (ρ) – as well as surface roughness and lubrication conditions. The coefficient of friction quantifies the resistance to motion between two forces, with values ranging from 0 (no friction) to 1 (maximum friction). It is a dimensionless unit for the frictional force concerning the contact force (F_N) between two bodies [101].

$$f = \frac{F_R}{F_N} \tag{1}$$

The typical sliding friction value for a steel-on-steel pairing in an unlubricated state is $f = 0.10 - 0.12$. For a steel-on-steel pairing in a lubricated state,

on the other hand, the value is $f = 0.04 - 0.07$ [102]. Surface roughness influences friction by affecting the real contact area. Additionally, the presence or absence of lubrication significantly impacts friction, as it minimizes wear and heat generation [43]. Kuhn more explicitly defines lubrication as influencing friction due to the different energy inputs resulting from the solid surface's separation [7]. Precise measurement and control of these variables are essential in various industries, from automotive engineering to materials science, ensuring optimal performance and durability in mechanical systems [43].

2.2.4 Wear

Focusing strongly on pure solids, DIN 50323-2 [103] defines wear as progressive: *"loss of material from the surface of a solid body caused by mechanical causes, i.e. contact and relative movement of a solid, liquid or gaseous counter-body"* [103]. Fleischer provided another definition worth mentioning. He defines wear as *"a permanent change in shape, size and/or material of the material areas forming the surface of solids as a result of friction"* [95]. More recently, Kuhn defined general wear in the tribological system as *"a production of irreversibility resulting from frictional energy and includes all elements of a tribological system"* [7].

In technical terms, wear is considered undesirable under normal circumstances. Exceptions arise in running-in processes, as the wear process can help to fulfil the technical requirements. Technological machining processes that enhance the workpiece's value are not classified as wear despite tribological processes at the interface between the workpiece and the tool, which are typically associated with wear [93].

2.2.4.1 Types of Wear according to movement

Similar to the types of friction, wear is also classified according to types of wear in tribotechnical applications. Depending on the type of tribological system and the existing type of movement, the wear is divided into open and closed tribosystems. In primarily closed tribosystems, sliding wear and rolling wear occur analogously to friction. In addition, impact wear, vibration wear and groove wear (counter-body groove) may occur. On the other hand, furrow wear (particle furrow), jet wear and erosion (flow wear) are found primarily in

open tribosystems. All types of wear can furthermore be attributed to different proportions of wear mechanisms [20, 43, 93, 97].

During a sliding movement of stressed materials or components, wear processes are caused, the sequence and result of which is called sliding wear. Rolling wear appears when components or materials rotate or roll. When two solid bodies collide or impact, impact wear emerges, triggered by the impulsive, force-like and energetic interactions acting in the process. These interactions result in changes in shape (plastic deformation, crack formation) and material changes, which increase the reactivity of the stressed contact partners with the surrounding medium. In the case of vibrancy wear, wear occurs due to low relative movement between contact partners in a tribological system. The amplitude of the relative movement is usually smaller than the diameter of the existing geometric contact area [43].

In the course of grooving wear, either roughness hills of contacting counterparts (counter-body grooving; two-body abrasion) or hard particles (particle grooving; three-body abrasion) penetrate the surface areas of a stressed material or component.

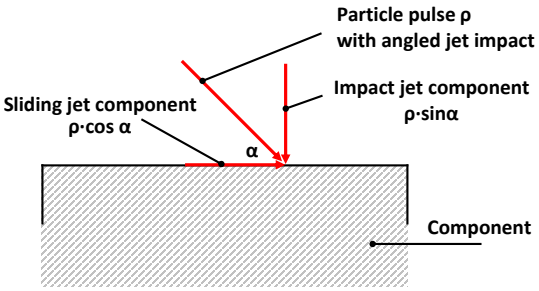

Figure 2.11: Particle impulse with angular jet wear and decomposition into impact jet and jet components according to Czichos and Habig [43]

As a result, scratches or grooves are created by abrasion processes. In abrasive blasting, a material or component surface is damaged by the impact of granular particles. Depending on the angle at which the particles strike the surface, jet wear (figure 2.11) can be divided into sliding jet wear $(\alpha \approx 0°)$, impact jet wear $(\alpha \approx 90°)$ and jet abrasion $(0° < \alpha < 90°)$. Erosion or flow wear caused by gas or fluid flows can cause damage to the material. This damage can be caused by the fluid itself or by particles in it. Different types of erosion result from the stressing medium (gas, vapour, liquid), the moving matter or a combination of all three. When classifying the types of wear, it should be noted that several wear mechanisms can be active simultaneously during the wear process. It means

that different forms of wear can occur with a single type of wear [43].

2.2.4.2 States of wear according to the wear surface

Wear conditions are described similarly to friction ones and are based on the physical condition of the material most affected by wear. The subdivision can be seen in figure 2.12.

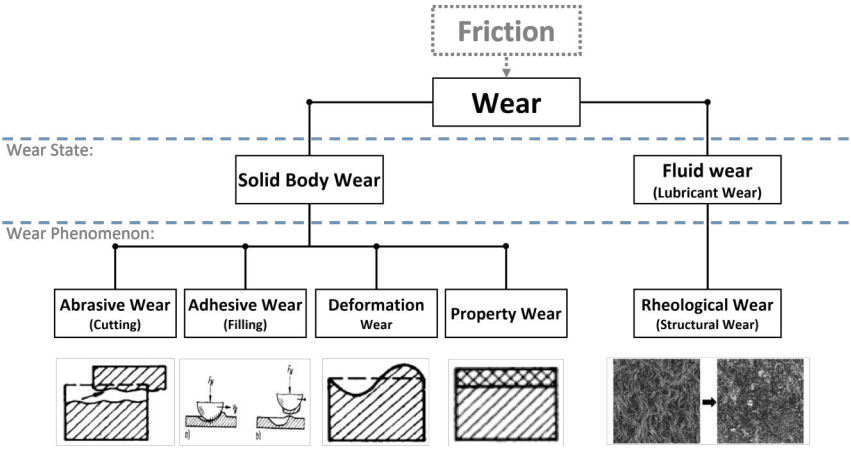

Figure 2.12: Classification of tribological wear into solid and fluid wear according to Kuhn and Fleischer et al. [7, 95]

Solid wear refers exclusively to wear on solid body surfaces due to friction and direct contact with asperities. The solid wear, according to the type of damage on the tribo-pair, is divided into abrasive, adhesive, deformation and property wear:

- Abrasive wear refers to material loss due to fracture or separation processes at submicroscopic, microscopic and macroscopic levels. It may include two-body and three-body abrasion [95]. Two-body abrasion occurs when hard particles or protuberances are forced against and move along a solid surface. Three-body abrasion occurs when the particles are not constrained and are free to roll and slide down a gradient.
- Adhesive wear is when two surfaces slide over each other under heavy load or pressure. Material is displaced from one surface and adheres to

the other during friction. It is common when the surfaces are of similar material.

- Deformation wear happens in contrast to abrasive and adhesive wear due to plastic deformation without material loss.
- Property wear refers to the friction bodies' altered physical and chemical properties due to increased internal energy. It is also known as corrosive wear when it occurs due to chemical or electrochemical reactions.

On the other hand, lubricant (grease) wear refers to the change of the lubricating grease structure in a tribological contact. Rheological wear , as described by Kuhn, includes the irreversible structural changes in material areas of a thixotropic lubricant due to tribological stress [7]. The wear states for liquid and mixed states are interpreted according to their specific properties.

2.2.4.3 Wear mechanisms

Wear mechanisms are physical and chemical interactions that appear on the mating surface due to the friction process. These interactions trigger elementary processes that ultimately lead to material and shape changes in the contact partners. A distinction is made between four main wear mechanisms: surface disruption (fatigue), abrasion, adhesion and tribochemical reactions (tribo-oxidation) [43, 93]:

- Fatigue and cracking in surface areas due to tribological alternating stresses are causes of surface disruption, leading to material separation and erosion, which is noticeable by the appearance of "dimples" [43, 93, 97].
- Abrasion is material removal that results from repeated furrowing and scoring stresses. There are two ways abrasion can happen: First, when hard particles are pressed into a tribologically stressed body, and second, when the mating body in tribological contact is significantly more rigid and rougher than the other [43, 93, 97].
- Adhesion refers to the formation of adhesive bonds at the interface between the base body and the mating body, whereby material interactions at the atomic level play a decisive role. When the adhesive bond is loosened, wear occurs outside the original interfaces, which is noticeable

in the material of the contact partner with the lower strength. Examples of such adhesive bonds are "cold welding" and "seizing" [43, 93, 97].

- In a tribochemical reaction, reaction layers or particles are formed by activated or promoted chemical reactions on or between the contacting surfaces between the elements of the Tribosystem [43, 93, 97].

Figure 2.13 shows all the wear mechanisms presented.

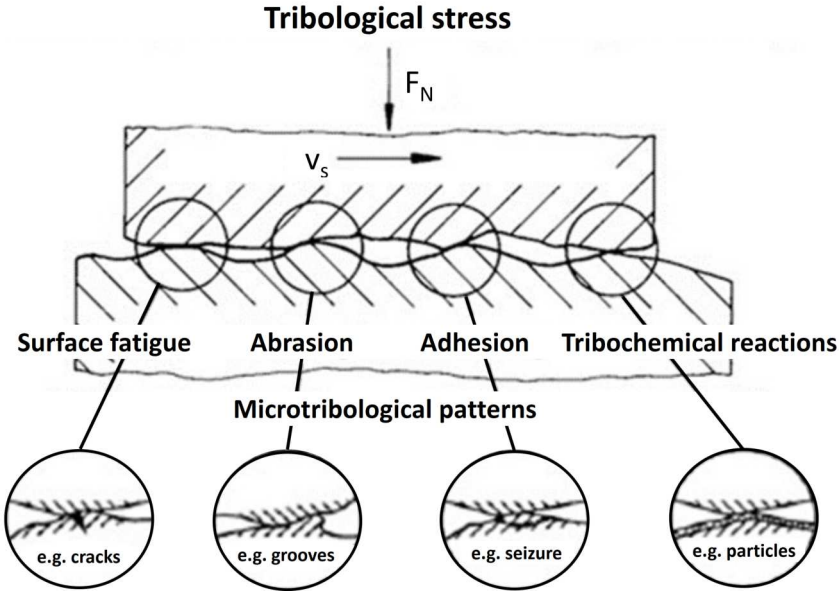

Figure 2.13: Basics of wear mechanisms according to Czichos and Habig [43]

2.2.4.4 Wear measurement variables

Wear parameters are used to quantify changes in the shape or mass of a body and the results of wear processes [43]. A distinction is made between direct, related and indirect wear measurement quantities [93].

Measured quantities that describe the change in mass, geometrical dimensions or volume of the wearing body are called direct wear measurement quantities. The amount of wear describes the change in length, area, volume or mass

of the wearing body [20, 93]. Measured quantities formed from the ratio of wear to reference quantities are called related wear-measured quantities or wear rates. Reference values are often the stress duration, path, or throughput [20, 93]. In the case of indirect wear measurement variables, the measurement is not aimed at determining wear-related changes in the geometrical dimensions or mass of the component or tribological system but rather at determining the point in time or throughput at which the functionality of the component or tribological system decreases [20, 93].

2.2.5 Tribological behaviour of lubricating greases

Kuhn [7] categorises greases' tribological performance into two distinct consideration levels. Firstly, grease behaviour impacts a higher-level tribological system involving three friction bodies (figure 2.7). Secondly, the characteristics of frictional grease and consequent wear behaviour are examined. Additionally, Kuhn [7] emphasizes that experimental studies primarily address these aspects.

When considering a grease volume element, the tribological behaviour describes the ability to lubricate a contact, whereby lubrication means the surface separation and absorption of the contact stress. Tribological behaviour refers to interactions concerning friction, wear, and lubrication. It should be described by the energy expended (friction) and the structural change (wear) [104]. Since this is essentially a phenomenon of flow and deformation, comprehensive rheological characterisations of greases provide helpful information. Through these, it is possible to look at their viscoelastic characteristics and structural degradation and understand lubricating grease behaviour under operating conditions [105]. It is noticeable that the performance of greases decreases due to chemical and physical degradation caused by extreme operating conditions (high or low temperatures), grease ageing and the shear stresses due to both the applied speed and the load [11]. Chemical degradation refers to the oxidation of the base oil and thickener. Physical degradation involves the destruction of the microstructure of the grease thickener, which results in an increased release of the base oil and a consequent change in consistency [11, 106, 107]. In his book, Kuhn [7] highlights, among others, the work of Kühl [108–110] and Karbacher [111–114], which deals with the investigation of grease in natural components and assemblies and its effects on their function and service life.

Another aspect is rheological wear, which was briefly described in Section

2.2.4.2. As the previous sections show, the available literature sources mainly explain that wear is decisively related to the geometric-material change of solid friction partners. However, lubricating greases are also characterised by a time-dependent tribological behaviour. Under tribological stress, we find that the material characteristics of grease are irreversibly changed. The change in material characteristics imitated due to friction (shear process) is called rheological wear [7, 115, 116] . Kuhn [7] defines rheological wear as: *"the irreversible change in the characteristics of stressed areas of a structurally viscous lubricant as a result of tribological stress"*.

2.3 Basic of Rheology

This section intends to explain the meaning and objectives of Rheology concerning lubricating greases. The term Rheology is derived from the Greek word combination rhei or rheo (ῥεῖν, in English: flow or stream) and lógos (λόγος, in English: Science) and thus means "Science of flow" [117, 118]. It primarily studies the flow of matter in a fluid state (liquid or gas), but also "soft solids" or solids under conditions where they respond with plastic flow rather than deforming elastically in response to an applied force.

Rheology applies to substances with a complex microstructure, such as muds, sludges, suspensions, polymers and other glass formers, lubricating greases, bitumen, and many foods and other biological materials. It involves the study of material properties under different shear stresses or strains besides pressure and temperature. Thus, Rheology is essential in many fields, such as materials science, pharmacy, the food industry, and the chemical industry, among many others [117, 118]. Rheology has roots in antiquity, with concepts that can be traced back to the Greek philosopher Heraclitus and the Jewish prophetess Deborah. However, it only came into prominence following the end of the Second World War. Notable figures such as Sir Isaac Newton and Robert Hooke are credited with setting the boundaries of modern Rheology hundreds of years earlier. Since the 20th century, Rheology has been regarded as a single discipline. However, even before then, many researchers were more or less scientifically involved with the behaviour of liquids and solids. For example, Markus Reiner (1931 and 1960) and George W. Scott Blair (1942) made attempts to classify all variants of rheological behaviour [117].

2.3.1 What is Rheology?

The term Rheology was significantly coined in 1920 by Eugene C. Bingham, a professor at Lafayette College and founder of the Society for Rheology in the USA, from a suggestion by a colleague, Markus Reiner. The term was inspired by the aphorism of Heraclitus, "panta rhei" (πάντα ῥεῖ), meaning 'everything flows'. He defined Rheology as the science of the deformation of materials in theory and the measurement of these properties in practice [119]. In 1949, Ludwig Prandtl provided the following definition in his work "Considerations on Rheology" [120]:

> *In the broader sense, Rheology can be defined as the study of the mechanical behaviour of deformable substances. Its range extends from almost solid substances to almost liquid ones; the substances can be homogeneous on the one hand but can also have any structures (macroscopic to submicroscopic) on the other. The objective of Rheology is to separate the mechanical properties into defined components and to determine the characteristic numbers of these components from measurements. Measurements of changes in shape and the corresponding forces provide means for this. The behaviour of the characteristic numbers with temperature variation is also necessary.*

Metzger [117] summarises the scientific discipline of Rheology as the *"study of the deformation and flow of substances"*. Rheology is a sub-discipline of physics that deals with science and technology and occurs when substances flow and deform under the influence of external forces. Rheology generally accounts for the behaviour of non-Newtonian fluids by characterizing the minimum number of functions needed to relate stresses with a rate of change of strain or strain rates [118].

2.3.2 Rheometry and Rheological tests

The experimental characterization of a material's rheological behaviour, i.e., the flow behaviour of liquids and viscoelastic materials, is known as rheometry. Rheometers are often used to perform continuous rotational or oscillatory movements. In both cases, there are two different operational modes, by specifying the rotational speed (controlled-shear rate, CSR) or by specifying the driving force (controlled-shear stress, CSS); in such modes, the reaction of a material to an applied shear rate or shear stress, respectively, is analysed. These experiments help investigate and determine the rheological properties of materials. These properties include, for example, viscosity, elasticity and

plasticity. In Rheology, there are three main types of rotational shear tests: steady-state flow tests, transient tests, and oscillatory tests.

- Steady State Flow Tests (viscous flow tests) involve applying a constant shear rate or shear stress to the material and measuring the resulting steady-state flow behaviour. It is often used to determine the viscosity of a material as a function of the shear rate.

- Transient Tests (shear stress growth tests) involve applying a step change in shear rate or stress and observing the material's response over time. Transient tests can provide information about the thixotropic behaviour and the material's relaxation time, which is the time it takes to return to its original state after deformation.

- Oscillatory Tests (small amplitude oscillation tests) involve applying an oscillating shear stress or strain and measuring the material's response. It used to be done inside the linear viscoelastic behaviour (LVE) to provide information about the material's viscoelasticity at an unperturbed structural state, describing its behaviour under viscous (flow) and elastic (deformation) conditions.

Each of these tests provides different insights into the rheological properties of a material, and the choice of test depends on the specific properties of interest [117]. The basic principle in all these tests is to place the material in a simple shear cell and apply a defined shear stress in a controlled way. The diagrams in figure 2.14 best illustrate shearing. Figure 2.14a shows two plane walls, where the lower one is stationary, and the upper one moves parallel to the lower one at a constant speed, U. The material adheres to both walls. The liquid's velocity $U(y)$ is zero at the lower wall and rises with increasing distance from the lower wall until it

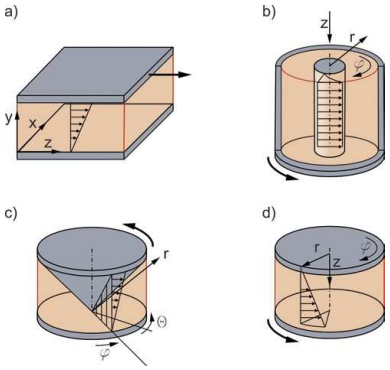

Figure 2.14: Shear possibilities of liquids and their application - a) plane and parallel plates, b) concentric annular gap, c) cone plate and plane base plate, d) circular plate and plane base plate [121]

reaches the velocity u at the upper
wall. A simple shear cell consists of a specific geometry (plate-plate, cone-plate, coquette cylinder and others) between which the material is placed. One of the surfaces is then moved at a controlled mode while the other remains static. Figure 2.14b-2.14d shows further possibilities for testing lubricants by rotational rheometry. For consistent substances such as lubricating greases, the cone-plate (CP) system (figure 2.14c) is often used, in which the shear stress occurring in the entire space between the cone and plate is constant [26]. The plate-plate (PP) system (figure 2.14d) is also frequently used, as the maximum particle size is not limited and variable measuring conditions can be specified by adjusting the measuring gap [118].

2.3.2.1 Transient tests: The time-dependent flow behaviour

Figure 2.15: Example of shear stress growth curve for a lubricating grease

For any thixotropic material, such as lubricating greases, the transient test is a useful rheological test to analyze how the shear stress behaves over time. It is often carried out at a constant shear rate, and, in the context of this research, it may be used to simulate the fluid friction condition in grease-lubricated tribological contacts [117, 118]. In their work, Kuhn [104], Delgado [105], and Czarny [122] describe the typical behaviour of greases in shear stress growth tests at specific shear rate values. Figure 2.15 shows the typical time evolution of the shear stress behaviour of lubricating greases, which may be correlated with the structural degradation over time. A stress overshoot is the maximum shear stress associated with the grease structure's elastic response. Immediately afterwards, the shear stress decreases continuously, which can be attributed to the grease's structural degradation and the resulting viscosity loss. Finally, the shear stress approaches an equilibrium value, representing a balance between the applied shear rate and the shear-induced residual stability of the microstructure [104, 123].

Depending on the grease specimen's consistency and the shear rate selected,

fracture and leakage phenomena can occur during transient tests, significantly affecting rheological results. Moreover, it is worth noting that rotational tests should be performance using rough surfaces to avoid undesirable phenomena such as wall slip [7, 28, 124].

2.3.2.2 Small amplitude oscillation tests (SAOS)

Small amplitude oscillation tests, performed within the linear viscoelastic region, are a type of oscillatory test used in Rheology. During these tests, a sample is exposed to a continuous sinusoidal excitation of either a deformation (controlled-strain mode) or a shear stress (controlled-stress mode). The deformation amplitude or shear stress varies while the frequency is kept constant (figure 2.16).

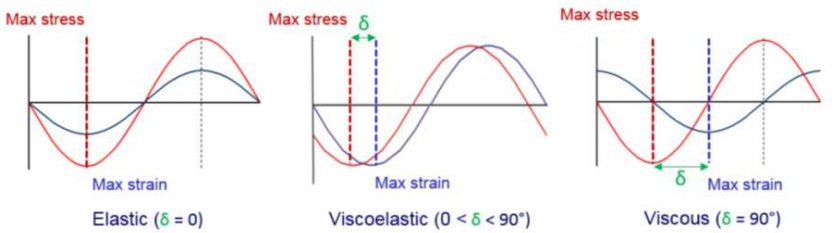

Figure 2.16: Stress and strain curve characteristics for elastic (ideal solid), viscoelastic and viscous (ideal liquid) materials [125]

The key benefit of small amplitude oscillation tests is that they are considered non-destructive when performed in the linear-viscoelastic (LVE) range. It means that the microstructure of the sample specimen was not disturbed or destroyed by the applied forces during the experiment. After exceeding this LVE limit, the behaviours are also interesting, as the deformation increases until the inner structure of the test sample collapses and begins to flow [118]. These tests determine the viscous and elastic properties of complex materials. In oscillation testing using a parallel plate measuring system, the sample is placed between plates with a known gap (h), and the upper plate oscillates at a given stress or strain amplitude and frequency. The motion is a sinusoidal wave, with stress or strain amplitude on the y-axis and time on the x-axis. An oscillating torque is applied in controlled stress measurement, and angular displacement is measured to calculate strain. In controlled strain experiments,

angular displacement is controlled, and the required torque is measured to calculate shear stress. The ratio of applied stress (or strain) to measured strain (or stress) yields the complex modulus (G*), a quantitative measure of material stiffness.

$$G^* = \frac{\sigma_{max}}{\gamma_{max}} \tag{2}$$

Viscoelastic materials exhibit a phase difference falling between these extremes (figure 2.16) [125]. The phase difference, represented by the phase angle δ, allows the determination of the viscous and elastic components contributing to the total material stiffness (G*). Depending on the sample type, the applied sinusoidal signal and the sample's response will show a phase shift, delta δ, between 0° (pure viscous behaviour) and 90° (pure elastic behaviour) [126]. Combining both characteristics, viscoelastic materials have a δ-value between 0 and 90°, with 45° indicating the boundary between solid-like and liquid-like behaviour [125]. In real life, most complex materials, like lubricating greases, show viscous and elastic behaviour, also known as viscoelastic behaviour. The elastic character is the ability to absorb mechanical energy from the outside and store it reversibly. At the same time, the viscous properties indicate that this portion of the energy is dissipated internally by irreversible conversion to heat [126].

Amplitude sweep test measurements are usually used for the rheological characterisation of complex materials to characterise the linear viscoelastic behaviour (LVE behaviour). For amplitude sweep tests on the rheometer, a sample specimen is sheared between an oscillating plate and a fixed plate, gradually increasing the amplitude of the oscillation at a constant frequency. The measurement results are then usually represented by the storage modulus (G') and the loss modulus (G'') on the ordinate against the deformation on the abscissa (figure 2.17). The storage modulus G' represents the elastic component of the viscoelastic response and reflects the reversibly stored deformation energy. Conversely, the loss modulus G'' describes the viscous component and provides information about the irreversibly expended energy. Usually, G' and G'' are constant at low deformation in the diagram's first area, called the linear viscoelastic range (LVE). In this range, the complex materials are still below their yield stress, behave like viscoelastic solids, and their structure remains undisturbed [117, 118]. According to DIN 51810-2 [127], the limit of the LVE range is defined by a change in G' or G'' of more than 10 % compared to the LVE plateau values. This "critical point" (γ_y) is marked by the first dashed

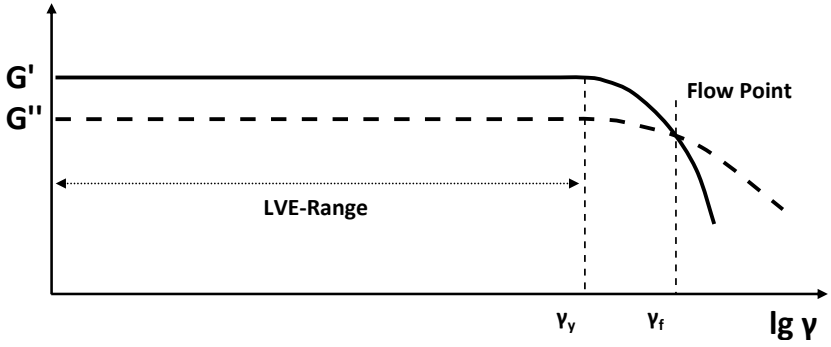

Figure 2.17: Example of a strain sweep test curve

vertical line in figure 2.17. At this point, the critical energy level is reached, where the structural degradation of the sample structure begins.

The SAOS test is also beneficial for investigating lubricating greases' storage behaviour and shelf-life stability. These measurements have established themselves as an essential investigation method for lubricating greases, which can be tested more intensively with the help of oscillatory measurements than with conventional measurements of grease consistency. In addition, amplitude sweep tests allow the yield stress to be determined as the value of the shear stress at the boundary of the LVE range [117, 118]. According to DIN 51810-2 [127], the limit of the LVE range is defined by a change in G' or G'' of more than 10 % compared to the LVE plateau values. This "critical point" (γ_y) is marked by the first dashed vertical line in figure 2.17. At this point, the critical energy level is reached, where the structural degradation of the sample structure begins. The crossing point (γ_f) of G' and G'' or yield point is marked by the second dashed vertical line. The sample structure has significantly changed, so the grease begins to flow [117, 118]. This point engages an energetic consideration, as the energy expended to reach the crossing point of G' and G'' can indirectly indicate sample structure degradation.

2.3.3 Rheological behaviour of lubricating greases

As briefly explained in the previous section, lubricating greases are viscoelastic materials exhibiting elastic and viscous characteristics depending on the ap-

plied stress. A relationship between the elasticity and the internal microstructure formed by the thickener can be observed. These unique characteristics help the grease stay in contact with the surfaces and move without leaking out of the tribological contact. In addition, the elasticity of the greases helps to store elastic energy. Conversely, the base oil determines the viscosity characteristics that allow the grease to flow under shear [7]. In the simplest form, the viscosity is linked to the base oil and the elasticity to the internal structure built up by the thickener [16].

In his book, Kuhn [7] characterises the rheological behaviour of greases by three criteria:

- With an increasing velocity gradient, the viscosity shows a decreasing course, which means that a structurally viscous, i.e. shear-thinning, flow behaviour is present.
- Lubricating greases can generally be described as thixotropic, as the viscosity decreases with increasing shear time. However, since lubricating greases do not regain their initial viscosity even after a longer resting time, they behave in a non-genuine thixotropic manner.
- In addition, lubricating greases have a yield point that must be overcome before they flow.

It should also be emphasised that the consistency and viscosity of lubricating greases are time-dependent properties. The intrinsic time of the flow behaviour of lubricating greases must always be included in a comprehensive rheological description of the material. This time dependency arises because lubricating greases are a thixotropic material. Even the elastic properties can determine the occurrence of normal stresses during the shearing movement of the grease [16].

In [16], the rheological behaviour of lubricating greases is summarised as follows: Under external deformation applied, the solid appearance of lubricating greases can break. The grease deforms plastically under a sufficiently high shear rate and flows as a liquid. Typically, lubricating greases exhibit shear-thinning properties, characterized by an asymptotically high constant value of viscosity at a zero shear rate and a non-linear function of viscosity with the increase of shear rate. At a high shear rate, the structure is permanently destroyed. This damages not only the weaker formations of the structure but also the more robust network. In addition, lubricating greases become thinner over time, decreasing the thickening effect.

Delgado and Franco carried out important work investigating the rheology of lubricating greases. Among other things, they dealt with the subtleties of thermorheological behaviour, steady-state flow, transient shear flow and the influence of various factors on the friction process and the microstructure of lithium greases [28–30, 105, 106, 123]. Delgado et al. [30] investigated the relationship between microstructure, rheology and the production of lithium lubricating greases. The focus was on the formation of the grease microstructures during the manufacturing process. It was found that lithium lubricating greases are highly structured systems based on a three-dimensional network due to the presence of metal soap crystallites. Also, Delgado et al. [105] investigated the shear-induced evolution of the grease microstructure in the transient shear flow analysis of model lithium lubricating greases. The results successfully described the transient stress behaviour and clarified the influence of soap concentration and oil viscosity on the elastic properties of lithium greases. Later, Delgado et al. [123] established empirical correlations between rheological parameters and the friction factor determined with a ball-and-disc tribometer. These provide information about the relationship between rheological behaviour and the friction process. Energetic evaluations of structural degradation during friction were carried out, whereby the storage and boundary energy density were correlated with the friction factor. Furthermore, the study by Delgado et al. [28] on the steady-state flow and yielding behaviour of lubricating greases showed that it was difficult to achieve proper steady-state flow conditions due to the thixotropic behaviour, among other phenomena. Accordingly, the study focused on understanding the microstructural features and their influence on the flow behaviour. Sánchez et al. [71] and Hamnelid [16] stated in their work that investigations of the rheological behaviour of greases have a significant effect on predicting their flow and deformation behaviour under operating conditions. They all contributed to understanding the microstructure of lubricating greases and the grease-reactive processes in the tribological system [16, 71].

Studies help better understand the influences of thickener concentration, base oil viscosity and temperature on the rheological characteristics of lubricating greases by providing valuable behavioural information [29, 106, 128–132]. Delgado et al. [29] showed the effects of thickener concentration and base oil viscosity on the rheology of greases. They also investigated their correlation with the microstructure of the grease. They found that an increase in thickener concentration leads to a more compact or interwoven microstructural network and, thus, to an increase in the values of the viscoelastic functions

in the linear viscoelastic range. The balance between the solubility of the thickener in the base oil and the entanglement of the soap fibres was identified as a decisive factor influencing the network of the lubricating grease [29].

In their study on thermorheological behaviour, Delgado et al. [106] investigated the effects of thermally induced changes on the viscous and viscoelastic behaviour of lithium lubricating greases. Among the most important results was a critical temperature of 110 °C, above which a drastic drop in the linear viscoelasticity functions was observed, indicating a thermal susceptibility of the lubricating grease. The effect of temperature on the flow behaviour of lubricating greases is similar to that of lubricating oils [7]. Mader [25] provides the following principal reasons for this - on the one hand, an increasing temperature changes the solubility of the metal soap in the base oil. On the other hand, the viscosity of the base oil decreases, and a change occurs in the crystal lattice. These interlinked studies contribute to a comprehensive understanding of the complex interplay between microstructure, rheology and performance characteristics of lubricating greases and provide valuable insights into the field.

2.4 The structural degradation of lubricating greases

In Tribology, the behaviour of greases under lubricating conditions, especially the effects of viscoelasticity on the friction process, is an ongoing problem. One way to solve this problem is to characterise the rheological properties of greases. Structural grease degradation, i.e., grease wear, can be divided into chemical and physical degradation [11, 12]. Chemical degradation mainly involves oxidation reactions, i.e. the oxidation of the base oil and the thickener, as well as the degradation of additives [11, 133]. Physical degradation includes destroying the thickener structure by mechanical stress, referred to as mechanical degradation of the grease. Oil separation is also included in physical degradation, resulting from oil evaporation at high temperatures or increased bleed rate and oil leakage [11–13]. Figure 2.18 shows that chemical degradation predominates at high operating temperatures, whereas mechanical degradation usually dominates at high speeds (shear rates) and low operating temperatures [11, 13, 14]. In this thesis, the focus is entirely on the mechanical

degradation of lubricating greases under shear stress.

Various studies have already been carried out on the friction process of grease-based lubricants using rheological measurements. Delgado et al. [123] and Kuhn [115] determined that in a friction process, the elastic deformation of the grease, the reversible alignment of the thickening particles and the final, irreversible dispersion of these particles in the oil are due to the progressive changes in the grease structure. Friction can be understood here as the supply (storage) and removal (loss) of energy in the tribosystem, and heat generation and wear are related to the dissipation of this energy [135]. Through stress growth (transient) experiments, an approach to investigate the structural degradation of lithium greases could be developed [123]. It was observed how a decreasing energy expenditure occurred during the shear process until a steady-state non-equilibrium condition was reached. It demonstrated that the intrinsic striving of energetically stressed systems results in mechanical degradation [135, 136]. The stressed grease is accordingly forced into an unstable state, striving for a way to release itself energetically. Changing the grease structure is one way to achieve stability and minimise energetic gradients.

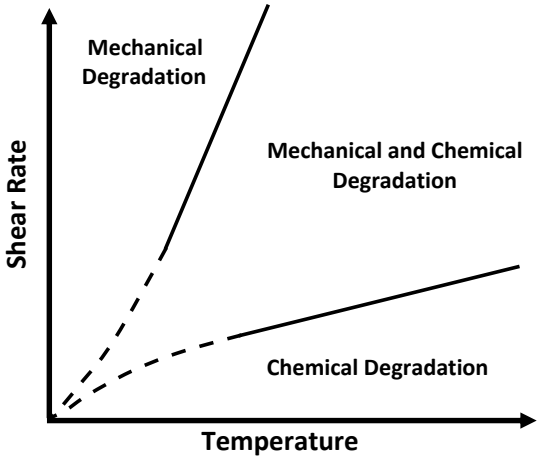

Figure 2.18: Grease degradation related to temperature [134]

Other researchers [12, 68, 87, 137–139] used different approaches to better describe grease structural degradation. Paszkowski and Olsztynska-Janus [87] used a rheometer to demonstrate how H-bonds between Li soap fibres are destroyed by shear stress. To define the mechanical degradation of greases, Rezasoltani and Khonsari [12] characterised the structural degradation of greases. They showed through penetration measurements that the shear process breaks

down the grease structure and leads to heat production, with simultaneous heat conversion caused by the structural degradation generating entropy. A comprehensive investigation from a thermodynamic point of view was carried out by Osara and Bryant [137]. They described the so-called degradation coefficient for lubricating greases as a correlation between the entropy generation rate and mechanical degradation. They used the degradation-entropy generation theorem and related it to the phenomenological entropy generation in stressed greases. Furthermore, Bryant, Khonsari and Ling [138] quantitatively described the structural degradation caused by mechanical energy. For this purpose, they introduced the term "degradation coefficient" for the first time, which describes the general relationship between thermodynamic and degradation-inducing forces. It makes it possible to determine the degradation rates based on the entropy concept and the degradation process instead of process variables. Roman et al. [68] use AFM and SEM images to show that the shear rate and shear time influence the microstructure of the grease. Zhou developed a master curve in his work [14], which includes the softening of greases as a function of shear rate, temperature, time, and the use of applied energy density. Chatra et al. [32, 140] determined that the grease's rolling bearing performance depends on the grease microstructure's flexibility and ability to rearrange. In addition, they performed an analysis of grease degradation using a temperature-corrected dissipated energy density approach.

From all these findings, three fields of research emerge with which this work is concerned. Firstly, the mechanical degradation of lubricating greases was observed from the point of view of the changes in the structural skeleton confirmed by the thickener as a result of the applied shear stress using rheological tests and the influence of the thickener (type and composition) and the base oil on the degradation process was investigated [79]. Furthermore, how greases behave in terms of heat development inside the bulk of grease was investigated. For this purpose, heat dissipation in a grease volume during the friction process was observed and evaluated in relation to the composition of the base oil and the thickener [141]. In addition, optical investigations visualised the structural changes of lubricating greases in more detail. For this purpose, different techniques such as optical light microscopy, scanning electron microscopy (SEM) and atomic force microscopy (AFM) were used to visualise the structural details at the micro and nano scale [73]. The following two sections deal with the derivation of the research gap. The aim is to provide an in-depth understanding of why this gap exists in the current research literature and how it has developed in the context of the research

field.

2.4.1 Shear-induced frictional energy calculation in rheometer tests

The research on energy translation components in the friction process and the cause-effect chain of friction and wear, which was started in the 60' of the last century, led to the development of an energetic approach in the 70' and 80', which can be applied to many problems [7]. Thus, friction is composed of two energetic parts. The energy needed to overcome the overlap is friction's mechanical or deformation component, and the energy needed to separate material bonds is the molecular part of friction. This energetic approach is essential to drawing conclusions about the longevity and reliability of friction couples based on the calculation of friction and wear. The basis of the energetic approach is based on the dual nature of friction [95]. According to the traditional energetic approach of Fleischer, friction's dual nature consists of Deformation and Adhesion.

In order to investigate the mechanical degradation of greases as regards changes in the structural skeleton as a result of the applied shear stress, a shear-induced friction energy calculation was conducted. For this purpose, data from rheological tests (rotational and oscillatory mode) were used to determine the energy released under shear stress. The energy described refers to the shear-induced frictional energy arising from shear forces within the grease. It occurs due to a structural rearrangement process, quantified as mechanical work. The rotation mode in the rheological tests was used to simulate flow conditions. The energy applied during the test leads to structural degradation of the grease lubrication structure, part of which is dissipated as heat. The shear-induced structural changes are influenced by the type and composition of the thickeners and the base oil. On the other hand, the oscillation measurements are used to analyse the previously applied mechanical work and the resulting structural changes [79]. The detailed calculations of the mechanical work for both the rotation (structure degradation) and the oscillation (unchanged structure) tests are described in the following equations. The method proposed by Yuxn Zhou [14] was engaged to calculate the mechanical work, W_R, delivered to the sample during the rotational test at a constant shear rate (equation 3).

$$W_R = \int_{t_i}^{t_{i+1}} \frac{M_{di} \cdot n_i \cdot 2\pi}{60} dt \tag{3}$$

The rheological test was designed to record a torque value every 15 seconds throughout the study (7200 s). Consequently, equation 3 was solved by considering a constant time segment of 15 seconds. Therefore, by individually considering each time segment with its measured torque value, the total mechanical work during the transient test of viscous flow for 7200 seconds can be calculated as the sum of all time segments, as illustrated below:

$$W_R = \int_{t_i}^{t_{i+1}} \frac{M_{di} \cdot n_i \cdot 2\pi}{60} dt = \sum_{i=1}^{m} \frac{M_{di} \cdot n_i \cdot \pi \cdot \Delta t_i}{30} \tag{3.1}$$

With:

M_{di} = Measured Torque [Nm]

n_i = Rotational velocity [min^{-1}]

Δt_i = Segment of time [s] (corresponding to each measured point)

m = total number of segments of time within the full-time range studied

In addition to the approach used in the work by Ahme et al. [79], there is another way of calculating the mechanical work in the rotation test. As the work is applied to the sample as a rotational movement, it can also be calculated using the mechanical rotational power approach [142].

$$P = \frac{W_R}{t} \tag{4}$$

Rearranging according to W_R results in:

$$W_R = P \cdot t \tag{4.1}$$

With:

$$P = M_d \cdot n \cdot 2 \cdot \pi \tag{4.2}$$

It follows:

$$W_R = M_d \cdot n \cdot 2 \cdot \pi \cdot t \tag{4.3}$$

With:

M_d = Measured Torque [Nm]

n = Rotational velocity [min^{-1}]

t = Segment of time [s]

Both calculation approaches provide identical results.

As mentioned, oscillation tests are widely used to assess the viscoelastic characteristics of lubricating greases directly linked to their structural attributes [29]. Within this test, particular emphasis was placed on the intersection of G' and G", marking the transition point from solid-like to liquid-like behaviour, essentially the point where the grease shifts from solid to liquid dominance. Consequently, it provides insights into structural degradation from prior shear conditions and its impact on viscoelastic behaviour.

Calculating mechanical work in the oscillation test is notably more intricate than in the rotational test. This complexity arises from the absence of an applied shear rate coupled with the test operating through sinusoidal oscillations. As a result, the output values for shear rate $\dot{\gamma}$ and torque M_d consistently reach their maximum. Nonetheless, a method has been proposed to ascertain the mechanical work during this test, estimating the effective shear rate from equation 5:

$$\dot{\gamma} = C_{SR} \cdot n \tag{5}$$

With:

$\dot{\gamma}$ = Shear rate [s^{-1}]

C_{SR} = Conversion factor shear rate [s^{-1}/min^{-1}]

n = Rotational velocity [s^{-1}]

The conversion factor C_{SR} for the specific grooved plate-plate geometry employed was determined using the prescribed standard procedure outlined by

Anton Paar, involving a calibration fluid. Consequently, the rotational velocity n is derived from equation 5.1.

$$n = \frac{\dot{\gamma}}{C_{SR}} \tag{5.1}$$

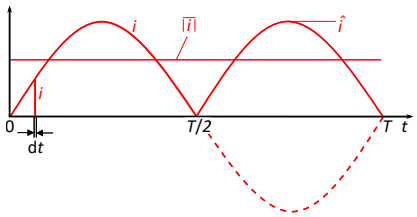

Figure 2.19: Sine current curve for a rectified value [143, as cited in 79]

The recorded values of the shear rate $\dot{\gamma}$ and torque M_d represent the maximum values (peak values) achieved during the sinusoidal movement. An approach commonly used in electrical engineering was applied to still use these values in our model. Consequently, a rectified value is determined for a sinusoidal current. This corrected value represents the mean value obtained from integrating the magnitudes of the sine wave [143]. Figure 2.19 aims to provide a more detailed diagram of this scenario. The sine curve depicts the second oscillation (dotted) mirrored upward. In the figure, $\widehat{i}$ represents the peak value and $\left|\bar{i}\right|$ signifies the rectified value. The following formula provides the ratio of the rectified value to the peak value:

$$\frac{\left|\bar{i}\right|}{\widehat{i}} = \frac{1}{T}\int_0^T \left|\sin\left(\omega t\right)\right| d\left(\omega t\right) = \frac{2}{\pi} \sim 0.6366 \tag{6}$$

In this thesis, the values obtained from the rheometer are peak values, specifically the shear rate $\widehat{\dot{\gamma}}$ and the torque $\widehat{M_d}$. However, rectified values are necessary to calculate the mechanical work during the oscillation test. These values were calculated from equations 6.1 and 6.2, respectively:

$$\left|\overline{\dot{\gamma}}\right| = \widehat{\dot{\gamma}} \cdot \frac{2}{\pi} \tag{6.1}$$

$$\left|\overline{M_d}\right| = \widehat{M_d} \cdot \frac{2}{\pi} \tag{6.2}$$

Therefore, employing the adaptations mentioned above, it is possible to effectively calculate the mechanical work during the oscillation test using equa-

tion 3.1. It is essential to note that, in this scenario, the time segment is not consistently fixed at 15 seconds, unlike in the viscous flow transient test; it varies.

$$W_{CP} = \int_{t_i}^{t_{i+1}} \frac{\left|\overline{M_d}\right| \cdot \frac{\left|\overline{\dot{\gamma}}\right|}{C_{SR}} \cdot 2\pi}{60} dt = \sum_{i=1}^{m} \frac{\left|\overline{M_{di}}\right| \cdot \frac{\left|\overline{\dot{\gamma}}\right|}{C_{SR}} \cdot \pi \cdot \Delta t_i}{30} \tag{6.3}$$

With:

$\left|\overline{M_{di}}\right|$ = Rectified Measured Torque [Nm]

$\left|\overline{\dot{\gamma}_i}\right|$ = Rectified Shear rate [s^{-1}]

C_{SR} = Conversion factor shear rate [s^{-1}/min^{-1}]

Δt_i = Segment of time [s] (corresponding to each measured point)

m = total number of segments of time within the full-time range studied

Based on the energetic approach to the structural degradation of greases, this thesis work has developed a parameter (R_{tee}) for the holistic interpretation of the mechanical energy expended in the stressed grease and thus involved in the structural degradation. For this purpose, the ratio of two mechanical energies is used. In the numerator is the mechanical energy expended to start and maintain the grease degradation process (W_{CP}), and in the denominator is the mechanical energy expended for structural degradation achieved in the transient viscous yield test at a given shear rate (W_R).

$$R_{tee} = \frac{W_{CP}}{W_R} \tag{7}$$

The decisive factor here is that a higher shear rate introduced more mechanical energy into the grease and thus destroyed the structural skeleton more during the viscous flow transient test. As a result, the crossing point in the oscillation test was reached more quickly. In other words, the greater the ratio of energy applied (R_{tee}), the less the structural damage to the stressed grease [79].

2.4.2 The internal friction-dependent temperature changes

It is well known that temperature has a strong influence on the viscosity and viscoelasticity of greases [144]. At the same time, viscoelasticity greatly influences the grease's friction process under fluid friction conditions [145]. Different studies on temperature investigation have different approaches. In most cases, heat is applied to the system externally [106, 139, 146–148]. Delgado et al. [106] identified a critical temperature of 110 °C in their studies on lithium greases, at which the grease's viscoelastic behaviour (i.e. plateau modulus) decreases drastically. Pan et al. [147] concluded that short thermal ageing of greases at 120 °C for 2 to 24 hours leads to a decrease in the cross-linking of the microstructure and especially the strength of the fibre skeleton structure. They pointed out that it is not the chemical composition but the physical interlacing strength responsible for the change in lubrication performance after this short-term heat treatment. Zhou et al. [139] developed a master curve for the ageing of greases with the help of a self-built Couette ageing machine. They investigated the influence of temperature and shear on the mechanical ageing of fibrous greases. They discovered that an increase in temperature accelerates shear degradation. A model to study greases at different shear rates and temperatures has been developed by Rezasoltani and Khonsari [146]. In this model, explicit entropy generation is used to predict the degradation of grease consistency under mechanical shear. In order to avoid chemical degradation or evaporation of the base oil, they restricted themselves to temperatures of 25 °C to 45 °C. Thus, mechanical degradation is the predominant process in this model. Only Osara and Bryant [148] performed differentiated temperature measurements to provide a pure heat effect analysis to evaluate thermal entropy generation. They combined primary thermal energy and thermodynamics with the degradation-entropy generation theorem. For this, they used the results of their study [137]. The study measured temperature using a motorised paint mixer (stirrer) with three thermocouples attached at different locations in the mixing vessel to record the temperature under shear conditions.

This thesis aims to provide information on heat dissipation during the process of friction in a lubricating grease volume [141]. The focus is on converting mechanical energy into heat as a function of the composition of the base oil and the thickener. In this context, a theoretical investigation of the grease temperature in the measuring gap was also carried out. The following approach

is designed as a theoretical temperature determination and is not intended to serve as a model. Instead, it is intended to be used later to compare experimental observations with theoretical predictions and to validate the results obtained. Although it is primarily based on the 1st Law of Thermodynamics, the heat transfer rate into the grease was not considered.

$$Q_{12} + W_{12} = U_1 - U_2 \tag{8}$$

With:

Q_{12} = quantity of energy supplied to the system as heat [J]

W_{12} = amount of thermodynamic work done by the system [J]

$U_1 - U_2$ = change in the internal energy of a closed system [J]

For the sake of simplicity, this approach assumes that the system has no heat transfer with the environment. Therefore, the system has been described as:

$$Q_{12} = 0 \tag{8.1}$$

However, it should be noted that despite using a climate chamber (bonnet), it is impossible to avoid heat exchange with the environment completely. Thus, it was stated that:

$$W_{12} = U_1 - U_2 = m_i \cdot c_i \cdot (T_1 - T_2) \tag{8.2}$$

With:

Q_{12} = quantity of energy supplied to the system as heat [J]

W_{12} = amount of thermodynamic work done by the system [J]

$U_1 - U_2$ = change in the internal energy of a closed system [J]

m_i = sample mass [g]

c_{pi} = sample specific heat capacity [J/(g·K)]

$(T_1 - T_2)$ = sample temperature change [K]

Rearranging according to ΔT results in:

$$\Delta T = \frac{W_{12}}{m_i \cdot c_{pi}} \tag{8.3}$$

Where:

$$m_i = \rho_i \cdot v_i \tag{8.4}$$

and:

$$W_{12} = W_R = \int_0^{15} \frac{M_d \cdot n \cdot 2\pi}{60} dt = \frac{M_d \cdot n \cdot \pi}{2} \tag{8.5}$$

Utilizing equation 8.3 facilitates the straightforward calculation of the corresponding theoretical temperature change value for each measuring point in the investigation. It is important to note that the theoretically derived temperature curves are not intended to replicate the experimentally obtained temperature curves but rather serve as a tool to enhance the result evaluation.

3 Materials and Experimental Methods

The following chapter describes the materials and the experimental methods used in this thesis. In addition, it contains information about the sample preparation, the instruments used, and the measurement methods used to obtain the results of this thesis. Thus, this chapter provides the basis for replicability and enables the readers to reproduce the experiments and verify the study results.

3.1 Materials

Eleven different lubricating greases, kindly provided by Fuchs Europe Schmierstoffe (Mannheim, Germany) and Fuchs Lubritech (Kaiserslautern, Germany), were studied. They differ in the base oil's type and viscosity and the thickener agent's type and concentration. These lubricating greases can be divided into two groups: one consists of traditional greases based on metal soap and polyurea (C1-C7); the second group consists of newly developed, purely biogenic greases based on vegetable oil and various combinations of biogenic thickeners (B1-B4). Deliberately, no additives were added to either group of greases to exclude other possible effects on the grease behaviour (i.e. temperature behaviour, structural degradation). The compositions of the eleven model greases used and their basic properties are shown in tables 3.1 and 3.2.

The conventional model greases with conventional thickeners (C1-C7) were prepared following the manufacturing protocol described by Delgado et al. [29]. The combination of base oil (type and viscosity) and thickener agent (type and weight concentration) was chosen because these parameters influence the microstructure skeleton and rheological behaviour of lubricating greases. It is worth pointing out that the lubricating greases produced belong to NLGI group 2, so the soap concentration varies. The changing soap concentration influences the consistency of the greases, but the influence on the

rheological behaviour is proportional and can be controlled [29].

Table 3.1: Composition and primary technical data of conventional lubricating grease samples studied

Lub. Grease	Thickener type	NLGI-grade	Thickener concentration [%]	Base oil	Base oil viscosity at 40°C [mm²/s]	Dropping point [°C]
C1	Lithium-12-hydroxystearate	2	16.1	Castor oil	240	≈ 190.11
C2	Lithium-12-hydroxystearate	2	10.6	PAO	240	≈ 210.50
C3	Lithium-12-hydroxystearate	2	13	PAO	48	≈ 208.48
C4	Lithium-12-hydroxystearate	2	9.5	Mineral oil	240	≈ 206.49
C5	Calcium-12-hydroxystearate	2	9.7	Castor oil	240	≈ 142.05
C6	Calcium-12-hydroxystearate	2	22.8	PAO	240	≈ 150.87
C7	Polyurea	2	19.6	PAO	240	≈ 296.91

The group of purely biogenic lubricating greases shown in table 3.2 were selected from a wide range of newly developed biogenic greases obtained in the TriBioGen research project by Acar et al. [65, 66]. The most promising ones compound this group (samples B1-B4) .

Table 3.2: Composition and primary technical data of pure biogenic lubricating grease samples studied

Lub. Grease	Thickener type	NLGI-grade	Thickener concentration [%]	Base oil	Base oil concentration [%]	Base oil viscosity at 40°C [mm²/s]	Dropping point [°C]
B1	Cellulose	1	1.5	Glycerine Glyceryl-monooleate	88.5 10	227.4 120.1	<≈ 100
B2	Polyhydroxy butyrate Ethylcellulose	0-1	5.3 7.7	MCT oil Castor oil HOSO	55 22 10	14.7 258.3 46.2	≈ 80
B3	Beeswax Glycerol monostearate Cetyl alcohol	00	7 5 2	HOSO Castor oil	50 36	46.2 258.3	≈ 45
B4	Chitosan Phosphoric acid (85%) Calcium hydroxide Glyceryl monostearate	1	2.35 4 3.15 5.1	Glycerol Sorbitan-monooleate	49.6 35.8	227.4 445.2	≈ 150

3.2 Rheological measurements

A stress-controlled rheometer, model MCR 302 (Anton Paar, Austria), carried out all rheological measurements. To ensure constant temperature conditions, an environmental control chamber (Anton Paar - Peltier systems with TruGap™) was supplemented to the rheometer in all experiments to prevent external influences such as heat loss due to draughts or other environmental influences. While the testing conditions for grease on the rheometer may vary considerably from the real operational settings, they can still offer valuable insights into the shear stresses experienced by the grease. Nevertheless, Kuhn [7] and Delgado et al. [28] state that undesirable phenomena such as wall slip and leakage can occur during rotational tests, significantly affecting the rheological results. Therefore, for each test procedure, special attention was paid to the choice of the measurement system and the selection of the maximum shear rate.

Three repetitions were performed on fresh samples for each grease to achieve high accuracy of the results for all rheological tests. Subsequently, a mean value was calculated for all results of these three repetitions. The results show statistical significance with a confidence level of 95 %.

3.2.1 Rheological test to analyse the expended energy on structural degradation

A combination of stress growth transient and strain sweep tests were performed to analyse the expended energy on structural degradation for all lubricating greases studied. A grooved plate-plate geometry of 25 mm diameter was chosen as the measuring system to prevent wall slip phenomena [7, 28]. A gap of 1 mm was set, and all tests were carried out at constant temperatures of 40 °C and 80 °C. In all measurements, the torque and the rotational speed were recorded each second, along with other parameters, and used to determine the mechanical energy.

The experimental procedure was conducted in three successive steps (figure 3.1). Firstly, all samples were kept at rest time for 900 s, such as all grease volumes achieving the specific temperature and eliminating the previous mechanical history. Previous analysis determined that a rest period of 900 s was enough to eliminate the previous mechanical history due to the specimen's placement. In the second test section, the grease samples were submitted to a stress growth transient test for 7200 s, at a constant shear rate within the

range from 0 to 1000 s^{-1}, to induce structural changes under fluid friction-friendly conditions. This long period was chosen to achieve a steady state condition for all greases investigated. Higher shear rates than 1000 s^{-1} were not considered, as leakage phenomena were observed above these shear rates. Finally, in the third test section, a strain sweep test was performed in oscillation mode at a constant frequency of 1 Hz, within the strain range from 0 to 100 %. This oscillation test determined the shear-induced structural degradation rate in the previous rotation test by analysing the strain range below the crossing point of G' and G'' (frequency at G'=G''). The equation for the basic shear-induced frictional energy calculation is described above in Section 2.4.1. The energy expended to reach the crossing point of G' and G'' is an indirect indicator of the structural degradation of the grease. For comparison, the strain sweep test in oscillation mode was also performed on all fresh greases.

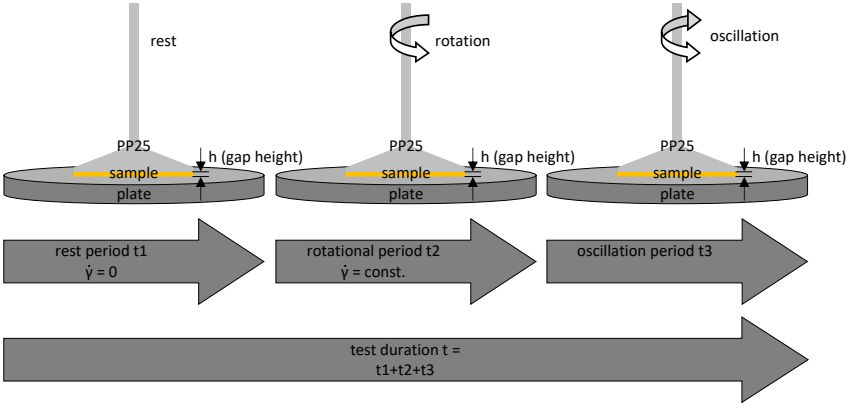

Figure 3.1: Schematic illustration of the experimental procedure - to evaluate the energy used for the structural degradation of lubricating greases [79]

3.2.2 Rheological test to analyse the internal friction-dependent temperature changes

Temperature changes inside the lubricating greases studied were monitored along the stress growth transient test. It made it possible to quantify the amount of energy introduced into the tested grease volume and to observe the evolution of the internal friction energy during the test. In addition, it allows statements about the greases' temperature behaviour and the mechanical

stress after the measurements. According to ISO 3219-2 standard, a smooth cone plate with a diameter of 50 mm and a cone angle of 1° was used as the measuring system, resulting in a gap of 0.103 mm. The cone plate geometry was explicitly selected for this experimental procedure as it allows the uniform shear conditions required for temperature measurements throughout the conical gap. In addition, the amount of sample required was small, which aids in the accurate temperature measurements. The torque, speed, and temperature were monitored during the test every 15 seconds (5320 measurement points in total).

The experimental procedure was conducted in two successive steps (figure 3.2) to avoid possible leakage effects due to the motor start-up to reach the high shear rate values commanded. Temperature changes inside the lubricating greases were tested at 250 and 500 s^{-1} shear rates, selected by the standard DIN 51810-1 [149]. It is worth mentioning that no shear rates higher than 500 s^{-1} were used to avoid leakage from the measuring gap. Furthermore, a short shear rate ramp of 600 s was selected in the first part of the test to avoid possible leakage effects due to a sudden high shear rate. In the first steps, the shear rate was linearly increased from 0 to the maximum values, 250 or 500 s^{-1}. The temperature changes were also monitored during this first test section. In the second test section, the grease sample was constantly stressed at the respective shear rate (250/500 s^{-1}) for 79200 s; this long stress period aimed to induce structural changes in the lubricating greases under liquid friction-friendly conditions while recording an extensive time range of the temperature change.

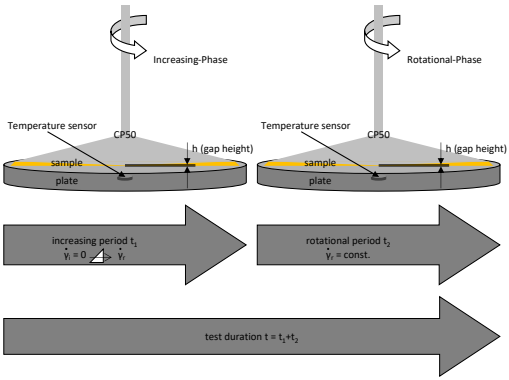

Figure 3.2: Schematic illustration of the experimental procedure – to analyse the temperature change inside lubricating greases [141]

3.2.3 Rheological test to analyse the Rheodestruction

For the rheo-destruction tests, a grooved plate geometry of 25 mm diameter was chosen as the measuring system. The tests were carried out at constant temperatures of 40 °C and 80 °C. The measuring gap was set to 1 mm. This series of tests consisted of four consecutive test sections (figure 3.3).

The first step consisted of a specific period to relax the grease specimen after squeezing. Conversely, the sample was heated to reach the most homogenous commanded temperature in all bulk grease. Previous investigations found that a rest period of 900 s was enough. Following the first test section, a small oscillation strain amplitude within the LVE range (a constant strain of 0.02 % and frequency of 10 Hz) was set for 900 s. This step represents the reference state for the grease samples tested. For the third test section, a shear strain outside the linear viscoelasticity (LVE) range, i.e., 5, 10, 20, 50 and 100 %, was applied to stress the sample for 900 s. After that, a small oscillation strain was again applied for 7200 s, and the subsequent recovery when a strain inside the linear region was again restored. This section shows the greases' phase of recovery (thixotropy behaviour). To recover all examined greases, a long period was deliberately chosen for the last test section to reach a stationary state. During the measurements, typical rheological parameters were again recorded every 15 seconds.

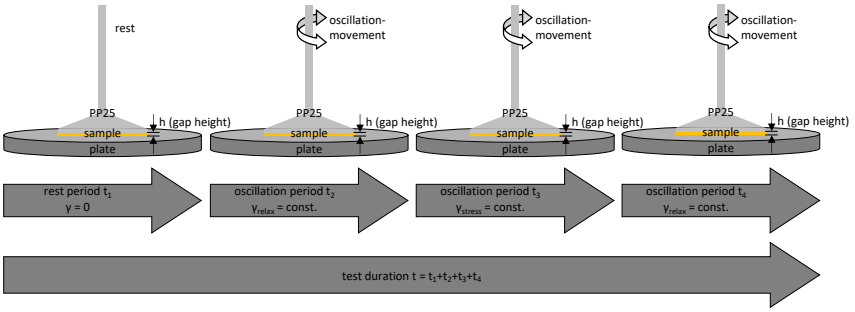

Figure 3.3: Schematic illustration of the experimental procedure - regarding the destruction of internal structures by rheo-destruction tests

3.2.4 Rheological test to analyse the Squeeze-Behaviour

The deformation tests performed (squeeze tests) are not traditional rheometer tests. Nevertheless, the rheometer was used for this series of experiments. Within the scope of this thesis, two different deformation tests were executed, for which a grooved plate geometry with a diameter of 25 mm was selected as the measuring system. All tests were conducted at constant temperatures of 20 °C, 40 °C and 80 °C and a measuring gap width of 1 mm was set before starting the tests.

The first series of tests consisted of two consecutive test sections (figure 3.4). To prevent the impact of mechanical history on the squeeze flow behaviour, the sample was left at rest for 900 s after placing the sample in the first test section. In addition, the sample was preheated to the appropriate temperature during this time. In the second test section, the grease sample was stressed with a logarithmically increased normal force of 0.1 to 30 Newton. The end of the test was defined as either reaching the maximum normal force of 30 Newton (maximum 361 seconds) or reaching a minimum gap width of 0.015 mm.

The second test section was divided into 17 segments (figure 3.5). After another 900 s resting phase for recovery and tempering of the grease sample, two identical test sequences were always carried out. In the first step, the grease was stressed with a linearly increased normal force of 5 Newton each for 50 seconds. Directly afterwards, a small amplitude oscillation in the LVE range with a constant deformation of 0.02 % and a constant frequency of 1 Hz for 100 s was set. The purpose of this segment was to document the respective starting position of the lubricating grease samples. In addition, the storage modulus and loss modulus are used for evaluation. These two test sections were repeated until a maximum normal force of 40 Newton was reached, resulting in 17 test segments and a test duration of 2100 s.

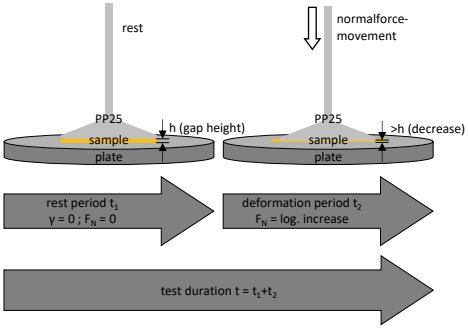

Figure 3.4: Schematic illustration of the experimental procedure of a squeeze test

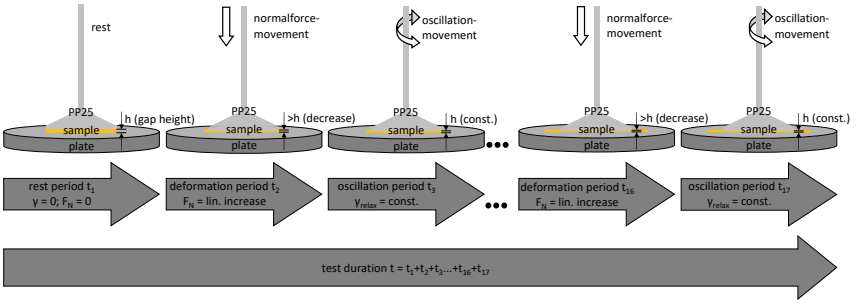

Figure 3.5: Schematic illustration of the experimental procedure of a combined squeeze test with a low oscillation strain

3.3 Microscopy measurements

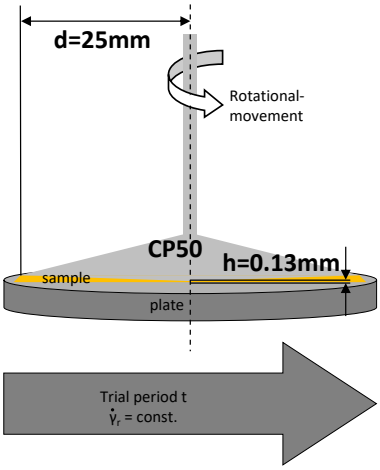

Figure 3.6: Schematic illustration of the experimental procedure - to produce stressed lubricating grease samples for optical analyses [73]

Microscopic measurements are used in many areas of research and industry. This technique can examine small details at the level of molecules and atoms. Furthermore, it describes objects' structure, shape, and size in detail, a valuable addition to other measurement methods. In the following, all microscopic measuring methods used in this thesis are briefly introduced, and the respective implementation of the measuring devices is explained.

All greases were microscopically analysed in both "as received" and stressed conditions. Stressed grease specimens were obtained after a stress growth transient test run similar to the one described in Section 3.2.2. A cone measuring system with an angle of 1° was used to ensure uniform sample shear, resulting in the smallest gap specified by the measuring system being 0.103 mm (figure 3.6). To ensure sufficient sample material for a

wide range of optical examinations, a diameter of 50 mm was chosen for the measuring system. All tests were carried out at room temperature to avoid influencing the structural degradation of the greases due to temperature.

To achieve a significant shear-induced structural change in the greases, as also occurs during fluid friction conditions, the sample was shear-stressed at a constant shear rate of 1000 s^{-1} for 79200 s. Although a high relative velocity can lead to material leakage from the measuring gap, this was deliberately accepted, as the investigation is mainly concerned with optical evaluations concerning the stressing of greases. Considering this limitation, the typical rheological values for further measurements were recorded.

3.3.1 Transmitted light optical microscopy measurements

A transmitted light microscope from Olympus (Hamburg, Germany) examined the stress and unstressed grease microstructure. An Olympus Plan Achromat objective (PLCN20x) with a magnification of 20x was used. Digital images were taken with an Olympus DP27 digital camera with 6.3x magnification, giving a cumulative magnification of 126x. The grease specimens were applied as a thin layer on standard glass holders, which allowed individual features and details of the specimen to become visible. At least three fresh samples were prepared, of which five images were taken at different locations. The aim was to obtain a structural characterisation that was as representative as possible for each grease studied. One challenge in these measurements was to ensure uniform illumination of the different coloured greases. Therefore, so-called High Dynamic Range (HDR) images were taken. The image processing software automatically selects a suitable illumination time, thus controlling brightness and darkness [150]. However, this thesis presents some images in black and white because distorted colour values can occur.

3.3.2 Scanning electronic microscopy (SEM) measurements

For the microstructural analysis of all greases studied, a scanning electron microscope (SEM) model EVO LS15 (ZEISS, Germany) with a voltage strength of 10 kV was used at room temperature. A magnification range of 1000x to 20000x was chosen for the images. As a novelty regarding previous SEM-based

investigations of greases [22, 74–77], all greases studied have been chemically fixed to affect the grease microstructure as little as possible. For this purpose, all samples were fixed on the holder with 2.5 wt% glutaraldehyde in 0.1 M cacodylate buffer for two hours, followed by three washes in 0.1 M cacodylate solution. Subsequently, all samples were subjected to a second fixation with 1 wt.% osmium tetraoxide solution for one hour. It was followed by three more washes with 0.1 M cacodylate solution. Finally, a critical point drying in acetone was performed before metallisation with Au/Pd. To ensure representative morphology prototypes, at least three samples were prepared for each grease studied, and then five images were taken at different locations and magnifications.

3.3.3 Atomic force microscopy (AFM) measurements

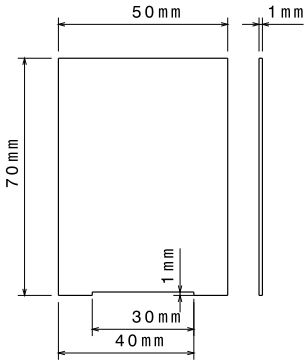

Figure 3.7: Schematic illustration of the AFM-Sample scraper [73]

An atomic force microscope (AFM), model JPK NanoWizard 3 (BRUKER, Bruker Nano Surfaces Division, Massachusetts, USA), was used for further microstructural analysis. All AFM measurements were carried out at room temperature, and the tapping mode with phase detection was preferred, as this mode is particularly suitable for soft imaging materials (lubricating greases). In this mode, the cantilever oscillates at or just below its resonance frequency, causing the cantilever tip to interact slightly with the surface of the grease, thus producing high-resolution images during the measurement. The cantilever was a High-Resolution Silicon AFM NSG01 with a typical resonant frequency of 150 kHz and a typical force constant of 5.1 N/m. The size of the scan windows for the investigations was 5 or 20 µm, and a scan speed of 0.2 Hz was set.

One of the most important and, at the same time, most difficult steps in AFM measurements is the preparation of the grease samples, as they are particularly adhesive and viscous. A smooth sample surface before starting the scan sequence is needed to ensure adequate quality of the AFM images. It has been common practice [68, 71, 85, 86] to preheat the greases at a temperature below the dropping point. However, this previous manipulation

of the grease specimen may disturb the equilibrium between thickener and oil. For this purpose, a specially developed scraper was preferred to produce a smooth and even grease surface (figure 3.7).

3.4 Determination of the density and the specific heat capacities

The specific densities were determined both experimentally and theoretically (table 3.4). Because measuring the specific densities of highly viscous materials experimentally is complex, theoretical values were calculated using equation 9 to verify the experimental results [141]. The specific densities of each component in the grease essential for this purpose are available in table 3.3.

$$\rho_{grease} = \rho_{thickener} \cdot wt.\%_{thickener} + \rho_{base\,oil} \cdot wt.\%_{base\,oil} \tag{9}$$

Table 3.3: Specific densities at 20 °C of the different grease components [151, 152, 153, 154, 155, 156, 157, 158, 159, 160, 161, 162, 163, 164, 165, as cited in 141]

Ingredient	specific density [g/cm³] at 20°C	Ingredient	specific density [g/cm³] at 20°C
Lithium 12-hydroxystearate	1.03	Glyceryl monooleate	0.94
Calcium 12-hydroxystearate	1.08	Polyhydroxybutyrate	1.22
Urea	1.33	Ethyl cellulose	1.14
Castor oil	0.97	Beeswax	0.97
PAO	0.85	HOSO	0.92
Mineral oil	0.90	MTC oil	0.96
Cellulose	1.50	Glycerol monostearate	1.03
Glycerol	1.26	Cetyl alcohol	0.82

The specific heat capacities could only be determined experimentally (table 3.4), as theoretical values were unavailable for all greases studied. For all experimental investigations, three tests were carried out on fresh samples. As a result, statistical significance was achieved for the determined data, as they did not exceed the significance level of 0.05 in the Student's t-test and had a 95 %

confidence interval. The specific densities were determined experimentally using a PNR 10 penetrometer crucible (Petrotest, Germany) with a defined volume of 3178 mm^3 and a precision balance, model 1602 MP8 (Sartorius, Germany). All samples were tempered at 20, 40 and 80 °C for 15 minutes using the penetrometer crucible in an F3 S circulating thermostat water bath (Haake, Germany). After heating, the crucible was removed evenly, and the weight of the filled crucible was determined immediately afterwards.

Table 3.4: Specific densities (experimentally and theoretically) and specific heat capacity at 20 °C of the greases used [141]

Lubricating greases	Experimental specific densities [g/cm³]	Theoretical specific densities [g/cm³]	Specific heat capacity [J/(g·K)]
C1	0.9357	0.9780	2.106
C2	0.8126	0.8691	1.948
C3	0.8299	0.8734	2.000
C4	0.8639	0.9124	1.847
C5	0.9481	0.9789	2.206
C6	0.8609	0.9024	2.063
C7	0.8498	0.9441	1.997
B1	1.2109	1.2318	2.245
B2	0.9643	0.9849	2.012
B3	0.9205	0.9414	2.144

A differential scanning calorimeter, model DSC 204 F1 (Netzsch, Germany), experimentally determined the specific heat capacities. The calorimeter worked with a nitrogen atmosphere, keeping the nitrogen flow at 20 mL/min. The grease samples (16.9 - 20.9 mg) filled into closed aluminium crucibles were heated from -40 °C to a maximum temperature of 300 °C at a heating rate of 10 K/min. The specific heat capacities were then determined following the standard protocol of DIN 51007 [166]. In this process, an equation in which the heating rate and the weight of the sample are significant was applied to three measurements made in the same way (baseline, sapphire, sample) [167]. A sapphire of 4 mm diameter and 0.5 mm height from a DSC

standard set by Netzsch was used as a standard reference.

3.5 Internal friction-dependent temperature change measurements

In rheological tests, different temperature environments are often simulated, and the reference temperature is kept constant or dynamic. However, if a defined temperature is specified, the behaviour of the lubricating greases differs from that under real, non-constant temperatures. In this thesis, measurements of the internal friction-dependent temperature changes during the transient flow test were recorded for all greases studied. It enables quantifying the dissipation energy, converted via mechanical energy into thermal energy and a gradient of intrinsic energy.

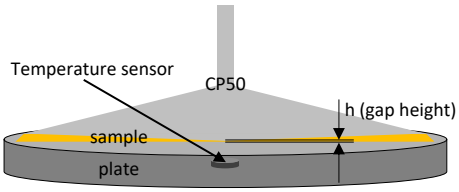

Figure 3.8: Schematic of standard plate PTD system with the temperature sensor [141]

For this purpose, two different approaches were used in this thesis to measure the temperature values during the shear stress test. On the one hand, the average temperature values of the grease samples were determined by a standard plate Peltier temperature control system (PTD) from Anton Paar (figure 3.8). The temperature sensor was located in the middle and directly under the base plate in this measuring system.

As a novelty, a new measuring cell called Calidus was developed for this type of temperature measurement. This modular measuring cell was installed in an Anton Paar MCR302 rheometer (figure 3.9). A threaded system allows different modules to be installed. The difference to the Anton Paar PTD system was that the thermoplastic base plate of the temperature module was equipped with two temperature sensors—one in the middle and one positioned slightly off-centre.

In both configurations, an Anton Paar environmental chamber (bonnet) was supplemented during all measurements. This chamber encloses the sample and thus minimises heat loss, allowing more precise recording of the temperature measurements.

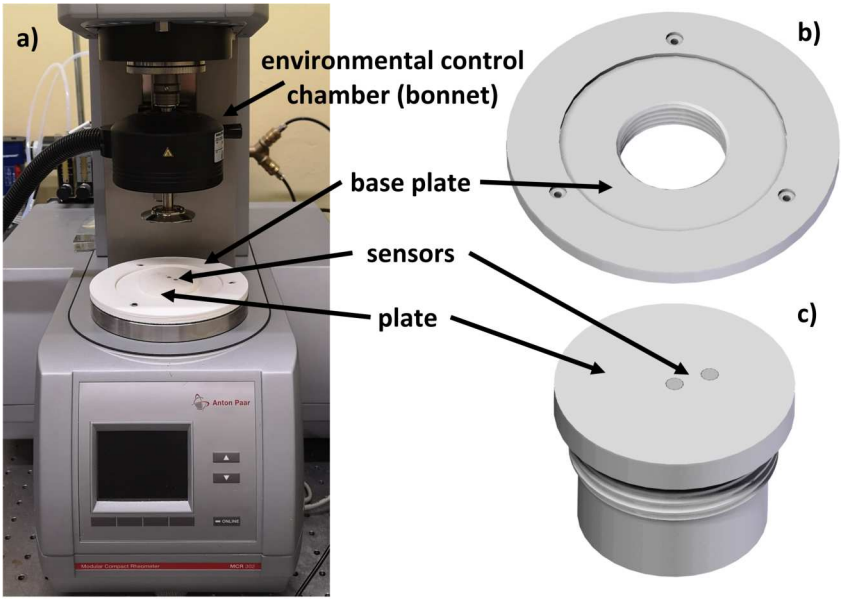

Figure 3.9: Calidus coupled to the rheometer (a), Schematic of Calidus base plate (b), Schematic of Calidus plate with two sensors (c) [141]

Figure 3.10: Thermal image of rheometer MCR 302 during operation [141]

In addition, a PT-100 sensor was used to record the room temperature in parallel with all measurements for verification. Different thermal imaging captures validated that the measuring instrument (Anton Paar Rheometer MCR 302 with Peltier temperature control system (PTD) measuring cell) did not introduce any significant heat into the grease system. Figure 3.10 displays one of these thermal imaging snapshots, providing evidence of this fact [141].

4 Results and discussion

This part of the thesis discusses the core aspects of the structural degradation of lubricating greases. The results are the outcome of an intensive examination of a group of lubricating greases regarding their composition (thickener type, thickener concentration, base oil type and base oil viscosity). They have been related to the thickener's microstructural organisation, the structural degradation, the expended energy, and the temperature changes when the greases studied were submitted to control shear-stress conditions. All these findings have been published in well-renowned indexed journals. In addition, further findings from both rheo-destruction and squeeze tests carried out as part of this research work are shown and discussed.

4.1 Evaluation of structural degradation by optical measurement methods

The structural degradation of all greases studied was evaluated using a transmitted light microscope, scanning electron microscope (SEM), and atomic force microscope (AFM). This combination of optical measurements lets us obtain different magnifications to ensure a comprehensive grease structure analysis from macroscopic and microscopical perspectives (figure 4.1). All greases were studied under unstressed and stressed conditions, which allowed the study of the changes in the structural skeleton caused by shear stress and related to the shear-induced mechanical profile. Moreover, through these investigations, it was possible to gain an insight into the wear behaviour of the grease structure.

Particular sample preparation protocols were developed to ensure all these optical analyses could be carried out on grease specimens without altering the grease structure. In the case of the transmitted light microscope measurements, care was taken to prepare a particularly thin-layered grease specimen so that several layers of the grease do not overlap. In addition, a thin-layered

grease specimen improves the primary exposure and prevents air bubbles from forming in the grease layer.

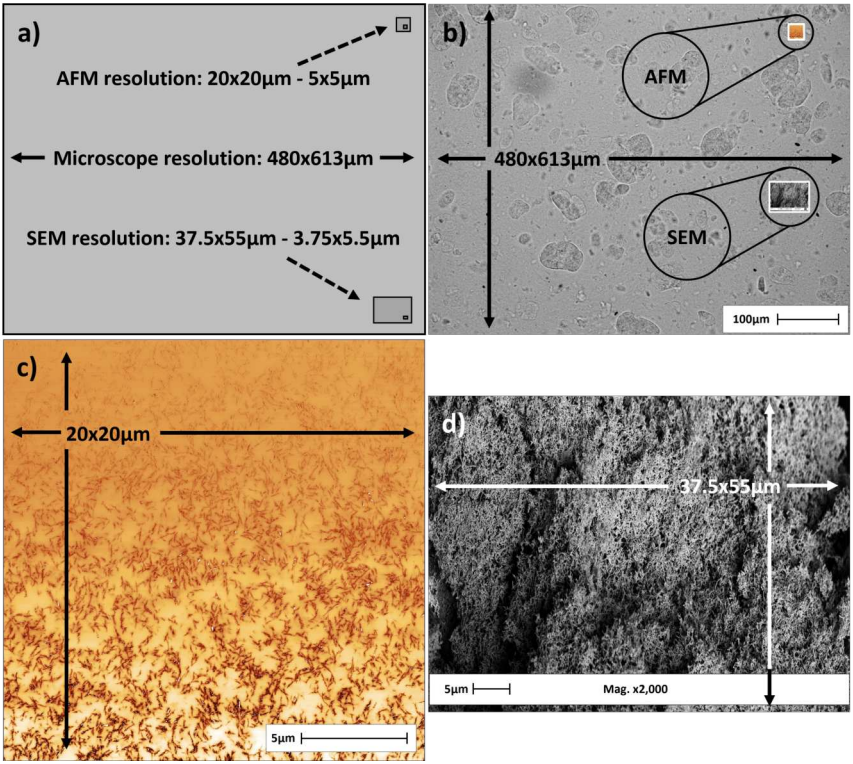

Figure 4.1: Comparison of the different optical resolutions for unstressed grease C1: a) Schematised optical resolutions, b) visual comparison of the different optical resolutions, c) detailed micrograph of AFM resolution, d) detailed micrograph of SEM resolution [73]

For the SEM measurements, the prior extraction of the base oil, which is necessary for analyses in a vacuum, was optimised. Specifically, the grease samples were chemically fixed before removing the base oil. This procedure helped to keep the original density of cavities and minimise the clumping of thickener particles. Furthermore, the images were very deep in focus and showed the structural skeletons of the thickener particles more clearly. Concerning the

AFM measurements, previous researchers slightly heated just below the dropping point of the grease sample to reach a smooth upper grease surface. However, this preparation protocol may induce changes in grease microstructure. Thus, this research work chose smoothing the grease surface with the help of a newly developed spatula at room temperature. This method avoided changing the microstructure's equilibrium between thickener and oil. The respective preparations were used to analyse the different structural patterns of the greases in both the stressed and unstressed states. The results showed that the optical light microscope is particularly suitable for visualising changes in the macrostructure of the grease (agglomerates) due to shear stress. SEM and AFM examinations, on the other hand, enable microstructural analysis.

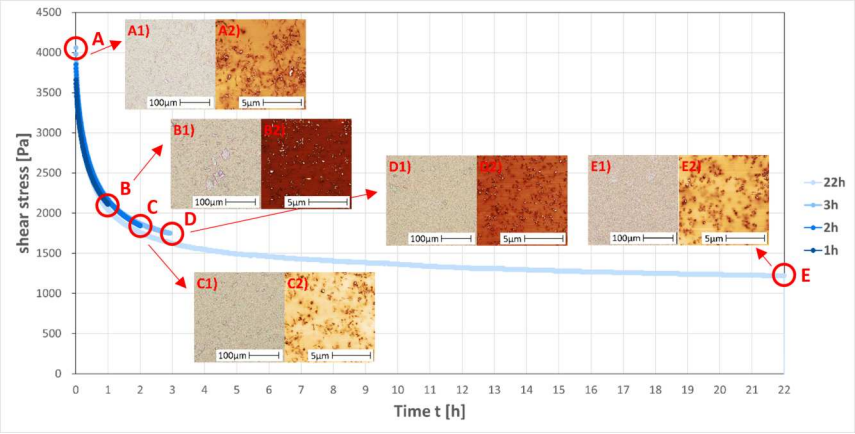

Figure 4.2: Transient shear stress curve of grease C7 – start (A), after 1 h (B), 2 h (C), 3 h (D) and 22 h (E) – with microscope images (left) and AFM images (right) for each spot

Combined analysis of the grease structure using both transmitted light and AFM microscopes during the transient shear stress test led to a suitable optical analysis of the grease wear, i.e., the rheological degradation of the grease, within all degradation time studied, form a macroscopic and microscopical point of view. For the sake of comparison, polyurea grease (C7) was selected. Figure 4.2 shows the transient shear stress curve of grease C7 with both transmitted light and AFM microscope images for each spot. It was found that both the amount of agglomerates and their sizes decreased with the shear

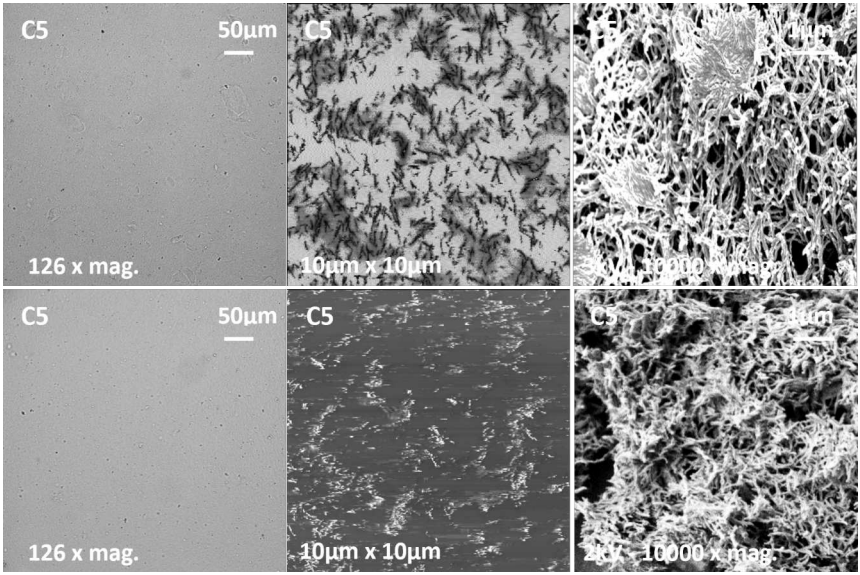

Figure 4.3: Calcium greases C5 (9.7 wt.%) – top row unstressed, bottom row stressed for 22 h – from left to right: transmitted light microscopy image, AFM image, SEM image unstressed

time. The polyurea grease showed significant changes in the macrostructural distribution within the first hour. After this time, the accumulation of cohesive polyurea agglomerates was no longer evident. Instead, the agglomerates' size and the polyurea particles' long rod-shaped structures continuously decreased. It should be emphasised that the structural degradation along the shear time correlates well with the course of the shear stress curve.

For all model greases studied, the structural pattern of unstressed grease changed into a pattern with a smaller grouping of particles and more oriented toward the flow direction due to the internal friction process and grease wear induced by the shear stress imposed. The process of internal friction favours the degradation of the internal grease structure, i.e., the grease wear, which is reflected in the transient shear stress curve by a decrease in the shear stress values recorded. It is worth emphasising that this decrease in shear stress values corresponds to the decrease in expended energy involved in the degradation of the grease structure during the internal friction process as a

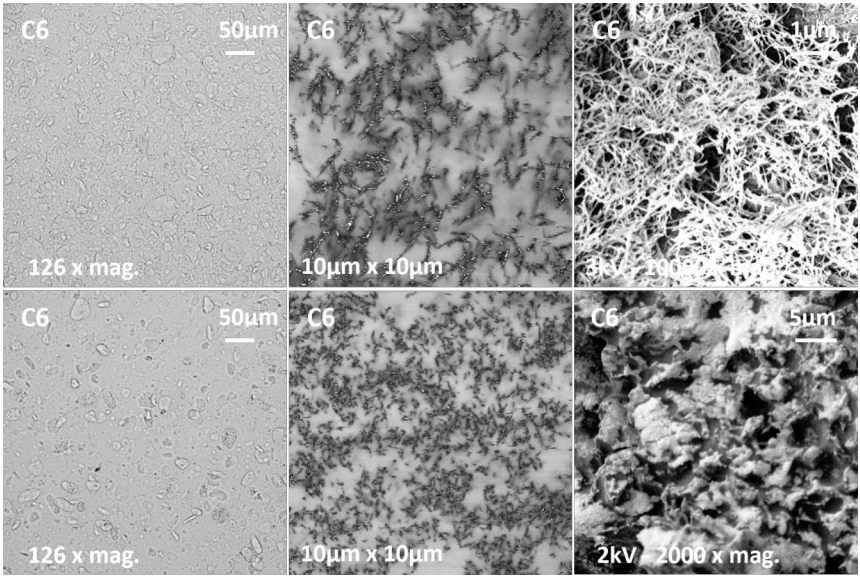

Figure 4.4: Calcium greases C6 (22.8 wt.%) – top row unstressed, bottom row stressed for 22 h – from left to right: transmitted light microscopy image, AFM image, SEM image unstressed

consequence of the shear rate imposed. Besides, it was found that the type of thickener also plays a significant role in influencing this expended energy. Thus, the structural skeletons of lithium and calcium greases, compared to the polyurea grease or biogenic greases (B3 and B4) studied, were able to dissipate less mechanical energy during shear processes, which corresponded to a minor change in the structural skeleton—on the other hand, lubricating greases with a higher thickener content led to more structural degradation in the stressed grease. It can be seen in particular in figures 4.3 and 4.4. The figures show the microscopic images of greases C5 (9.7 wt.%) and C6 (22.8 wt.%). The greases are shown unstressed in the top row and stressed in the bottom row. The order of the images is from left to right, transmitted light microscopy, SEM and AFM.

This part of the research contributes to understanding the structural degradation of greases during the internal friction process and how the applied shear rate influences this degradation through optical assessments. The knowledge

gained provides insight into the structural degradation behaviour of greases and can be used to promote replacing conventional ingredients with biogenic substances. The detailed elaboration can be found in Appendices A.1 and A.3.

4.2 Structural degradation of lubricating greases related to the expended mechanical energy

In this section, the structural degradation induced by shear stress applied in rheological tests (rotational and oscillation mode) on the expended mechanical energies is analysed and correlated with the structural changes observed by the optical measurements. Other influences, such as thermal energy or chemical energy, were neglected. The mechanical degradation caused by the shear stress applied in the rheological tests is analysed in the context of the structural skeleton changes of the thickener. Special attention was also given to the influence of the thickener, both in terms of its nature and composition, as well as the base oil on the degradation process.

A better understanding of the influence of the grease composition (thickener and base oil) on the macroscopic structural degradation of lubricating greases could be gained. In addition, a holistic approach was developed for the expended energy involved in the internal structural degradation that occurred in the stressed greases using the parameter (R_{tee}) (see equation 7). As commented in the previous section, R_{tee} relates the mechanical energy involved within the grease degradation process to start and keep the flow process, with the mechanical energy involved in the structural degradation achieved along with the viscous flow transient test at a specific shear rate. Thus, this ratio of expended energies provides a suitable energetical approach for describing the mechanical stability of the lubricating greases according to the shear-induced structural changes observed in each case. Accordingly, a more considerable value for R_{tee} means a lower degradation of the structure of the stressed grease. Thus, more internal frictional energy is required to make the stressed grease flow, or less mechanical energy is dissipated during the structural degradation.

$$R_{tee} = \frac{W_{CP}}{W_R} \tag{7}$$

With:

R_{tee} = Ratio of the total expended energy

W_{CP} = Mech. work until the crossing point at the oscillation test [J]

W_R = Mech. work supplied from the viscous flow transient test [J]

The transmitted light microscope images showed that although all the examined conventional model greases belong to NLGI class 2, they show considerable differences in the structural pattern of the unstressed grease. As commented above, numerous thickener-based agglomerates with different shapes and sizes were detected in the unstressed samples, whose size was influenced mainly by the amount of thickener and the type of base oil used. On the other hand, the type of thickener-based influencing on the microstructural framework significantly affected the internal friction energy more than the base oil or the content of the thickener. Consequently, differences in the expended energy by the stressed greases to start the flow process were appreciated. Thus, it was found that the structural skeleton of lithium and calcium greases dissipated less mechanical energy during the shearing process than polyurea and biogenic B3 greases (see figure 4.5). At the same time, the highest mechanical energy dissipated was found for the biogenic grease B3. It is worth mentioning that greases with a higher thickener content had a lower R_{tee}-value, which indicates a more intensive degradation of the structural skeleton in the stressed grease.

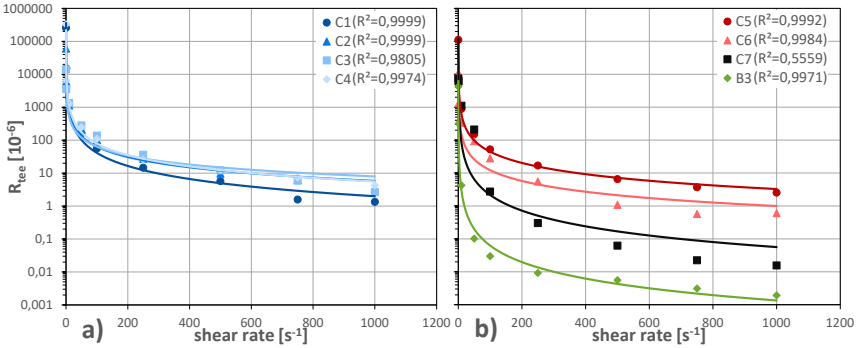

Figure 4.5: Ratio of expended energies (R_{tee}) 40 °C for a) lithium greases and b) other greases. Power curve fittings are shown by a discontinuous line indicating each R-squared (R2) in the legend [79]

The expended mechanical energies were also analysed within a temperature range of 40-80 °C. For most greases studied, the temperature drastically affected the expended energy-shear rate dependence, being higher overall in the case of lithium greases when PAO was used and less for the calcium and polyurea greases. The R_{tee}-value of polyurea grease C7 was the only one that was hardly influenced by temperature. It implies that the structural skeleton of polyurea grease supports the shear-induced structural degradation in the temperature range considered more efficient than the other greases. The detailed results are in the first publication (Appendix A.1).

4.3 Structural degradation-based temperature changes in stressed lubricating greases

In assessing the structural degradation of lubricating greases, this investigation aimed to learn about the internal heat changes in the lubricating greases reached during the stress-growth rheological tests performed, which could later be used in engineering calculations. Temperature measurements are primarily registered by the PTD measuring cell couplet to the plate-plate cell used for rheological tests. In addition, the temperature change was to be related to the components of the greases studied (thickener, base oil, and weight composition), and a comparison was to be made with both the shear-induced structural changes observed by optical measurements and the dissipated mechanical energy of the stressed greases studied. It should lead to quantifying the dissipation energy converted via mechanical energy into thermal energy and a gradient of intrinsic energy. It is worth mentioning that the focus was placed solely on the lubricating greases studied and not on lubrication pairings, even though in mixed friction conditions, the frictional energy is due to solid and liquid friction. Thus, to obtain precise information on the liquid friction behaviour of greases, the greases studied in this work were subjected to stress-growth rheological tests (mechanical energy) at room temperature and using a conventional rotational rheometer measuring cell. It should be noted that no physicochemical interactions between the components were considered in any of the investigations either. In addition to the empirical observation, a simple theoretical approach for calculating the temperature change of stressed greases was developed. The experimental observations and the theoretical predictions were compared. These approaches can be understood to validate the

knowledge gained and are not intended to represent a specific model.

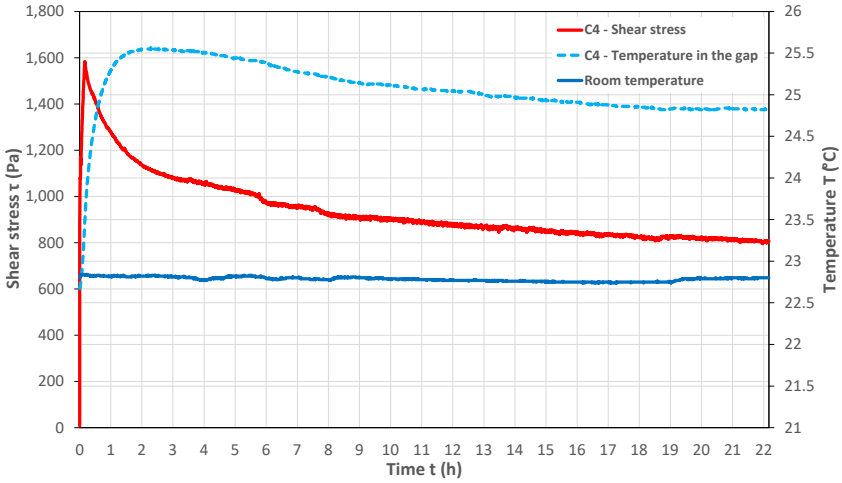

Figure 4.6: Experimental room temperature, shear stress, and temperature profile of lithium grease C4, with the standard PTD measuring [141]

The investigations demonstrated a correlation between the structural degradation and the temperature changes associated with the stressed grease at a high shear rate (see figure 4.6). All greases showed an internal temperature profile characterised by an abrupt increase in ΔT. This increase resulted from the pronounced internal friction due to the high structural consistency of the grease. A decrease followed this in ΔT until a steady-state value was reached. The examined conventional model greases showed pronounced differences in the temperature profiles. The grease C1, which had a thickener content of 16.1 wt.%, showed the most substantial heating (3.2 Kelvin) and a pronounced drop in ΔT. Grease C5, with the same base oil and a thickener content of 9.7 wt.%, had slightly less heating and was at the same level as grease C7, which had a thickener content of 19.6 wt.% and PAO as the base oil. It showed that not only the absolute thickener concentration is decisive for the internal frictional heating, but rather the type of both the thickener and the base oil. At the same time, these three greases (C1, C5 and C7) exhibited not only the highest specific densities but also the largest heat capacities. It demonstrates that the specific heat capacity of these greases is involved in

the temperature change profile. In particular, the grease C5, with the more significant decrease in ΔT, had the highest specific heat capacity, followed by the greases C1 and C7. In contrast, grease C4, which had the lowest specific heat capacity, showed a uniform decrease in ΔT until reaching equilibrium (table 4.1).

Table 4.1: Composition and technical data of conventional lubricating grease samples studied

Lubricating greases	Thickene type	Thickener conc. [%]	Base oil	Temp. change [K]	max. ΔT reached [K]	R_{tee} (10^{-6})	C_p [J/(g·K)]
C1	Lithium-12-hydroxystearate	16.1	Castor oil	1.97	3.20	5.74	2.106
C2	Lithium-12-hydroxystearate	10.6	PAO	2.13	2.63	9.65	1.948
C3	Lithium-12-hydroxystearate	13	PAO	0.86	1.42	12.15	2.000
C4	Lithium-12-hydroxystearate	9.5	Mineral oil	1.83	2.63	11.67	1.847
C5	Calcium-12-hydroxystearate	9.7	Castor oil	1.58	3.13	6.52	2.206
C6	Calcium-12-hydroxystearate	22.8	PAO	---	---	1.08	2.063
C7	Polyurea	19.6	PAO	1.87	3.07	0.06	1.997

Furthermore, a direct correlation between the structural degradation described in Section 4.2 (reciprocal of R_{tee}) and the internal temperature change of the stressed lubricating greases could be established. A higher ratio of the applied energies (R_{tee}) was accompanied by lower temperature changes (ΔT). Thus, the greases (C2, C3 and C4) with the lowest structural degradation under stress also showed the lowest temperature changes (see figure 4.7). Accordingly, the greases C1, C5 and C7, each with the lowest R_{tee}-values, had the highest maximum ΔT-values and the steepest drops until a constant ΔT-value was reached. The viscosity of the base oil also played a decisive role in deriving this internal temperature increase. Thus, the grease C3 with the lowest base oil viscosity and with 13 wt.% lithium soap, despite having a high R_{tee}-value similar to grease C4 and C2, showed a temperature change of about 52 % lower. In addition, this grease also had the lowest maximum ΔT and the temperature profile was characterised by a moderate variation of ΔT during the test.

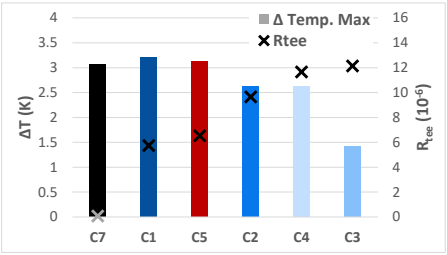

Figure 4.7: Comparison of the maximum ΔT-values with the ratio of expended energies (R_{tee}) [141]

A novel temperature-measuring cell called Calidus was developed based on the knowledge gained to work deeper in temperature generation in stressed greases. The measurements carried out with the newly developed Calidus measuring cell provided more precise results regarding the grease's internal temperature. Another advantage is the material of the Calidus measuring cell, as this better isolates the internal temperature measurements from the geometry to minimise the influence of heat conduction. This results from the lower mass inertia of the measuring cell material (Calidus: polylactide, PTD: titanium), which means the temperature values achieved can be stabilised more quickly. At the same time, the sensors used in the Calidus measuring cell have an optimised installation position located directly at the measuring gap. However, it should also be emphasised that for future measurements, the aim is to optimise the surface properties so that the rheological measurements more closely match those of the PTD measuring cell.

Concerning the theoretical approach, it can be stated that there was a much better correlation between the experimental data of the Calidus measuring cell (see figure 4.8). The determination of the theoretical temperature values is mainly based on the first law of thermodynamics:

$$Q_{12} + W_{12} = U_1 - U_2 \tag{8}$$

In this case, the determined temperature values were consistently higher than those determined experimentally. It is plausible, as the theoretically determined temperature values were based on the assumption that the energy supplied to the system as heat (Q_{12}) was zero. Future investigations should aim to determine a theoretical value for Q_{12} so that the theoretical approach corresponds closer to reality. It could lead to further development of the theoretical approach towards a model that considers the heat transfer rate within the grease. In this way, temperature values could be determined as input variables without being determined beforehand in experimental temperature measurements. The full article can be found in Appendix A.2.

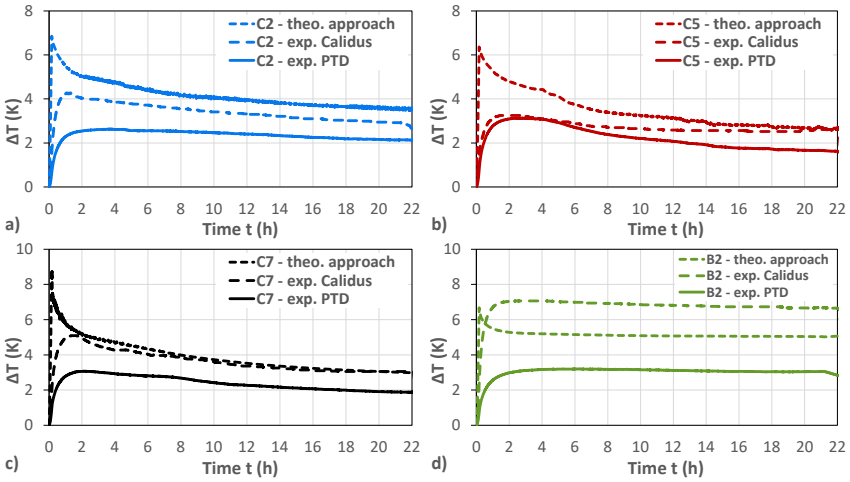

Figure 4.8: Comparison of the rheometer measuring Cell–Calidus and Anton Paar PTD–with the use of lubricating greases (a) C2, (b) C5, (c) C7, and (d) B2 concerning the experimental ΔT profile and the theoretical approach curve [141]

4.4 Further insights from other investigations (Rheo-destruction & Squeeze Test)

In addition to the main focuses of this work described in the previous three sections, further investigations were carried out in this research work. However, the compiled results of the investigations were not thoroughly evaluated within the scope of this thesis. Nevertheless, they will be briefly presented to provide an outlook for future investigation tasks.

Rheo-destruction tests offer another possibility to investigate grease wear from a rheological point of view. The lubricating greases were examined with a strain-controlled rheometer by SAOS test, within the LVE range, at 10 Hz, and two temperatures, 40 °C and 80 °C, were studied. Through this investigation, correlations with the composition and microstructure can be obtained. Strain sweep tests at 10 Hz from 0.01 to 100 % were previously carried out to determine the LVE range of each lubricating grease studied. Thus, it ensures suitable comparability among all lubricating greases tested. It is worth mentioning that the strain value selected within the LVE range for

the rheo-destruction tests was also not chosen to be too small to achieve a reasonable resolution of all measurements. Figure 4.9 shows the strain sweep curves at 40 °C for all greases studied.

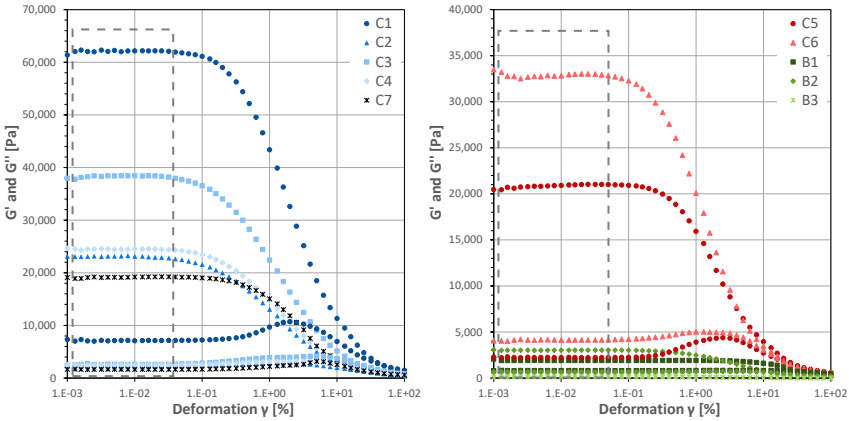

Figure 4.9: Strain sweep test for all conventional greases at 40 °C

The results were evaluated based on the time-dependent curves of the complex shear modulus (G*) inside and outside the LVE range at temperatures of 40 °C and 80 °C (figures 4.10 and 4.11). As expected, the complex modulus continuously decreases as the magnitude of the sinusoidal shear strain applied increases outside the LVE range because of a much larger structural breakdown. A partial recovery of G*-values was observed once the shear strain outside the LVE range applied for 2 h ceased. Generally, the higher the shear strain outside the LVE range applied, the lower the final value of G* reached at the end of the rheo-destruction tests. This partial recovery of G* tends to an asymptotic value with the shear strain value outside the LVE range applied just over 20 %. On the one hand, it is worth noting that the grease microstructure exhibits a maximum ability to reach its original consistency once the deformation outside the LVE range has ceased, and it is dependent on the energy applied till the maximum value is reached. On the other hand, this asymptotic limit seems to be reached by shear strain values equal to or higher than the corresponding value at the crossing point of G' and G''. Furthermore, it can be observed that the greases studied, within the shear strain range analysed, show a maximum permanent structural degradation. This G*-value

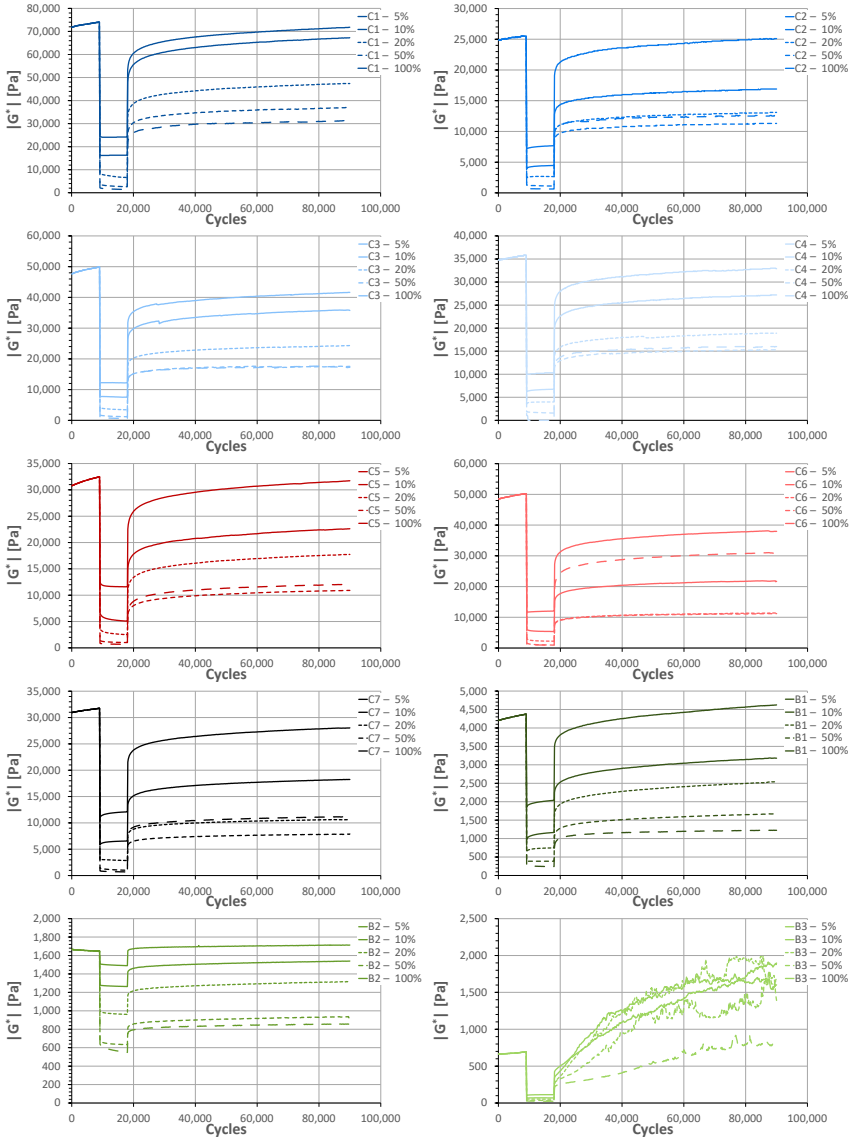

Figure 4.10: Complex shear modulus of all tested greases at 40 °C, at a frequency of 10 Hz, after changing the shear strain from linear (=0.2 %) to the non-linear viscoelastic range (=5, 10, 20, 50, 100 %) and back (=0.2 %)

is related to different properties of the grease, such as microstructural characteristics, composition, and viscoelastic properties. This fact will affect the corresponding tribological behaviour. In addition, more significant structural degradation at higher input energies was observed for all greases [168].

In comparing the subsequent ability to recover the initial G*-value when a shear strain inside the linear region is again restored, all examined lubricating greases showed similar progressions at a temperature of 40 °C (figure 4.10). The curves are almost parallel and differ mainly in the absolute values of the shear modulus. Despite the expected behaviours of the complex shear modulus and dissipated energy when changing the shear strain, isolated exceptions were found. For example, unusual behaviour occurred at 40 °C with some lubricating greases. For the greases C2, C4 and C5, higher recoveries of G*-values were obtained after submitting the greases to a shear strain value of 100 % than 50 %. The effect was even more pronounced with the greases C6 and C7, which have the highest thickener content. For grease C7, the recovery of the G*-value (third test phase - with asymptotic behaviour) was above the value after a deformation of 20 %. For grease C6, it was above the recovery of the G*-value after a deformation of 10 %.

In a first evaluation of the examined conventional greases at 40 °C and 80 °C, it was observed that the rheo-destruction results strongly depend on the temperature. Thus, it was found that the complex modulus values of the undisturbed sample decreased with temperature for six out of seven greases studied. An example is exposed in figure 4.11: grease C1. It can be attributed to the fact that the consistency of the lubricating greases decreases with increasing temperature, which may be a consequence of both viscosity-temperature dependence of base oil, capillary forces, and a weakening of the Van der Waals that provide linking in the structural skeleton of the lubricating greases. Thus, it can be pointed out that the shear strain and temperature level are critical for the permanent degradation of the lubricating grease microstructure, i.e., the asymptotic limit of partial recovery of G*-values. These observations can be confirmed by the investigations of Delgado et al. [106], who established in their studies that the irreversible structural degradation increased with increasing temperature. Cann and Spikes [169] emphasise that the base oil, held within the soap network by van der Waals and capillary forces, leaks out under high shear stresses and temperatures. In this context, Cann and Spikes explained that when the soap network is damaged, the ability of this structure to hold a certain amount of base oil is reduced, and a separation of the soap and oil phase occurs [169]. Only the grease C7 was an

exception, reflected in the highest dropping point of all greases.

At a temperature of 80 °C, grease C1 showed an unusual property to regain the original G*-value after the shear stress. Thus, this grease achieved a higher G*-value after being subjected to a shear stress of 5 % (figure 4.11b). It may be related to the high thickener content of this grease. Moreover, this grease could recover its structure network better. Lithium grease C1 was the most effective at recovering the original structure, but it is also affected by the magnitude of the shear strain applied. Furthermore, at 80 °C, only grease C6 showed recovery values of G* at 100 % higher than 50 %. This described anomaly could be due to a destruction of the lubricating grease structure at a deformation of 100 %. It means the structural degradation of greases with a higher thickener content was much more pronounced than that of greases with less thickener content.

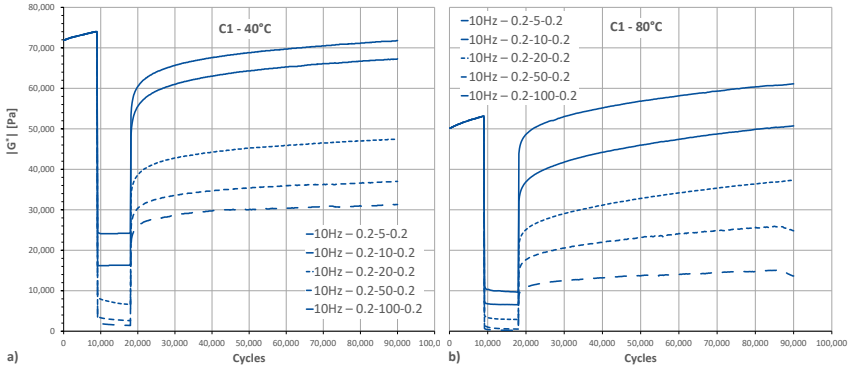

Figure 4.11: Complex shear modulus of grease C1 at 40 °C (a) and 80 °C (b) at a frequency of 10 Hz, after changing shear strain from the linear (=0.2 %) to the nonlinear viscoelastic region and reaching higher values when the former shear strain is reimposed

The results for the pure biogenic greases were similar to those for the conventional greases. Grease B1 reacted with identical curves to the conventional greases at 40 °C and 80 °C. Only at a shear strain of 5 % could the grease reach the initial value of G* during the rest period. For the pure biogenic grease B2, the curves at 40 °C were at least comparable to those of the conventional greases. However, the temperature of 80 °C was too high for the tests, as this is very close to the dropping point of the grease. Therefore, the results ob-

tained at 80 °C cannot be evaluated. Unfortunately, the lubricating grease B3 cannot be evaluated meaningfully either since the dropping point was also too close to the test temperature for this lubricating grease. Thus, although tests were only carried out for this grease at 40 °C, the recovery stage investigated in the fourth section cannot be evaluated.

As part of this research, squeeze tests were carried out on all model greases. These tests aimed to assess the bleeding oil capacity, mechanical network resistance, and capillary forces affected by the base oil that provides linking in the structural skeleton of selected model greases using load tests on the rheometer. In these tests, the greases were subjected to a compressive force in two different test series. As commented in Section 3.2.4, in the first test series, a defined normal force was applied in different steps up to a maximum value of 30 N or a previously achieved minimum gap height of 0.015 mm. The normal force and the gap height were recorded during the complete test period. The tests were conducted at three different temperature settings (20 °C, 40 °C and 80 °C). For comparison, the gap height "d" was plotted against the normal force F_N in a diagram (figure 4.12), in this case for 20 °C.

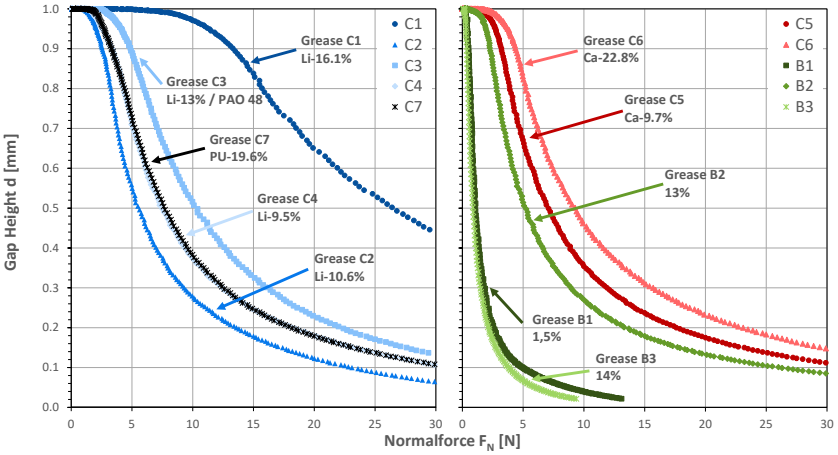

Figure 4.12: Normal force-dependent course of the lubrication grease deformation (Squeeze-Test) at 20 °C

As previously stated by Kuhn [7], all squeeze curves show a characteristic shape that can be divided into three sections: A progressive behaviour can

describe the first range; in the second range, the behaviour is approximately linear or stationary; in the third range, there is a degressive behaviour as illustrated in figure 4.12. As can be appreciated in figure 4.12, when examining the respective conventional lubricating greases, it can be determined that, in principle, the greases with a higher thickener content are generally more difficult to squeeze. Thus, the greases C1, C3, C6 and C7 with higher thickener content are more difficult to deform than the greases with lower thickener content, which hinders the squeezed flow. A comparison of the different thickener types showed that lithium greases are more challenging to squeeze than calcium greases, which, in turn, are more complicated to squeeze than PU greases. Therefore, the shape and size of thickener particles, the structural network or agglomerates distribution, and the thickener content might affect the squeezed flow. The combination of thickener and base oil proved that the base oil used in each case also influences the structural network and the particle agglomerates. Thus, the lubricating grease C3 with a PAO base oil with a base oil viscosity of 48 mm^2/s need higher normal forces to squeeze than the lubricating grease C2, which also consists of a PAO base oil but has a base oil viscosity of 240 mm^2/s. As Delgado et al. [28, 29] pointed out, the oil viscosity affects both the development and size of fibres occurring during crystal growth in the final steps of the manufacturing process and the size of hollow spaces among fibres where oil is trapped. Thus, a lower oil viscosity favours a more compact structural skeleton that can hold relatively large amounts of lubricating oil. This compact microstructure easily implies a more robust structural integrity, i.e., higher consistency, that better tolerates the action of mechanical stress. However, the microstructural network of greases with higher oil viscosities is much weaker, showing large spaces among fibres and resulting in lower consistency. It is also evident in the greases C4 and C2, which have similar thickening proportions. However, the grease C4 with a mineral oil base had different solvency (affinity of the base oil for a given thickener) and stronger capillary forces than the grease C2 with a PAO base oil. The biogenic greases behaved differently from the conventional greases due to their different NLGI classes and dropping points. Regarding the temperature behaviour of all lubricating greases, it can be observed that higher temperatures ensure that the capillary forces become weak. The viscosity of the lubricating greases decreased by a higher temperature, simultaneously reducing the flow resistance force.

The difference in the second series of tests was that short deformation intervals were carried out, i.e., a short oscillation stage was always carried out

between the increase steps of the normal force up to 40 N, in which the storage and loss modulus were recorded. It allows the behaviour of the storage and loss modulus to be observed. For example, figure 4.13 shows the four tested lithium greases with different proportions of thickener at the tested temperature of 20 °C. It can be seen that the greases with a higher thickener content, C1 and C3, show a more constant course of the storage and loss modulus. However, even in the case of greases with a higher thickener content, the lower the thickener content, the more significant the change in the property of the grease per stress section (increase in the applied normal force). For example, the storage and loss modulus of grease C3 increases slightly with increasing squeeze pressure. Furthermore, it can be determined for greases C1 and C3 that the distance between the storage and loss modulus remains constant. For the greases with a lower thickener content (C2 and C4), it can be seen that the storage modulus continues to decrease throughout the stress and approaches the loss modulus. The results suggest that, in addition to the dependence on the soap content, the base oil also influences the behaviour of the lubricating greases in this series of tests.

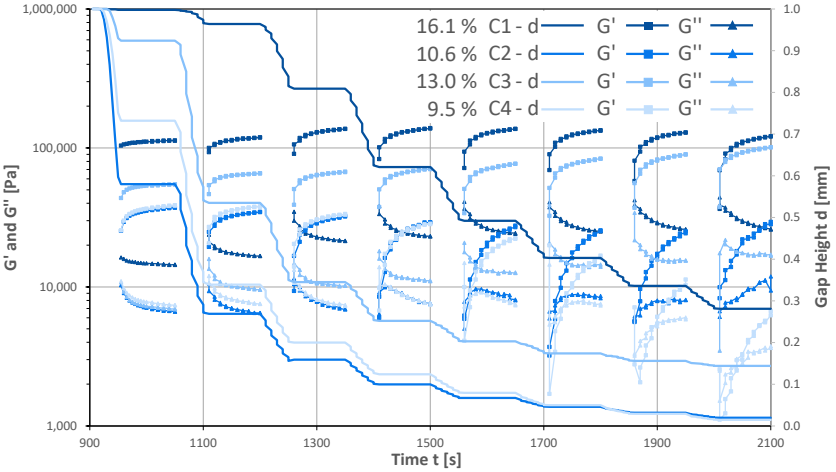

Figure 4.13: Short normal force-dependent lubrication grease deformation intervals with oscillation phases between the normal force increase up to 40 N at 20 °C

In addition, the bottom plate of the rheometer was replaced by a reflective

surface for some of the squeeze tests to asses any changes in the microstructural network of the greases analysed during the squeeze tests. After the squeeze tests, it allowed the samples to be examined directly under a reflected-light microscope, both in the centre and at the edge of the sample. These respective images could check the homogeneity and the distribution of the agglomerates. It could be observed that the greases did not show any significant changes regarding the agglomerates in the outer area and the centre of the mirror. The shape and size of the agglomerates were unchanged in all greases. Thus, it can be stated that the applied normal force did not cause any change in the number and shape of thickener agglomerates within the greases, i.e., that no significant plastic deformation of the agglomerates occurred, but only the lubricant squeeze flow between the two parallel surfaces. Figure 4.14, in which the grease C1 is shown, is an example.

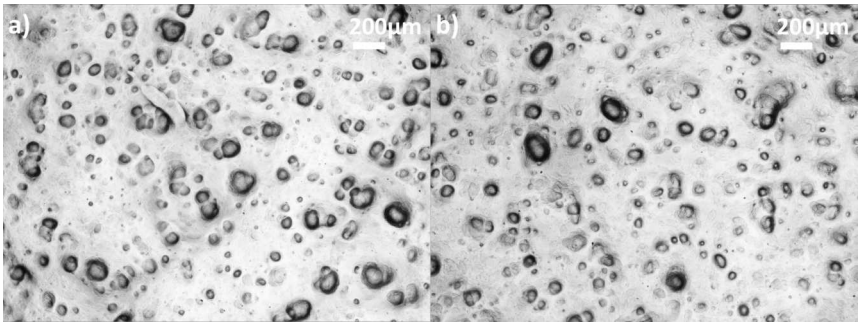

Figure 4.14: Reflected light microscope image of grease C1 after squeeze test a) in the centre of the sample, b) at the edge of the sample

Further exciting aspects regarding the squeeze tests can provide future investigations of lubricating greases subjected to rheological stress. The results of this series of measurements can then be compared with the findings obtained in this thesis. Furthermore, evaluating the area under the curve for $d(F_N)$ is interesting. The area represents the applied energy for the deformation of the grease and can serve as a critical figure for the losses due to deformation in real bearing applications. It could show how the grease is compressed between the cage pocket, the rolling elements, and the cage and its guiding surface.

5 Conclusions and Outlook

This thesis aims to investigate the mechanisms of lubricating grease's mechanical structural degradation through various experimental investigations to model them and present them in analytical form. The investigations were carried out as part of the "Tribiofett" research project in cooperation with the University of Huelva and the Hamburg University of Applied Sciences. The experimental investigations were carried out with various measuring devices, which led to a detailed analysis of the structural degradation of a significant number of lubricating greases, conventional and completely biogenic model greases, from an energy point of view.

The following chapter summarises the experiments' results and provides the corresponding conclusions. A brief assessment is made of the knowledge gained from the results by evaluating them. In addition, future test procedures and further possibilities for ongoing research on structural degradation of lubricating greases are presented.

5.1 Conclusions

The following conclusions can be drawn from the experiments performed.

1. An optical light microscope was suitable for visualising the macrostructure and agglomerates within the lubricating greases. SEM and AFM measurements were suitable for microstructural analyses. A suitable sample preparation protocol was necessary for the optical observations of the structural degradation behaviour of lubricating greases. The methods used in this work allowed minor changes to the structural skeleton of the grease.

2. The combination of thickener and base oil proved that the base oil used in each case also influences the structural network. The higher the thickener content of the lubricating grease, the larger the agglomerates in the lubricating grease.

3. The grease wear parameter R_{tee} provided essential results on the structural degradation of lubricating greases caused by mechanical stress. It was found that the higher the parameter is, the lower the structural degradation in the lubricating grease under stress. Thus, it was found that greases with a higher thickener content led to lower R_{tee}-values, which meant more significant structural degradation in the stressed grease.

4. The type of thickener, which affects the macro and microstructural skeletons, significantly influences the internal frictional energy, even more than the thickener content or the base oil used. Thus, lithium and calcium greases showed less structural degradation, i.e., less shear-induced structural changes, than polyurea or biogenic greases. It means that the structural skeletons of lithium and calcium greases dispel less mechanical energy during the shearing process.

5. The new Calidus measuring cell provides accurate temperature results that are close to the values of the PTD measuring cell. The conventional PTD configuration provided the average grease mass temperature, while the Calidus cell indicated the local temperature within the gap. In addition, the Calidus-based temperature measurements were more thorough, unlike the PTD cell, as the sensors almost touched the grease.

6. The grease's wear can be attributed mainly to the structural skeleton of the thickener, which also means that in the case of the base oil, there is no dissipation of the energy introduced into the tribological system. It means that all the energy introduced is dissipated in heat, generating wear volume on the solid.

7. It was found that it is not the absolute concentration of the thickener that is decisive for internal frictional heating; it is also the thickener and base oil type. Thus, lubricating greases, which showed the most negligible structural degradation due to stress, exhibited the lowest temperature changes within the grease. Thus, the higher values of the parameter R_{tee} meant that the temperature change (ΔT) within the lubricating grease was low. In this sense, R_{tee}-values showed that the polyurea grease investigated was hardly influenced by temperature, which indicates that the structural skeleton of polyurea greases supports shear-induced structural degradation within a tested temperature range better than other lubricating greases.

8. The specific heat capacities of the conventional greases analysed correlate with their specific density values, so a higher specific density is associated with a higher heat capacity. The specific heat capacities of the respective greases were directly involved in the temperature change profile.

9. None of the pure biogenic greases tested could be examined at temperatures above 40 °C, which is significant compared to conventionally produced greases, as pure biogenic greases should also be developed for use in high-temperature ranges.

10. The rheo-destruction tests provided a further opportunity to quantify grease wear better. The findings emphasise that shear stress and temperature are decisive factors for the permanent degradation of the microstructure of lubricating greases. It was confirmed that the consistency of the greases decreases at higher temperatures, which is due to both the viscosity-temperature dependence of the base oil and a weakening of the Van der Waals and capillary forces, which are responsible for the linkage in the structural skeleton of the greases.

11. The shape and size of the thickener particles, the structural network or agglomerates distribution, and the thickener content affected the squeeze flow behaviour. Summarising, the squeeze tests showed that the particle density significantly influences the results, the capillary forces - which depend on the base oil's viscosity - and the oil separation capacity.

Despite all the results obtained, it should be noted that this thesis examined a small selection of lubricating greases and that further investigations should verify the transferability of the findings. Nevertheless, the parameter R_{tee} should be emphasised in particular. It provides an opportunity to quantify the wear of lubricating greases better through practical tests. Regarding sustainability, it should be considered that the pure biogenic lubricating greases used in this thesis do not yet represent a possible alternative to conventional lubricating greases. The investigations showed that pure biogenic lubricating greases need further development regarding their reliability and temperature resistance. The newly developed Calidus temperature measuring cell should also be emphasised, as it can provide more precise temperature values due to the measuring cell material's lower inertia and the sensors' better installation position.

5.2 Outlook

Finally, it is worth pointing out that all lubricating greases analysed should generally be investigated by further research. In principle, it would be helpful to analyse the rheo-destruction and squeeze tests comprehensively. In addition, a further series of squeeze tests could be added. Stressed lubricating greases should also be analysed using the same test procedure. The results obtained could then be compared with those in this thesis concerning the behaviour of the lubricating greases after stress. Modifying the Calidus measuring cell would also be helpful, as it can provide more precise temperature values due to the measuring cell material's lower inertia and the sensors' better installation position. Only the plate surface requires adaptation to correspond to that of a conventional PTD measuring cell in terms of stability (compression) and texture (roughness) and to achieve more accurate rheological measurement results in the future. This improvement of the measuring cell surface would lead to even more precise temperature measurements. As a result, developing a model that combines the temperature developments of a lubricating grease during the friction process with those of a wear model could also be advanced. Further results could also be provided by investigations using a tribocell or a tribometer, which could also analyse different temperature ranges.

It is recommended that the research carried out as part of this thesis be extended. Lubricating greases with the same ingredients should be used, but the percentage of thickener should not vary. For example, the percentages should be set at 10 wt.%, 15 wt.% and 20 wt.%. In addition, all base oil-thickener combinations should be used, resulting in many greases to be analysed. This measure enables a detailed estimation of the weighted percentage of the thickener on the structural degradation of lubricating greases. Biogenic lubricating greases also require adaptation or further development in order to replace conventional lubricating greases in the near future. Tests with deliberately high temperatures are interesting for these further developed, purely biogenic lubricating greases. In addition, investigations into the material ageing process of these lubricating greases may also be of interest. It would allow better conclusions to be drawn about the service life of the ingredients used, particularly the thickeners.

Besides the Tribiofett research project, further research is also being conducted into developing environmentally friendly lubricants. In 2017, the "PHAT" research project was launched on the topic of "Bio-based alternative for thickeners and binders in lubricant applications", which was funded by the Federal

Ministry of Education and Research (BMBF) with 1.25 million euros. One of the companies involved in the project was FUCHS Schmierstoffe GmbH, which produced the lubricating greases for this thesis. The research project, which has now been completed, focussed on thickeners and binders made from biotechnologically produced PHA (polyhydroxyalkanoates) to obtain a sustainable alternative to conventional thickener products. The chemically modified samples tested during the project showed promising thickening properties in laboratory tests. In addition, initial samples showed a positive thickening effect in base oils and proved advantageous in the end application [170]. At the end of the PHAT project period, it became clear that although the overarching aim was already within reach, further research was needed.

For this reason, the follow-up project "PHATICUS" was launched, which is planned to run for three years until the end of March 2024 [171]. This research project aims to focus on the scale-up of the fermentation process. At the same time, the life cycle and end-of-life properties of the PHA-based thickener and the lubricant formulations developed are to be investigated. In addition, the field of application of PHA-based lubricants is to be expanded to increase the viscosity of all common base oils, including mineral oil, among other aspects [172]. However, it remains to be discovered to what extent biogenic lubricating greases, in general, can reduce or even replace the proportion of conventional lubricating greases and how long this will take.

Bibliography

[1] W. J. Bartz, *Energieeinsparung durch tribologische Maßnahmen* (Handbuch der Tribologie und Schmierungstechnik), in German. Ehningen bei Böblingen: Expert-Verlag, 1988, vol. 2, 92 pp., ISBN: 978-3-816-90314-7.

[2] W. Dresel and R.-P. Heckler, "Lubricating grease", in *Lubricants and Lubrication*, T. Mang and W. Dresel, Eds., 2., vollst. überarb. u. erw. Auflage, Weinheim: Wiley-VCH, 2007, pp. 603–646, ISBN: 978-3-527-61033-4.

[3] R. Shah, R. Chen and M. Woydt, "The effects of energy efficiency and resource consumption on environmental sustainability", *Lubricants*, vol. 9, no. 12, 2021. DOI: 10.3390/lubricants9120117.

[4] M. Woydt, "The importance of tribology for reducing CO2 emissions and for sustainability", *Wear*, vol. 474-475, 2021, ISSN: 0043-1648. DOI: 10.1016/j.wear.2021.203768.

[5] F. Bongardt and M. König, "Additive für biologisch rasch abbaubare Schmierstoffe", in German, *Tribologie + Schmierungstechnik*, vol. 03, no. 58, pp. 56–61, 2011.

[6] P. M. Lugt and D. M. Pallister, *Grease lubrication in rolling bearings* (Tribology in practice series), 1. ed. Chichester: Wiley, 2013, 444 pp., ISBN: 978-1-1184-8397-8.

[7] E. Kuhn, *Zur Tribologie der Schmierfette, Eine energetische Betrachtungsweise des Reibungs- und Verschleißprozesses*, in German, 2., neu bearbeitete und erweiterte Auflage. Renningen: Expert-Verlag, 2017, 227 pp., ISBN: 978-3-816-93339-7.

[8] European Commission, Ed. "Reach regulation, To protect human health and the environment against the harmful effects of chemical substances". (2023), [Online]. Available: https://environment.ec.europa.eu/topics/chemicals/reach-regulation_en (visited on 15/08/2023).

[9] National Lubricating Grease Institute, Ed., "Lubricating greases guide", Kansas City, 2006.

[10] J. M. Franco, M. A. Delgado, C. Valencia, M. C. Sánchez and C. Gallegos, "Mixing rheometry for studying the manufacture of lubricating greases", *Chemical Engineering Science*, vol. 60, no. 8, pp. 2409–2418, 2005, 5th International Symposium on Mixing in Industrial Processes (ISMIP5), ISSN: 0009-2509. DOI: 10.1016/j.ces.2004.10.042.

[11] A. Rezasoltani and M. M. Khonsari, "On monitoring physical and chemical degradation and life estimation models for lubricating greases", *Lubricants*, vol. 4, no. 3, 2016. DOI: 10.3390/lubricants4030034.

[12] A. Rezasoltani and M. M. Khonsari, "On the correlation between mechanical degradation of lubricating grease and entropy", *Tribology letters*, vol. 56, no. 2, pp. 197–204, 2014, ISSN: 1573-2711. DOI: 10.1007/s11249-014-0399-8.

[13] A. Gurt and M. Khonsari, "The use of entropy in modeling the mechanical degradation of grease", *Lubricants*, vol. 7, no. 10, 2019. DOI: 10.3390/lubricants7100082.

[14] Y. Zhou, "On the mechanical ageing of lubricating greases", PhD Thesis, University of Twente, Enschede, 2018. [Online]. Available: 10.3990/1.9789036546140.

[15] R. M. Mortier, M. F. Fox and S. T. Orszulik, Eds., *Chemistry and Technology of Lubricants*, 3. ed., Dordrecht: Springer Netherlands and Springer, 2010, 560 pp., ISBN: 978-1-4020-8662-5.

[16] L. Hamnelid, "Introduction to rheology of lubricating grease publication", in *ELGI Rheology Book, The Rheology of Lubricating Grease*, C. Balan, Ed., Amsterdam, Netherlands, 1999-08-07, pp. 2–19. [Online]. Available: https://www.elgi.org/wp-content/uploads/Introduction-to-Rheology-of-Lubricating-Grease-Publication.pdf (visited on 02/04/2022).

[17] Kyodo Yushi Co., Ltd., Ed. "History of grease, Early history of lubricant". (2023), [Online]. Available: https://www.kyodoyushi.co.jp/english/knowledge/grease/history (visited on 11/12/2023).

[18] W. J. Bartz, *Zur Geschichte der Tribologie* (Handbuch der Tribologie und Schmierungstechnik), in German. Ehningen bei Böblingen: Expert-Verlag, 1988, vol. 1, 148 pp., ISBN: 9-783-816-90313-0.

[19] R. Zechel *et al.*, *MOLYKOTE*, in German. München, 1990, 552 pp., ISBN: 978-3-407-25082-7.

[20] W. J. Bartz, *Einführung in die Tribologie und Schmierungstechnik, Tribologie - Schmierstoffe - Anwendungen ; mit 142 Tabellen*, in German. Renningen: Expert-Verlag, 2010, 372 pp., ISBN: 9-783-816-92830-0.

[21] Exxon Mobil Corporation, Ed., "Grease, Its components and characteristics", 2009. [Online]. Available: https://www.mobil.com.de/industrial/-/media/files/global/us/industrial/tech-topics/tt-components-and-characteristics-of-grease_en.pdf (visited on 19/12/2023).

[22] G. Gow, "Lubricating grease", in *Chemistry and Technology of Lubricants*, R. M. Mortier, M. F. Fox and S. T. Orszulik, Eds., 3. ed., Dordrecht: Springer Netherlands and Springer, 2010, pp. 411–432, ISBN: 978-1-4020-8662-5. DOI: 10.1023/b105569_14.

[23] LUMITOS AG, Ed. "Öle". in German, Chemie.de. (2017), [Online]. Available: https://www.chemie.de/lexikon/%C3%83%C2%B6le.html (visited on 04/12/2017).

[24] LUMITOS AG, Ed. "Schmieröl". in German, Chemie.de. (2017), [Online]. Available: http://www.chemie.de/lexikon/Schmier%C3%83%C2%B6l.html (visited on 04/12/2017).

[25] W. Mader, *Hinweise zur Anwendung von Schmierfetten*, in German. Hannover: Vincentz, 1979, 148 S, ISBN: 978-3-878-70164-4.

[26] W. J. Bartz, *Schmierfette, Zusammensetzung, Eigenschaften, Prüfung und Anwendung* (Kontakt & Studium), in German, 2., vollst. neu bearb. Aufl. Renningen: Expert-Verlag, 2010, vol. 500, ca. 400 S. ISBN: 978-3-816-92959-8.

[27] DIN 51825:2004-06, *Schmierstoffe - Schmierfette - Einteilung und Anforderungen*, in German (Berlin), 1st Jun. 2004. [Online]. Available: https://www.beuth.de/de/norm/din-51825/64088036 (visited on 07/12/2017).

[28] M. A. Delgado, S. Secouard, C. Valencia and J. M. Franco, "On the steady-state flow and yielding behaviour of lubricating greases", *Fluids*, vol. 4, no. 1, 2019, ISSN: 2311-5521. DOI: 10.3390/fluids4010006.

[29] M. A. Delgado, C. Valencia, M. C. Sánchez, J. M. Franco and C. Gallegos, "Influence of soap concentration and oil viscosity on the rheology and microstructure of lubricating greases", *Industrial & Engineering Chemistry Research*, vol. 45, no. 6, pp. 1902–1910, 2006, ISSN: 0888-5885. DOI: 10.1021/ie050826f.

[30] M. A. Delgado, M. C. Sánchez, C. Valencia, J. M. Franco and C. Gallegos, "Relationship among microstructure, rheology and processing of a lithium lubricating grease", *Chemical Engineering Research and Design*, vol. 83, no. 9, pp. 1085–1092, 2005, ISSN: 0263-8762. DOI: 10.1205/cherd.04311.

[31] R. Mas and A. Magnin, "Rheology of colloidal suspensions: Case of lubricating greases", *Journal of Rheology*, vol. 38, no. 4, pp. 889–908, 1994. DOI: 10.1122/1.550598.

[32] S. Chatra K. R. and P. M. Lugt, "Channeling behavior of lubricating greases in rolling bearings: Identification and characterization", *Tribology International*, vol. 143, p. 106 061, 2020, ISSN: 0301-679X. DOI: 10.1016/j.triboint.2019.106061.

[33] G. Klucker and P. Baumgartner, "Tribologische Untersuchungen zum Reibungs- und Verschleißverhalten von Modellfetten an einem Kugel-Scheibe-Tribometer", Maschinenbau und Produktion, in German, Diplomarbeit, Hochschule für Angewandte Wissenschaften Hamburg, Hamburg, 2011-10-01.

[34] CASTROL Austria GmbH, Ed. "Fette". in German. (2017), [Online]. Available: https://www.castrol.com/de_at/austria/services/schmierstofftechnik-uebersicht/schmierstofftechnik-fette.html (visited on 07/12/2017).

[35] K. Meyer and H. Kloß, *Reibung und Verschleiß geschmierter Reibsysteme, Eine physikalisch-chemische Betrachtung geschmierter Reibsysteme* (Reihe Technik), in German. Ehningen bei Böblingen: Expert-Verlag, 1993, 199 pp., ISBN: 978-3-816-90564-6.

[36] O. Pigors, *Werkstoffe in der Tribotechnik, Reibung, Schmierung und Verschleissbeständigkeit von Werkstoffen und Bauteilen; mit 189 Tabellen*, in German, 1. Aufl. Leipzig: Dt. Verl. für Grundstoffindustrie, 1993, 546 pp., ISBN: 978-3-342-00658-9.

[37] W. H. Dresel, "Moderne Schmierfette mit verlängerter Lebensdauer", in German, *Tribologie und Schmierungstechnik*, vol. 36, no. 6, pp. 305–311, 1989.

[38] API 1509, *Base oil interchangeability guidelines for passenger car engine oils and diesel engine oils*, 1st Feb. 2022. [Online]. Available: https://www.api.org/products-and-services/engine-oil/documents/api-1509-documents (visited on 23/10/2023).

[39] Noria Corporation, Ed. "Base oil groups explained". (2012), [Online]. Available: https://www.machinerylubrication.com/Read/29113/base-oil-groups (visited on 18/10/2023).

[40] G. Schmidt, "Synthetische Schmierfette, Stand der Technik - Industrielle Anwendung", in German, *Tribologie und Schmierungstechnik*, vol. 35, no. 1, 1988.

[41] U. J. Möller and J. Nassar, *Schmierstoffe im Betrieb, Mit 351 Tabellen* (ExxonMobil), in German, 2. Aufl. Berlin: Springer, 2002, 873 pp., ISBN: 978-3-540-41909-9.

[42] D. Kempkes, "Einsatz biogener Schmierstoffe in Windkraftanlagen", in German, *Tribologie und Schmierungstechnik*, vol. 54, no. 3, 2007.

[43] H. Czichos and K.-H. Habig, Eds., *Tribologie-Handbuch, Tribometrie, Tribomaterialien, Tribotechnik*, in German, 4., vollst. überarb. und erw. Aufl., Wiesbaden: Springer Vieweg, 2015, 794 pp., ISBN: 9783834822369.

[44] DIN 51818:1981-12, *Schmierstoffe - Konsistenz-Einteilung für Schmierfette - NLGI-Klassen*, in German (Berlin), 1st Dec. 1981. DOI: 10.31030/1258019. (visited on 09/03/2023).

[45] H. Wittel, D. Jannasch, J. Voßiek and C. Spura, *Roloff/Matek Maschinenelemente, Normung, Berechnung, Gestaltung*, in German, 23. Aufl. 2017. Wiesbaden: Springer Fachmedien Wiesbaden and Springer Vieweg, 2017, ISBN: 978-3-658-17895-6. DOI: 10.1007/978-3-658-17896-3.

[46] R. Luther, "Lubricants in the environment", in *Lubricants and Lubrication*, T. Mang and W. Dresel, Eds., 2., vollst. überarb. u. erw. Auflage, Weinheim: Wiley-VCH, 2007, pp. 115–165, ISBN: 978-3-527-61033-4.

[47] W. J. Bartz, "Lubricants and the environment", *Tribology International*, vol. 31, pp. 35–47, 1998, ISSN: 0301-679X.

[48] B. Wilson, "Lubricants and functional fluids from renewable sources", *Industrial Lubrication and Tribology*, vol. 50, no. 1, pp. 6–15, 1998, ISSN: 0036-8792. DOI: 10.1108/00368799810781274.

[49] S. Boyde, "Green lubricants. environmental benefits and impacts of lubrication", *Green Chemistry*, vol. 4, no. 4, pp. 293–307, 2002, ISSN: 1463-9262. DOI: 10.1039/B202272A.

[50] J. Salimon, N. Salih and E. Yousif, "Biolubricants: Raw materials, chemical modifications and environmental benefits", *European Journal of Lipid Science and Technology*, vol. 112, no. 5, pp. 519–530, 2010, ISSN: 1438-7697. DOI: 10.1002/ejlt.200900205.

[51] V. F. Medina, "Evaluation of environmentally acceptable lubricants (eals) for dams managed by the u.s. army corps of engineers victor f. medina", ERDC-WQTN-MS-9, 2015.

[52] D. Theodori, R. J. Saft, H. Krop and P. V. Broekhuizen, "Development of criteria for the award of the european eco-label to lubricants, Ivam research and consultancy on sustainability", 2004. [Online]. Available: https://produktinfo.blauer-engel.de/uploads/criteriafile/en/DE-UZ%20178-201407-en%20Criteria-V5.pdf (visited on 25/06/2022).

[53] Blue Angel - The German Ecolabel, Ed., "Biodegradable lubricants and hydraulic fluids, Basic award criteria", Version 5, 2014. [Online]. Available: https://produktinfo.blauer-engel.de/uploads/criteriafile/en/DE-UZ%20178-201407-en%20Criteria-V5.pdf (visited on 12/05/2022).

[54] European Commission Publications Office, Ed., "Revision of the european ecolabel criteria for lubricants, Final technical report", Criteria proposal for revision of EU ecolabel criteria, 2018. DOI: 10.2760/58736.

[55] R. Sánchez, J. M. Franco, M. A. Delgado, C. Valencia and C. Gallegos, "Effect of thermo-mechanical processing on the rheology of oleogels potentially applicable as biodegradable lubricating greases", *Chemical Engineering Research and Design*, vol. 86, no. 10, pp. 1073–1082, 2008, ISSN: 0263-8762. DOI: 10.1016/j.cherd.2008.05.002.

[56] R. Sánchez, J. M. Franco, M. A. Delgado, C. Valencia and C. Gallegos, "Development of new green lubricating grease formulations based on cellulosic derivatives and castor oil", *Green Chemistry*, vol. 11, no. 5, pp. 686–693, 2009, ISSN: 1463-9262. DOI: 10.1039/B820547G.

[57] R. Sánchez, M. Fiedler, E. Kuhn and J. Franco, "Tribological characterization of green lubricating greases formulated with castor oil and different biogenic thickener agents: A comparative experimental study", *Industrial Lubrication and Tribology*, vol. 63, pp. 446–452, 2011, ISSN: 0036-8792. DOI: 10.1108/00368791111169034.

[58] R. Sánchez, J. Franco, M. Delgado, C. Valencia and C. Gallegos, "Thermal and mechanical characterization of cellulosic derivatives-based oleogels potentially applicable as bio-lubricating greases: Influence of ethyl cellulose molecular weight", *Carbohydrate Polymers*, vol. 83, pp. 151–158, 2011. DOI: 10.1016/j.carbpol.2010.07.033.

[59] R. Sánchez, G. B. Stringari, J. M. Franco, C. Valencia and C. Gallegos, "Use of chitin, chitosan and acylated derivatives as thickener agents of vegetable oils for bio-lubricant applications", *Carbohydrate Polymers*, vol. 85, no. 3, pp. 705–714, 2011. DOI: 10.1016/j.carbpol.2011.03.049.

[60] J. E. Martín Alfonso, R. Yañez, C. Valencia, J. M. Franco and M. J. Díaz, "Optimization of the methylation conditions of kraft cellulose pulp for its use as a thickener agent in biodegradable lubricating greases", *Industrial & Engineering Chemistry Research*, vol. 48, no. 14, pp. 6765–6771, 2009, ISSN: 0888-5885. DOI: 10.1021/ie9002766.

[61] N. Núñez, J. E. Martín-Alfonso, C. Valencia, M. C. Sánchez and J. M. Franco, "Rheology of new green lubricating grease formulations containing cellulose pulp and its methylated derivative as thickener agents", *Industrial Crops and Products*, vol. 37, no. 1, pp. 500–507, 2012, ISSN: 0926-6690. DOI: 10.1016/j.indcrop.2011.07.027.

[62] R. Sánchez, J. M. Franco, M. A. Delgado, C. Valencia and C. Gallegos, "Rheological and mechanical properties of oleogels based on castor oil and cellulosic derivatives potentially applicable as bio-lubricating greases: Influence of cellulosic derivatives concentration ratio", *Journal of Industrial and Engineering Chemistry*, vol. 17, no. 4, pp. 705–711, 2011, ISSN: 1226-086X. DOI: 10.1016/j.jiec.2011.05.019.

[63] R. Sánchez, C. Valencia and J. M. Franco, "Rheological and tribological characterization of a new acylated chitosan–based biodegradable lubricating grease: A comparative study with traditional lithium and calcium greases", *Tribology Transactions*, vol. 57, no. 3, pp. 445–454, 2014. DOI: 10.1080/10402004.2014.880541.

[64] N. Acar, "An energetical approach to study the structural degradation of traditional and biogenic lubricating greases", PhD Thesis, University of Huelva, Huelva, 2022.

[65] N. Acar, E. Kuhn and J. M. Franco, "Tribological and rheological characterization of new completely biogenic lubricating greases: A comparative experimental investigation", *Lubricants*, vol. 6, no. 2, 2018. DOI: 10.3390/lubricants6020045.

[66] N. Acar, J. M. Franco, E. Kuhn, D. E. P. Gonçalves and J. H. O. Seabra, "Tribological investigation on the friction and wear behaviors of biogenic lubricating greases in steel–steel contact", *Applied Sciences*, vol. 10, no. 4, 2020, ISSN: 2076-3417. DOI: 10.3390/app10041477.

[67] B. B. Farrington, "The fine structure of lubricating greases", *Annals of the New York Academy of Sciences*, vol. 53, no. 4, pp. 979–986, 1951, ISSN: 0077-8923. DOI: 10.1111/j.1749-6632.1951.tb54248.x.

[68] C. Roman, C. Valencia and J. M. Franco, "Afm and sem assessment of lubricating grease microstructures: Influence of sample preparation protocol, frictional working conditions and composition", *Tribology letters*, vol. 63, no. 2, pp. 1–12, 2016, ISSN: 1573-2711. DOI: 10.1007/s11249-016-0710-y.

[69] Y. L. Ishchuk, *Lubricating Grease Manufacturing Technology*. New Delhi: New Age International (P) Ltd. Publishers, 2005, 224 pp., ISBN: 978-8-1224-1668-8.

[70] C. J. Boner, *Modern Lubricating Greases*. Shropshire: Scientific Publications, 1976, ISBN: 978-0-9006-4511-2. [Online]. Available: https://books.google.de/books?id=zL1ZAAAAYAAJ.

[71] M. C. Sánchez, J. M. Franco, C. Valencia, C. Gallegos, F. Urquiola and R. Urchegui, "Atomic force microscopy and thermo-rheological characterisation of lubricating greases", *Tribology letters*, vol. 41, no. 2, pp. 463–470, 2011, ISSN: 1573-2711. DOI: 10.1007/s11249-010-9734-x.

[72] E. Kuhn, "Friction and wear of a grease lubricated contact — an energetic approach", in *Tribology*, J. Gegner, Ed., Rijeka: IntechOpen, 2013, Ch. 9. DOI: 10.5772/55837.

[73] L. Ahme, E. Kuhn and M. A. Delgado, "On the optical assessment of the structural degradation of rheologically stressed lubricating greases", *Tribology International*, vol. 187, 2023, ISSN: 0301-679X. DOI: 10.1016/j.triboint.2023.108771.

[74] P. J. Shuff and L. J. Clarke, "Imaging of lubricating oil insolubles by electron microscopy", *Tribology International*, vol. 24, no. 6, pp. 381–387, 1991, ISSN: 0301-679X. DOI: 10.1016/0301-679X(91)90009-X.

[75] J. L. Mansot, P. Terech and J. M. Martin, "Structural investigation of lubricating greases", *Colloids and Surfaces*, vol. 39, no. 2, pp. 321–333, 1989, ISSN: 0166-6622. DOI: 10.1016/0166-6622(89)80283-5.

[76] S. Hurley and P. Cann, "Examination of grease structure by sem and afm techniques", *NLGI Spokesman*, vol. 65, pp. 17–26, 2001.

[77] I. Radulescu, A. V. Radulescu and F. Vasiliu, "Structure of lubricating greases by electron microscopy", *Journal of the Balkan Tribological Association*, vol. 11, pp. 453–459, 2005.

[78] P. Baart, B. van der Vorst, P. M. Lugt and R. A. van Ostayen, "Oil-bleeding model for lubricating grease based on viscous flow through a porous microstructure", *Tribology Transactions*, vol. 53, no. 3, pp. 340–348, 2010. DOI: 10.1080/10402000903283326.

[79] L. Ahme, E. Kuhn and M. A. Delgado, "Experimental study on the expended energy on structural degradation of lubricating greases", *Tribology letters*, vol. 70, no. 3, p. 81, 2022, ISSN: 1573-2711. DOI: 10.1007/s11249-022-01622-2.

[80] A. Hodapp, A. Conrad, B. Hochstein, K.-H. Jacob and N. Willenbacher, "Effect of base oil and thickener on texture and flow of lubricating greases: Insights from bulk rheometry, optical microrheology and electron microscopy", *Lubricants*, vol. 10, no. 4, 2022. DOI: 10.3390/lubricants10040055.

[81] P. Sengupta and J. W. Noordermeer, "A comparative study of different techniques for microstructural characterization of oil extended thermoplastic elastomer blends", *Polymer*, vol. 46, no. 26, pp. 12 298–12 305, 2005, ISSN: 0032-3861. DOI: 10.1016/j.polymer.2005.10.075.

[82] E. Vámos, J. Szamos and G. Bede, "Structural changes in lubricating greases and their mixtures during service", *Wear*, vol. 25, no. 2, pp. 189–197, 1973, ISSN: 0043-1648. DOI: 10.1016/0043-1648(73)90071-9.

[83] N. W. Rizzo, L. Irwin, M. D. Foster and M. Funk, "Extracting, imaging, and quantifying soap fibers in grease", *NLGI Spokesman*, vol. 60, pp. 24–25, 1996.

[84] F. Cyriac, P. M. Lugt, R. Bosman, C. J. Padberg and C. H. Venner, "Effect of thickener particle geometry and concentration on the grease ehl film thickness at medium speeds", *Tribology letters*, vol. 61, no. 2, p. 18, 2016, ISSN: 1573-2711. DOI: 10.1007/s11249-015-0633-z.

[85] G. Moreno, C. Valencia, M. V. de Paz, J. M. Franco and C. Gallegos, "Rheology and microstructure of lithium lubricating greases modified with a reactive diisocyanate-terminated polymer: Influence of polymer addition protocol", *Chemical Engineering and Processing: Process Intensification*, vol. 47, no. 4, pp. 528–538, 2008, ISSN: 0255-2701. DOI: 10.1016/j.cep.2006.11.006.

[86] G. Moreno, C. Valencia, J. M. Franco, C. Gallegos, A. Diogo and J. Bordado, "Influence of molecular weight and free nco content on the rheological properties of lithium lubricating greases modified with nco-terminated prepolymers", *European Polymer Journal*, vol. 44, no. 7, pp. 2262–2274, 2008, ISSN: 0014-3057. DOI: 10.1016/j.eurpolymj.2008.04.047.

[87] M. Paszkowski and S. Olsztyńska-Janus, "Grease thixotropy: Evaluation of grease microstructure change due to shear and relaxation", *Industrial Lubrication and Tribology*, vol. 66, no. 2, pp. 223–237, 2014, ISSN: 0036-8792. DOI: 10.1108/ILT-02-2012-0014.

[88] R. Gallego, J. F. Arteaga, C. Valencia, M. J. Díaz and J. M. Franco, "Gel-like dispersions of hmdi-cross-linked lignocellulosic materials in castor oil: Toward completely renewable lubricating grease formulations", *ACS Sustainable Chemistry & Engineering*, vol. 3, no. 9, pp. 2130–2141, 2015. DOI: 10.1021/acssuschemeng.5b00389.

[89] S. Chatra K. R. and P. M. Lugt, "The process of churning in a grease lubricated rolling bearing: Channeling and clearing", *Tribology International*, vol. 153, p. 106 661, 2021, ISSN: 0301-679X. DOI: 10.1016/j.triboint.2020.106661.

[90] M. Behrendt, "Entwicklung eines Systemtribometers mit Abbildung mehrachsiger instationärer Beanspruchungskollektive zur Analyse von Reibung und Verschleiß im Mischreibungsgebiet im Kontext nasslaufender Umschlingungs-CVT", Institut für Produktentwicklung, in German, Dissertation, Universität Karlsruhe, Karlsruhe, 2009-05-01. [Online]. Available:

http://www.ipek.kit.edu/downloads/IPEK_FB_Band36_M_Behrendt.pdf (visited on 30/11/2017).

[91] DIN 50323-1:1988-11, *Tribologie - Teil 1: Begriffe*, in German (Berlin), 1st Nov. 1988. [Online]. Available: https://www.beuth.de/de/norm/din-50323-1/3118612 (visited on 07/12/2017).

[92] Great Britain. Department of Education and Science, *Lubrication (tribology), Education and Research: A Report on the Present Position and Industry's Needs*, in collab. with H. P. Jost. London: Her Majesty's Stationery Office, 1966. [Online]. Available: https://books.google.de/books?id=IkRUAAAAYAAJ.

[93] Gesellschaft für Tribologie e.V., Ed., "Arbeitsblatt 7, Verschleiß, Reibung. Definitionen, Begriffe, Prüfung", in German, Aachen, Arbeitsblatt 7, 2002. [Online]. Available: https://neu.gft-ev.de/wp-content/uploads/2002_AB_7_Tribologie.pdf (visited on 02/12/2017).

[94] T. Mang, "Lubricants in the tribological system", in *Lubricants and Lubrication*, T. Mang and W. Dresel, Eds., 2., vollst. überarb. u. erw. Auflage, Weinheim: Wiley-VCH, 2007, ISBN: 978-3-527-61033-4.

[95] G. Fleischer, H. Gröger and H. Thum, *Verschleiss und Zuverlässigkeit*, in German. Berlin: Verlag Technik, 1980, 244 pp.

[96] DIN 50281:1977-10, *Reibung in Lagerungen; Begriffe, Arten, Zustände, physikalische Größen*, in German (Berlin), 1st Oct. 1977. [Online]. Available: https://www.beuth.de/de/norm/din-50281/1619289 (visited on 07/12/2017).

[97] M. Woydt, *Reibung und Verschleiß von Werkstoffen und Dünnschichten, Bauteilen und Konstruktionen, Ursachen, Analyse, Optimierung ; mit 14 Tabellen* (Kontakt & Studium), in German. Renningen: Expert-Verlag, 2010, vol. 687, 227 pp., ISBN: 978-3-816-92793-8.

[98] E. Kuhn, "Tribologie - Masterkurs Skript Teil 1, Einführung - Geschichte der Tribologie - Allgemeine Terminologie", in German, 2016.

[99] DIN 50323-3:1993-12, *Tribologie - Reibung - Teil 3: Begriffe, Arten, Zustände, Kenngrößen*, in German (Berlin), 1st Dec. 1993. [Online]. Available: https://www.beuth.de/de/norm/din-50323-3/2197987 (visited on 07/12/2017).

[100] R. Gohar and H. Rahnejat, *Fundamentals of tribology*. London: Imperial College Press, 2008, 391 pp., ISBN: 978-1-8481-6184-9.

[101] M. S. Agerer. "Der Reibungskoeffizient". in German, Maschinenbau-Wissen.de. (2017), [Online]. Available: http://www.maschinenbau-wissen.de/skript3/mechanik/kinetik/289-reibungskoeffizient (visited on 27/11/2017).

[102] J. Ihme, *Schienenfahrzeugtechnik* (Lehrbuch), in German, 1. Auflage. Wiesbaden: Springer Vieweg, 2016, 270 pp., ISBN: 978-3-658-13540-9. DOI: 10.1007/978-3-658-13541-6.

[103] DIN 50323-2:1995-08, *Tribologie - Verschleiß - Teil 2: Begriffe*, in German (Berlin), 1st Aug. 1995. [Online]. Available: https://www.beuth.de/de/norm/din-50323-2/2571492 (visited on 07/12/2017).

[104] E. Kuhn, "Experimental grease investigations from an energy point of view", *Industrial Lubrication and Tribology*, vol. 51, no. 5, pp. 246–251, 1999, ISSN: 0036-8792. DOI: 10.1108/00368799910290935.

[105] M. A. Delgado, J. M. Franco, C. Valencia, E. Kuhn and C. Gallegos, "Transient shear flow of model lithium lubricating greases", *Mechanics of Time-Dependent Materials*, vol. 13, no. 1, pp. 63–80, 2009, ISSN: 1573-2738. DOI: 10.1007/s11043-008-9070-9.

[106] M. Delgado, C. Valencia, M. C. Sánchez, J. Franco and C. Gallegos, "Thermorheological behaviour of a lithium lubricating grease", *Tribol. Lett.*, vol. 23, pp. 47–54, 2006. DOI: 10.1007/s11249-006-9109-5.

[107] P. Cann, M. Webster, J. Doner, V. Wikstrom and P. Lugt, "Grease degradation in r0f bearing tests", *Tribology Transactions*, vol. 50, pp. 187–197, 2007. DOI: 10.1080/10402000701261003.

[108] R. W. Kühl, "Schmierfrist und Nachschmierung fettgeschmierter Wälzlager", in German, in *Einsatz von Wälzlagern bei extremen Betriebs- und Umgebungsbedingungen: Optimierung durch geeignete Konstruktion und Entwicklung von Wälzlagern, Schmierung und Abdichtung*, ser. Kontakt & Studium 574, W. J. Bartz, Ed., vol. 8, Expert-Verlag, 1998, pp. 141–151, ISBN: 9-783-816-91608-6.

[109] R. W. Kühl, "Prüfung von Gebrauchtschmierfetten aus Wälzlagern", in German, Göttingen, 2006.

[110] R. W. Kühl, "Aggressiv oder verträglich?, Verhalten von Schmierstoffen gegenüber Wälzlager-Werkstoffen", in German, Göttingen, 2007.

[111] R. Karbacher, "Fettschmierung von Wälzlagern bei oszillierender Beanspruchung; Grease lubrication of oscillating roller bearings, Technische Berichte", in German, *Tribologie und Schmierungstechnik*, vol. 45, no. 5, pp. 23–31, 1998.

[112] R. Karbacher, "Betrieb von Wälzlagern bei hohen Drehzahlen mit rotierendem Innen- oder Außenring", in German, in *Einsatz von Wälzlagern bei extremen Betriebs- und Umgebungsbedingungen: Optimierung durch geeignete Konstruktion und Entwicklung von Wälzlagern, Schmierung und Abdichtung*, ser. Kontakt & Studium 574, W. J. Bartz, Ed., vol. 11, Expert-Verlag, 1998, pp. 182–211, ISBN: 9-783-816-91608-6.

[113] R. Karbacher, "Steigerung der Gebrauchsdauer durch gezielte Auswahl der Lager und des Schmierstoffs, Technische Berichte", in German, *Tribologie und Schmierungstechnik*, vol. 45, no. 6, 1998.

[114] R. Karbacher, "Entwicklung und Prufung eines neuen Hochleistungsfettes fur hohe Drehzahlen", in German, *VDI BERICHTE*, vol. 1706, pp. 309–324, 2002, ISSN: 0083-5560.

[115] E. Kuhn, "Correlation between system entropy and structural changes in lubricating grease", *Lubricants*, vol. 3, no. 2, pp. 332–345, 2015. DOI: 10.3390/lubricants3020332.

[116] E. Kuhn, "Analysis of a grease-lubricated contact from an energy point of view", *International Journal of Materials & Product Technology - INT J MATER PROD TECHNOL*, vol. 38, 2010. DOI: 10.1504/IJMPT.2010.031891.

[117] T. Mezger, *Das Rheologie Handbuch, Für Anwender von Rotations- und Oszillations-Rheometern* (Farbe und Lack), in German, 5., vollständig überarbeitete Auflage. Hannover: Vincentz Network GmbH & Co. KG, 2016, 512 pp., ISBN: 978-3-866-30633-2.

[118] T. Mezger, *Angewandte Rheologie, Mit Joe Flow auf der Rheologie-Straße*, in German, 3. Auflage. Graz: Anton Paar GmbH, 2017, 196 Seiten, ISBN: 978-3-200-03652-9.

[119] D. I. Wilson, "What is rheology?", *Eye*, vol. 32, no. 2, pp. 179–183, 2018, ISSN: 1476-5454. DOI: 10.1038/eye.2017.267.

[120] L. Prandtl, "Betrachtungen zur Rheologie", in German, *Physikalische Blätter*, vol. 5, no. 4, pp. 161–172, 1949, https://doi.org/10.1002/phbl.19490050402, ISSN: 0031-9279. DOI: 10.1002/phbl.19490050402.

[121] K. Wilczyński, *Rheology in Polymer Processing, Modeling and Simulation* (Hanser eLibrary). Munich and Cincinnati: Carl Hanser Verlag GmbH & Co. KG, 2021, 377 Seiten, ISBN: 978-1-5699-0660-6.

[122] R. Czarny, "Effects of changes in grease structure on sliding friction", *Industrial Lubrication and Tribology*, vol. 47, no. 1, pp. 3–7, 1995, ISSN: 0036-8792. DOI: 10.1108/00368799510078638.

[123] M. A. Delgado, J. M. Franco and E. Kuhn, "Effect of rheological behaviour of lithium greases on the friction process", *Industrial Lubrication and Tribology*, vol. 60, no. 1, pp. 37–45, 2008, ISSN: 0036-8792.

[124] C. Balan and J. M. Franco, "Influence of the geometry on the transient and steady flow of lubricating greases", *Tribology Transactions*, vol. 44, no. 1, pp. 53–58, 2001. DOI: 10.1080/10402000108982426.

[125] Malvern Instruments Limited, Ed., "A basic introduction to rheology", 2016. [Online]. Available: https://cdn.technologynetworks.com/TN/Resources/PDF/WP160620BasicIntroRheology.pdf (visited on 30/01/2024).

[126] A. Y. Malkin, *Rheology Fundamentals* (Fundamental topics in rheology). Toronto, Ontario, Canada: ChemTec Publishing, 1994, 315 pp., ISBN: 978-1-895198-09-6. [Online]. Available: https://chemtec.org/products/1-895198-09-7 (visited on 15/06/2022).

[127] DIN 51810-2:2017-04, *Testing of lubricants - Testing rheological properties of lubricating greases*, in German (Berlin), 1st Apr. 2017. DOI: 10.31030/2639274. (visited on 07/12/2022).

[128] M. Paszkowski, "Some aspects of grease flow in lubrication systems and friction nodes", in *Tribology*, J. Gegner, Ed., Rijeka: IntechOpen, 2013, Ch. 3. DOI: 10.5772/55929.

[129] I. Couronne, G. Blettner and P. Vergne, "Rheological behavior of greases: Part i—effects of composition and structure", *Tribology Transactions*, vol. 43, no. 4, pp. 619–626, 2000. DOI: 10.1080/10402000008982386.

[130] C. Yanhai, J. Pan and J. Yang, "Effect of thermorheological properties on shear flow of grease in pipes", *Journal of chemical engineering of Japan*, vol. 49, pp. 815–823, 2016. DOI: 10.1252/jcej.15we235.

[131] T. E. Karis, R.-N. Kono and M. S. Jhon, "Harmonic analysis in grease rheology", *Journal of Applied Polymer Science*, vol. 90, no. 2, pp. 334–343, 2003, ISSN: 0021-8995. DOI: 10.1002/app.12548.

[132] M. Paszkowski, "Assessment of the effect of temperature, shear rate and thickener content on the thixotropy of lithium lubricating greases", *Proceedings of the Institution of Mechanical Engineers, Part J: Journal of Engineering Tribology*, vol. 227, no. 3, pp. 209–219, 2013, ISSN: 1350-6501. DOI: 10.1177/1350650112460950.

[133] A. Rezasoltani and M. M. Khonsari, "Experimental investigation of the chemical degradation of lubricating grease from an energy point of view", *Tribology International*, vol. 137, pp. 289–302, 2019, ISSN: 0301-679X. DOI: 10.1016/j.triboint.2019.05.006.

[134] H. Ito, M. Tomaru and T. Suzuki, "Physical and chemical aspects of grease deterioration in sealed ball bearings", *Lubrication Engineering*, vol. 44, pp. 872–879, 1988. [Online]. Available: https://api.semanticscholar.org/CorpusID:113442893.

[135] E. Kuhn, "Application of a thermodynamic concept for the analysis of structural degradation of soap thickened lubricating greases", *Lubricants*, vol. 6, no. 1, 2018. DOI: 10.3390/lubricants6010007.

[136] H. A. Abdel-Aal, "Thermodynamic modeling of wear", in *Encyclopedia of Tribology*, Q. J. Wang and Y.-W. Chung, Eds., Boston, MA: Springer US, 2013, pp. 3622–3636, ISBN: 978-0-387-92897-5. DOI: 10.1007/978-0-387-92897-5_1313.

[137] J. A. Osara and M. D. Bryant, "Thermodynamics of grease degradation", *Tribology International*, vol. 137, pp. 433–445, 2019, ISSN: 0301-679X. DOI: 10.1016/j.triboint.2019.05.020.

[138] M. Bryant, M. Khonsari and F. Ling, "On the thermodynamics of degradation", *Proceedings of The Royal Society A: Mathematical, Physical and Engineering Sciences*, vol. 464, pp. 2001–2014, 2008. DOI: 10.1098/rspa.2007.0371.

[139] Y. Zhou, R. Bosman and P. Lugt, "A master curve for the shear degradation of lubricating greases with a fibrous structure", *Tribology Transactions*, vol. 62, pp. 1–21, 2018. DOI: 10.1080/10402004.2018.1496304.

[140] S. Chatra K. R., J. A. Osara and P. M. Lugt, "Impact of grease churning on grease leakage, oil bleeding and grease rheology", *Tribology International*, vol. 176, p. 107 926, 2022, ISSN: 0301-679X. DOI: 10.1016/j.triboint.2022.107926.

[141] L. Ahme, E. Kuhn and M. A. Delgado, "An approach of the internal friction-dependent temperature changes for conventional and pure biogenic lubricating greases", *Friction*, vol. 12, no. 4, pp. 780–795, 2024, ISSN: 2223-7704. DOI: 10.1007/s40544-023-0818-7.

[142] R. Erbrecht Ed. and H. König Ed., *Das große Tafelwerk interaktiv, Ein Tabellen- und Formelwerk für den mathe-matisch-naturwissenschaftlichen Unterricht in den Sekundarstufen I und II*, Mathematik, Informatik, Astronomie, Physik, Chemie, Biologie ; für das Abitur empfohlen, in German, 1. Aufl. Berlin: Cornelsen, 2003, 168 pp., ISBN: 978-3-464-57144-6.

[143] H. Fricke, H. Frohne and P. Vaske, *Grundlagen der Elektrotechnik, Elektrische Netzwerke*, in German, 17., neubearb. Aufl. Stuttgart: Teubner, 1982, 733 pp., ISBN: 978-3-519-06403-9.

[144] A. Adhvaryu, C. Sung and S. Z. Erhan, "Fatty acids and antioxidant effects on grease microstructures", *Industrial Crops & Products*, vol. 21, no. 3, pp. 285–291, 2005. DOI: 10.1016/j.indcrop.2004.03.003.

[145] Y. Wang, P. Zhang, J. Lin and X. Gao, "Rheological and tribological properties of lithium grease and polyurea grease with different consistencies", *Coatings*, vol. 12, no. 4, 2022, ISSN: 2079-6412. DOI: 10.3390/coatings12040527.

[146] A. Rezasoltani and M. Khonsari, "An engineering model to estimate consistency reduction of lubricating grease subjected to mechanical degradation under shear", *Tribology International*, vol. 103, 2016, ISSN: 0301-679X. DOI: 10.1016/j.triboint.2016.07.012.

[147] J. Pan, C. Yanhai and J. Yang, "Effect of heat treatment on lubricating properties of lithium lubricating grease", *RSC Adv*, vol. 5, 2015. DOI: 10.1039/C5RA08917D.

[148] J. Osara and M. Bryant, "Temperature-only system degradation analysis", Austin Texas, USA, 2020. [Online]. Available: https://www.researchgate.net/publication/342110517_Temperature-Only_System_Degradation_Analysis (visited on 18/08/2022).

[149] DIN 51810:2017-04, *Prüfung von Schmierstoffen - Prüfung der rheologischen Eigenschaften von Schmierfetten*, in German (Berlin), 1st Apr. 2017. [Online]. Available: https://www.beuth.de/de/norm/din-51810-1/269916043 (visited on 09/11/2021).

[150] OLYMPUS EUROPA SE & CO. KG, Ed., "OLYMPUS Stream Online-Help, Stream 2.2", in German, Hamburg, 2016-08. (visited on 14/10/2020).

[151] European Chemicals Agency, Ed. "Lithium stearate, Density". (2022), [Online]. Available: https://echa.europa.eu/es/registration-dossier/-/registered-dossier/22040/4/5 (visited on 19/07/2022).

[152] National Center for Biotechnology Information, Ed. "Glyceryl monooleate, Density", PubChem. (2022), [Online]. Available: https://pubchem.ncbi.nlm.nih.gov/compound/Glyceryl-monooleate#section=Solubility (visited on 19/07/2022).

[153] European Chemicals Agency, Ed. "Fatty acids, tallow, calcium salts, Density". (2022), [Online]. Available: https://echa.europa.eu/es/registration-dossier/-/registered-dossier/5720/4/5 (visited on 19/07/2022).

[154] Polymer Properties Database, Ed. "Polyhydroxybutyrate, Density". (2022), [Online]. Available: https://polymerdatabase.com/polymers/poly3-hydroxybutyrate.html (visited on 19/07/2022).

[155] European Chemicals Agency, Ed. "Urea, Density". (2022), [Online]. Available: https://echa.europa.eu/de/registration-dossier/-/registered-dossier/16152/4/5 (visited on 19/07/2022).

[156] ChemicalBook Inc., Ed. "Ethyl cellulose, Density", chemicalbook.com. (2022), [Online]. Available: https://www.chemicalbook.com/ChemicalProductProperty_EN_CB6165620.htm (visited on 19/07/2022).

[157] European Chemicals Agency, Ed. "Castor oil, Density". (2022), [Online]. Available: https://echa.europa.eu/de/registration-dossier/-/registered-dossier/14599/4/5 (visited on 19/07/2022).

[158] W. F. Tinto, T. O. Elufioye and J. Roach, "Chapter 22 - waxes", in *Pharmacognosy*, S. Badal and R. Delgoda, Eds., Boston: Academic Press, 2017, pp. 443–455, ISBN: 978-0-12-802104-0. DOI: 10.1016/B978-0-12-802104-0.00022-6.

[159] OKS Spezialschmierstoffe GmbH, Ed. "Oils with high-performance additives for reliable lubrication, Properties of base oils". (2022), [Online]. Available: https://www.oks-germany.com/en/tribology/types-of-lubricants/oils/ (visited on 02/03/2022).

[160] AMD Oil Sales, Ed. "Sunflower oil, high oleic rbdw, Density", AMD Special Oil LLC. (2022), [Online]. Available: https://www.amdoilsales.com/products/ho-sunflower/ (visited on 19/07/2022).

[161] Kraft Chemical, Ed. "Safety data sheet mtc oil, Density". (2022), [Online]. Available: https://greenfield.com/wp-content/uploads/2018/11/MCT-Oil-SDS.pdf (visited on 19/07/2022).

[162] National Center for Biotechnology Information, Ed. "Cellulose, Density", PubChem. (2022), [Online]. Available: https://pubchem.ncbi.nlm.nih.gov/compound/CELLULOSE (visited on 19/07/2022).

[163] Wikipedia. "Glycerol monostearate, Density". I. Wikimedia Foundation, Ed. (2022), [Online]. Available: https://en.wikipedia.org/wiki/Glycerol_monostearate (visited on 19/07/2022).

[164] National Center for Biotechnology Information, Ed. "Glycerol, Density", PubChem. (2022), [Online]. Available: https://pubchem.ncbi.nlm.nih.gov/compound/Glycerol#section=Density (visited on 19/07/2022).

[165] National Center for Biotechnology Information, Ed. "1-hexadecanol (cetyl alcohol), Density", PubChem. (2022), [Online]. Available: https://pubchem.ncbi.nlm.nih.gov/compound/1-Hexadecanol#section=Density (visited on 19/07/2022).

[166] NETZSCH-Gerätebau GmbH, Ed. "Precise determination of the specific heat capacity by means of dsc". (2022), [Online]. Available: https://analyzing-testing.netzsch.com/en/training-know-how/tips-tricks/dsc/precise-determination-of-the-specific-heat-by-means-of-dsc (visited on 25/02/2022).

[167] NETZSCH-Gerätebau GmbH, Ed. "Specific heat capacity (cp)". (2022), [Online]. Available: https://analyzing-testing.netzsch.com/en/training-know-how/glossary/specific-heat-capacity-cp (visited on 25/02/2022).

[168] M. A. Delgado, "Rheo-destruction", Letter, Huelva, 4th Apr. 2019.

[169] P. M. Cann and H. A. Spikes, "Stle 1991 annual meeting", 1991.

[170] Fraunhofer-Institut für Umwelt-, Sicherheits- und Energietechnik UMSICHT, Ed. "PHAt: Natürliche Verdickungsmittel für abbaubare Schmierstoffe, Neue Rohstoffe für biobasierte Schmierstoffe durch Aufbereitung spezieller Polymere". in German. (2023), [Online]. Available: https://www.umsicht.fraunhofer.de/de/projekte/phat-natuerliche-verdickungsmittel.html (visited on 15/12/2023).

[171] Fraunhofer-Institut für Umwelt-, Sicherheits- und Energietechnik UMSICHT, Ed. "Aus PHAt wird PHAtiCuS, Forschung und Entwicklung umweltverträglicher Schmierstoffe geht in die nächste Phase". in German. (2023), [Online]. Available: https://www.phat-projekt.de/aktuelles/aus-phat-wird-phaticus-forschung-und-entwicklung-umweltvertr%C3%A4glicher-schmierstoffe-geht-in-die-n%C3%A4chste-phase (visited on 15/12/2023).

[172] Fraunhofer-Institut für Umwelt-, Sicherheits- und Energietechnik UMSICHT, Ed. "Über das Projekt, PHAtiCuS: Marktfähige Schmierstoffe auf PHA-Basis". in German. (2023), [Online]. Available: https://www.phat-projekt.de/ (visited on 15/12/2023).

A Scientific publications in this thesis

Annex Contents

A Scientific publications in this thesis

A.1 Experimental Study on the Expended Energy on Structural Degradation of Lubricating Greases

Leif Ahme[1], Erik Kuhn[1], Miguel Ángel Delgado Canto[2]

[1]Department of Mechanical Engineering and Production Management, Hamburg University of Applied Sciences, Hamburg, Germany

[2]Department of Chemical Engineering, University of Huelva, Huelva, Spain

Published in: Tribology Letters

Publishing company: Springer Nature

Editor-in-Chief: Nicholas D. Spencer

Volume 70, Issue 3, Article Number 81

Year: June 2022

DOI: 10.1007/s11249-022-01622-2

ISSN:1023-8883

E-ISSN:1573-2711

Impact Factor (2022): 3.2

CiteScore (2022): 5.3

JCR Category	Rank
Engineering (Mechanical Engineering)	153/631
Engineering (Mechanics of Materials)	106/391
Physics and Astronomy (Surfaces and Interfaces)	17/55
Materials Science (Surfaces, Coatings and Films)	41/131

Tribology Letters (2022) 70:81
https://doi.org/10.1007/s11249-022-01622-2

ORIGINAL PAPER

Experimental Study on the Expended Energy on Structural Degradation of Lubricating Greases

Leif Ahme[1] · Erik Kuhn[1] · Miguel Ángel Delgado Canto[2]

Received: 3 January 2022 / Accepted: 26 May 2022

Abstract
One of the keystones of tribological studies is the energetical approach to the lubrication process. In the particular case of lubricating greases, part of the lubrication process's energy dissipates due to a shear-induced structural rearrangement of the 3D network of the thickening agent dispersed in the base oil. This fact confers them a particular consistency, mechanical stability, rheological and tribological behaviour. In this research work, we investigate the mechanical structural degradation induced by shear stress applied in rheological tests (rotational and oscillation mode) and the influence of thickener (type and composition) and base oil on both the degradation process and the expended mechanical energies. For this purpose, lithium, calcium and polyurea-based greases of NLGI grade 2 were used. These greases have been manufactured with a different base oil (mineral, synthetic and vegetable oils) and kinematic viscosity of 48 or 240 mm^2/s. Some biogenic greases were also included in this research. The optical microscopy analysis revealed thickener particles-based agglomerates with different shapes and sizes that reduced notably, if not almost completely destroyed, after stress. Due to the thickener particles-based agglomerates distribution, significant differences in the shear-induced frictional energy inside the bulk grease during the shear process were detected. The size of agglomerates depended on both the thickener content and the base oil viscosity and not the type of base oil.

Keywords Lubricating greases · Shear-induced structural degradation · Energetic approach · Microscopy · Rheology

1 Introduction

Lubricating greases are semi-solid lubricants with a markedly viscoelastic behaviour [1]. We find usability in various applications, especially in ball bearings under boundary or mixed friction.

Lubricating greases have a significant behaviour under friction stress compared with lubricating oils. There are many investigations of the particular tribological and rheological behaviour [2–5]. The Non-Newtonian behaviour, characterised by thixotropy, yield stress and viscoelastic behaviour, are the main differences compared with others [6].

✉ Leif Ahme
leif.ahme@haw-hamburg.de

[1] Department of Mechanical Engineering and Production Management, Hamburg University of Applied Sciences, Hamburg, Germany

[2] Department of Chemical Engineering, University of Huelva, Huelva, Spain

Lubricating greases are classified by the consistency gained by their microstructural skeleton developed by the thickener agent, according to the ASTM D217. This viscoelastic lubricant is generally a highly 3D structured suspension consisting of 70–90 wt% of base oil (mineral, synthetic or vegetable oil) and 3–30 wt% of thickener agent and additives [7]. The thickener is added to increase the consistency of greases and prevent loss of lubricant under operating conditions, but this implies a considerable resistance to the flow of these materials. Furthermore, the thickener forms an interconnected network, characterised by physical bonds like H-bridge or Van der Waals forces and stearic hindrances, which trap the oil and confers the appropriate rheological and tribological behaviour to the grease. As Delgado et al. [1] pointed out, this structural skeleton (size and shape of the disperse phase particles) is hugely affected by the processing conditions and grease composition (mainly, thickener content and base oil viscosity).

Since lubrication is mainly a deformation and flow problem, the knowledge of the rheological properties of lubricating greases may contribute to elucidating one of the

Published online: 17 June 2022

unresolved problems in tribology: the effect of viscoelasticity on the friction process and, consequently, how a lubricating grease behaves under lubricating conditions. Thus, greases undergo structural degradation due to friction stress, which divides into two groups—mechanical degradation and chemical degradation. Some attempts were made to analyse the grease-based friction process through rheological measurements. Thus, Delgado et al. [8] and Kuhn [9] stated that grease elastic deformation, thickener particles' reversible orientation and the final, irreversible dispersion of these particles in the oil could be attributed to progressive changes in the structure of the grease when it is transferred to the friction process. They developed an approach to study the structural degradation of lithium greases in the friction process using stress-growth experiments. This test displayed a decreasing energy expenditure during the shear process until a steady-state situation was reached, i.e. a stationary non-equilibrium state. This intrinsic reaction of the observed mechanical degradation is an expression of a general effort of energetically stressed systems [10, 11]. It means that the stressed lubricating grease is pushed into a non-stable situation and looks for a possibility to get an energetic release. Consequently, a change of the grease structure is involved as a path to minimise the energetic gradients to reach a stable situation.

In this context, Roman et al. [12] showed that grease microstructure was influenced by shear rate and shear time with the help of AFM and SEM micrographs. Paszkowski and Olsztynska-Janus [13] found a process of destroying H-bonds between Li-soap fibres during shear stress by a rheometer. In addition, the quantitative description of the structural degradation caused by mechanical energy can be found in different ways. Bryant, Khonsari and Ling [14] first defined the term “degradation coefficient”. They described it as the generalised thermodynamic and degradation forces ratio. It can elucidate the rates associated with the degradation equation based on the entropy concept and degradation process rather than process variables. Rezasoltani and Khonsari [5] used entropy generation and penetration measurements to define the mechanical degradation of lubricating greases. Osara and Bryant [15] did an extensive investigation from a thermodynamic point of view. They describe the so-called degradation coefficient for lubricating greases by applying the degradation-entropy generation theorem to phenomenological entropy generation for stressed greases. Finally, the work done by Zhou [4] delivers a Master curve. Softening of grease as a function of shear rate, temperature, time and use of the input energy density were investigated.

In this paper, we investigate the mechanical degradation observed in the rheometer tests from the point of view of the changes in the structural skeleton confirmed by the thickener as a consequence of shear stress applied, and we study the influence of thickener (type and composition) and base oil on the degradation process. We only investigate the effect of mechanical energy (shear process); other influences such as thermal energy chemical energy are neglected.

2 Materials and Experimental Methods

2.1 Materials

Ten different lubricating greases differing in composition were tested. The type and concentration of thickener and type and viscosity of the base oil were specifically selected because they influence grease microstructural and rheological behaviour [1]. All of them were NLGI group 2 that soap concentration had to be modified appropriately to get this NLGI grade. Although the soap concentration changes the rheology of greases, the influence is proportional and can be controlled [1].

No additives were included to exclude other possible effects on structural degradation. Greases were classified into two groups. The first group with conventional greases is based on metal soap and polyurea (C1–C4 lithium greases; C5–6 calcium greases, and C7 polyurea grease). The second group are newly developed pure biogenic lubricating greases based on vegetable oil and a combination of lignocellulosic material, esters compound and beeswax as a thickener (B1–B3). The composition of the different lubricating greases analysed in this study and their basic properties are listed in Tables 1 and 2, respectively. Greases were kindly supplied by Fuchs Europe Schmierstoffe (Mannheim, Germany) and Fuchs Lubritech (Kaiserslautern, Germany) as part of the TriBioGen research project. The biogenic lubricating greases were investigated in various studies by Acar [16, 17]. The most promising ones were recommended for further investigation, and therefore, samples B1–B3 were selected for this work.

2.2 Microscopy Measurements

A transmitted light microscope from Olympus (Hamburg, Germany) was used to evaluate both unstressed and stressed structural skeletons of lubricating greases. A very thin layer was spread on a specimen's standard glass-based holder to get transmitted light microscope samples. At least three different fresh samples of each grease were analysed, taking five pictures at various locations to obtain a natural representative morphology for each grease studied. The objective used was a Plan Achromat objective (PLCN20x) from Olympus, specially designed for liquid substances with a 20× magnification. An Olympus DP27 digital camera with 6.3× magnification was used to take the images at room temperature, giving a cumulative magnification of 126. At the bottom right of all images, the white scale indicates 100 µm

Table 1 Conventional lubricating greases

Lubricating greases	Thickener type	Thickener concentration [%]	Base oil	Base oil viscosity at 40 °C [mm^2/s]	NLGI grade	Dropping point [°C]
C1	Lithium-12-hydroxystearate	16.1	Castor oil	240	2	≈190,111
C2	Lithium-12-hydroxystearate	10.6	PAO	240	2	≈210,497
C3	Lithium-12-hydroxystearate	13	PAO	48	2	≈208,479
C4	Lithium-12-hydroxystearate	9.5	Mineral oil	240	2	≈206,493
C5	Calcium-12-hydroxystearate	9.7	Castor oil	240	2	≈142,055
C6	Calcium-12-hydroxystearate	22.8	PAO	240	2	≈150,872
C7	Polyurea	19.6	PAO	240	2	≈296,913

Table 2 Biogenic lubricating greases

Lubricating greases	Thickener type	Thickener concentration [%]	Base oil	Base oil concentration [%]	Base oil viscosity at 40 °C [mm^2/s]	NLGI grade	Dropping point [°C]
B1	Cellulose	1.5	Glycerine	88.5	227.4	1	<≈100?
			Glyceryl-monooleate	10	120.1		
B2	Polyhydroxy butyrate	5.3	MCT oil	55	14.7	0–1	≈80
	Ethylcellulose	7.7	Castor oil	22	258.3		
			HOSO	10	46.2		
B3	Beeswax	7	HOSO	50	46.2	00	≈45
	Glycerol monostearate	5	Castor oil	36	258.3		
	Cetyl alcohol	2					

at the magnification. It is worth mentioning that much effort was made to ensure a similar illumination for all images captured. Despite this, some samples showed slight differences in brightness, which made it impossible to find an illumination time suitable for all areas of these samples. In these cases, the so-called High Dynamic Range (HDR) image recordings were made, which brought the opportunity to control both brightness and darkness on the image processing software [18].

Morphological observations of each representative grease's microstructure were conducted at room temperature with a scanning electron microscope (SEM), model ZEISS EVO LS15 (ZEISS, Germany), at 10 kV. A magnification of 7000 × was used. Previously, all samples were chemically fixed on the holder with 2.5 wt% glutaraldehyde in 0.1 M cacodylate buffer for two hours, followed by three washes in 0.1 M cacodylate solution. Subsequently, all samples were subjected to a second fixation with one wt% osmium tetraoxide solution for 1 h, again followed by three washes with 0.1 M cacodylate solution. Finally, all samples were submitted to critical point drying in acetone before being metallised with Au/Pd. Representative morphology prototypes were assured by using, for each formulation studied, at least three different samples and taking five pictures at various locations.

Although presenting SEM images, the optical microscope images were deliberately preferred in this experimental study on the expended energy on structural degradation. These images were used to discuss a more applied and macroscopic observation of the structural degradation of the bulk grease and to obtain an overview of the agglomerates.

2.3 Rheological Measurements

The most common friction regimen in most machine elements work is mixed friction. The frictional energy of the overall system results from both solid and liquid friction. Rheological investigations provide accurate data on both the internal friction and the structural degradation of the stressed lubricating greases and lead to measuring the mechanical work expended due to the implemented shearing process.

All rheological tests were performed using a grooved plate–plate geometry of 25 mm diameter and 1 mm gap at constant temperatures of 40 °C (MCR 302) and 80 °C (MCR 300) in controlled-stress rheometers (Anton Paar, Austria). Grooved surfaces were selected to prevent wall slip phenomena [19]. To ensure constant temperature conditions, a Peltier temperature control system (Anton Paar—Peltier systems with TruGap™) with an environmental control chamber, as described above, was used.

The experimental procedure with rheometers was organised in three consecutive steps (Fig. 1). During all rheological measurements, both torque and rotational velocity, among other parameters, were recorded every second and used to quantify the involved mechanical energy on the grease.

In the first step, no strain on the sample was imposed during the 900 s to allow the grease to relax or rather to compensate the squeezing process and, second, to allow the grease to reach the commanded temperature. In previous investigations in our laboratory, it was determined that a rest time of 900 s was enough. In the second step, the sample was stressed within the shear rate range from 0 to 1000 s^{-1} for 7200 s to induce structural changes in the lubricating greases under liquid friction-liked conditions. The long period was selected to achieve a stationary state with all lubricating greases studied. Higher shear rates than 1000 s^{-1} were not considered because a notable leakage phenomenon was appreciated. Finally, a third step consisting of a strain-sweep test in oscillation mode at a constant frequency of 1 Hz was performed within the strain range from 0 to 100%. This oscillation test aimed to determine the shear-induced structural degradation rate in the previous rotational test by analysing the strain region below the crossing point of G′ and G″ (frequency at G′ = G″) was reached. We consider that the energy expended to reach the crossing point of G′ and G″ is an indirect indicator of grease structural degradation. The strain-sweep test in oscillation mode was also carried out on unstressed greases for comparative purposes. Three replicates were performed on fresh samples for each grease to ensure the accuracy of the results. The results have shown a statistical significance at a 95% confidence level. In addition, a mean value was calculated for all three outcomes.

3 Results and Discussion

3.1 Basics of Energetic Calculation

The data from rheological tests (rotational and oscillation mode) were used to determine the expended energy under shear stress conditions. This energy is shear-induced frictional energy inside the bulk grease due to a structural rearrangement process quantified as mechanical work. Thus, rotational mode implies flow conditions. The energy supplied into the lubricating greases during the test leads to structural degradation of the grease, apart from a portion of it is dissipated as heat energy. On the other hand, the oscillation mode allows the expended mechanical work to analyse the shear-induced structural changes to achieve a predominant liquid-like behaviour. The thickener (type and composition) and the base oil affect the shear-induced structural changes (i.e. the expended mechanical energies). Details about the calculation of the mechanical work involved in both rotational (structural degradation) and oscillation (non-degraded structure) tests follow below.

3.1.1 Mechanical Work During the Viscous Flow Transient Test

All greases were stressed using a controlled-stress rheometer, which imposed specific shear stress conditions. Thus, the viscous flow transient test under simple shear conditions may provide a feasible measure of the shear-induced frictional energy on the grease at fixed shear stress.

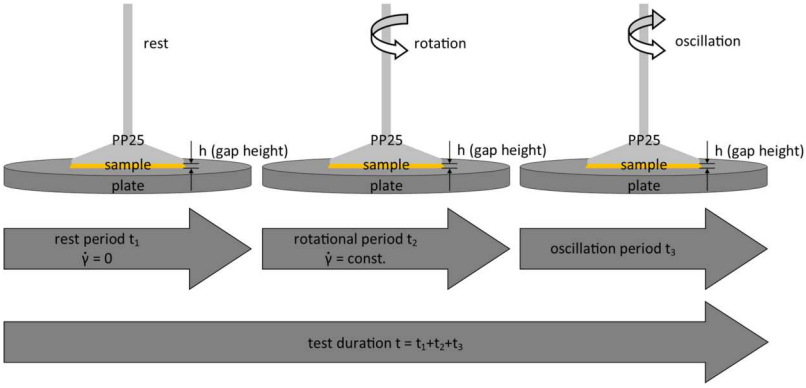

Fig. 1 Schematic illustration of the experimental procedure

The approach of Zhou [4] was used to determine the mechanical work W_R supplied to the sample during the rotational test at a constant shear rate (Eq. 1).

$$W_R = \int_{t_i}^{t_{i+1}} \frac{M_{di} \bullet n_i \bullet 2\pi}{60} dt. \tag{1}$$

The rheological test was programmed to measure a torque value each 15 s within the full-time range studied (7200 s). Therefore, equation one was solved considering a constant segment of time (15 s). Thus, if each segment of time is considered individually with its torque value measured, the total mechanical work during the viscous flow transient test for 7200 s can be calculated as the sum of all segments of time, as follows:

$$W_R = \int_{t_i}^{t_{i+1}} \frac{M_d \bullet n \bullet 2\pi}{60} dt = \sum_{i=1}^{m} \frac{M_{di} \bullet n_i \bullet \pi \bullet \Delta t_i}{30}, \tag{2}$$

with

M_{di} = Measured Torque [Nm].

n_i = Rotational velocity [min^{-1}].

Δt_i = Segment of time [s] (corresponding to each measured point).

m = total number of segments of time within the full-time range studied.

3.1.2 Mechanical Work During Oscillation Test

The oscillation test is widely used to determine the viscoelastic behaviour of the lubricating greases, which is directly related to their structural features [1]. In this test, attention was paid to the intersection of G′ and G″, a transition point from solid-like to liquid-like, i.e. a point above which the grease loses the solid-like behaviour and the liquid-like behaviour becomes dominant. Thus, it will provide information about the structural degradation caused by previously applied shear conditions and how it affected viscoelastic behaviour.

The calculation of the mechanical work in the oscillation test is much more complicated than in the rotational test because, on the one hand, no shear rate was applied. On the other hand, the test runs in oscillating sinusoidal movements. It means that the output values for the shear rate $\dot{\gamma}$ and the torque M_d are always maximum values. Nevertheless, a method was proposed to determine the mechanical work during the test. The effective shear rate is estimated from Eq. 3:

$$\dot{\gamma} = C_{SR} \bullet n, \tag{3}$$

with

$\dot{\gamma}$ = Shear rate [s^{-1}].

C_{SR} = Conversion factor shear rate [s^{-1}/min^{-1}].

n = Rotational velocity [s^{-1}].

The conversion factor of C_{SR} for the respective grooved plate–plate geometry used was determined according to the necessary standard procedure according to Anton Paar with calibration fluid. Thus, the rotational velocity n is estimated from Eq. 4.

$$n = \frac{\dot{\gamma}}{C_{SR}} \tag{4}$$

As values of the shear rate $\dot{\gamma}$ and the torque M_d registered were the maximum values (peak values) reached under the sinusoidal movement, we used an approach from Electrical Engineering. Thus, a rectified value is determined for a sinusoidal current. This corrected value is the occurring mean value of the integral over the amounts of the sine wave [20]. Figure 2 intended to illustrate the situation in more detail.

The sinus curve shows the second oscillation (dotted) reflected upwards. In the figure, $\hat{i}$ represents the peak value and $|\bar{i}|$ represents the rectified value. The following formula gave the ratio of rectification value to peak value:

$$\frac{|\bar{i}|}{\hat{i}} = \frac{1}{T}\int_0^T |\sin(\omega t)| d(\omega t) = \frac{2}{\pi} \sim 0.6366. \tag{5}$$

In our case, the values obtained from the rheometer are peak values, i.e. the shear rate $\hat{\dot{\gamma}}$ and the torque $\widehat{M}_d$. However, rectified values are required to calculate the mechanical work during the oscillation test. These were calculated from Eqs. 6 and 7, respectively:

$$|\bar{\dot{\gamma}}| = \hat{\dot{\gamma}} \bullet \frac{2}{\pi}, \tag{6}$$

$$|\bar{M}_d| = \widehat{M}_d \bullet \frac{2}{\pi}. \tag{7}$$

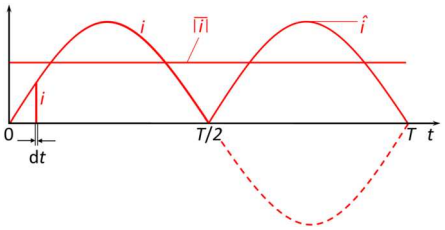

Fig. 2 Sine current curve for a rectified value cf. [20]

Thus, with the help of these adaptations described above, it can successfully determine the mechanical work during the oscillation test by using Eq. 2. Please note that the segment of time, in this case, is not always constant 15 s as in the case of the viscous flow transient test; it varies.

3.2 Structure of Unstressed and Stressed Lubricating Greases

As it is well known, lubricating greases are essentially highly structured two-phase colloidal suspensions consisting of a thickening agent dispersed in a base oil. The thickener forms a three-dimensional gelling network that traps the oil by capillary phenomena and molecular attraction and confers them to the appropriate consistency, rheological and tribological behaviour. Figure 3 shows the SEM micrographs corresponding to representative lithium soap, calcium soap and polyurea-based greases manufactured with the same synthetic oil (PAO 240 mm^2/s). No SEM micrographs of pure biogenic greases studied (B1, B2 and B3) were obtained because their dropping points were much lower. That is why it is technically impossible to observe these samples by SEM. However, all of them showed a high density of entangled soap fibres. Li-soap-based greases showed a spongy and entangled structural skeleton with the largest fibres, while polyurea-based grease showed more heterogeneous soap particles, which looked like aggregates of fibres [1, 6].

However, from a macroscopical point of view, these microstructural skeletons can be organised as agglomerates of different shapes and sizes, demonstrated by optical microscopy, as a consequence of the process of crystallisation of the thickener particles [1]. Figures 4, 5, 6 and 7 show the optical microscopic images of both unstressed and stressed states for lithium, calcium, polyurethane and pure biogenic greases. These visual images differ in colour due to firstly the greases having different primary colours and, secondly, each prepared sample experiences different refraction of the light under the microscope. As can be well appreciated, the structural pattern of unstressed grease was changed into a pattern with a smaller grouping of particles and more oriented toward the flow direction. In addition, as Paszkowski and Olsztynska-Janus [13] and Delgado et al. [6] pointed out, lubricating greases show a highly shear-thinning behaviour for which the structural skeleton undergoes elastic and plastic deformation and even disintegration when a high shear rate is applied. For this aim, optical microscopy images were taken for all greases studied and compared with the knowledge gained from rheological tests to identify further possible correlations between the different components of the model greases, the structural degradation process and the expended mechanical energies involved.

All greases were highly stressed by a transient flow test at 1000 s^{-1} for 22 h using a cone plate of 50 mm diameter to ensure a consistent shear of the sample and avoid any leakage phenomenon characteristic of lubricating greases [6]. After this time, a stressed grease specimen was deposited on a standard glass holder to observe it microscopically. Thus, any possible disturbance of the aggregates pattern was avoided due to the thixotropy effects. As expected, the number of agglomerates decreased and became smaller than unstressed samples, and the aggregate pattern of stressed greases studied was more homogeneous and cohesive (Figs. 4, 5, 6, 7).

Concerning lithium greases (Fig. 4), the characteristic fibre-based microstructural skeleton of lithium greases could not be identified macroscopically with an optical microscope. However, it is noteworthy that numerous lithium soap-based agglomerates with different shapes and sizes can be recognised in the unstressed sample. It was detected that the size of these agglomerates depended on both the soap content and the base oil. Thus, the Li grease with the highest soap content (grease C1) or the lowest oil viscosity (grease C3) showed the most oversized agglomerates. According to Delgado et al. [1], either low-viscosity base oil or high soap content leads to a high density of entanglements with

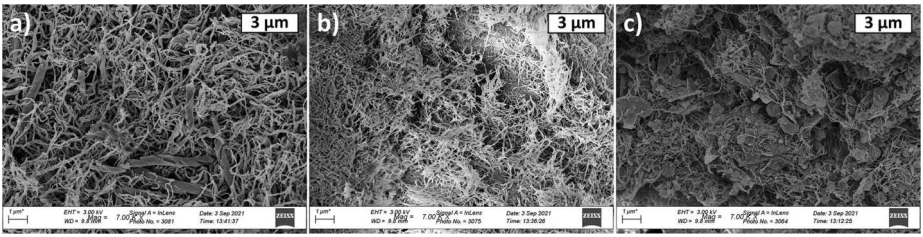

Fig. 3 SEM (15 kV and 7000 magnification) micrographs corresponding to **a** lithium grease (C2); **b** Calcium grease (C6); **c** Polyurea grease (C7)

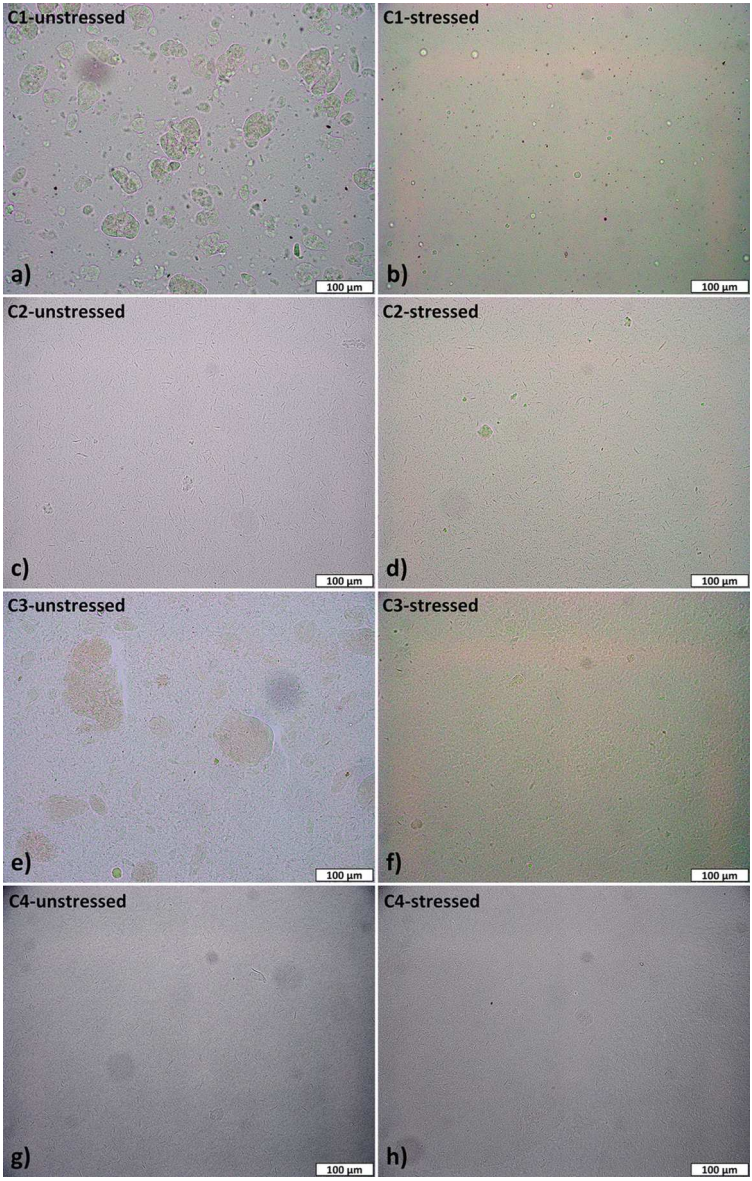

Fig. 4 Optical microscopic images of the lithium greases: **a**, **b** C1; **c**, **d** C2; **e**, **f** C3; **g**, **h** C4—left-side column are unstressed greases and right-side column are stressed greases (1000 s^{-1} for 22 h)

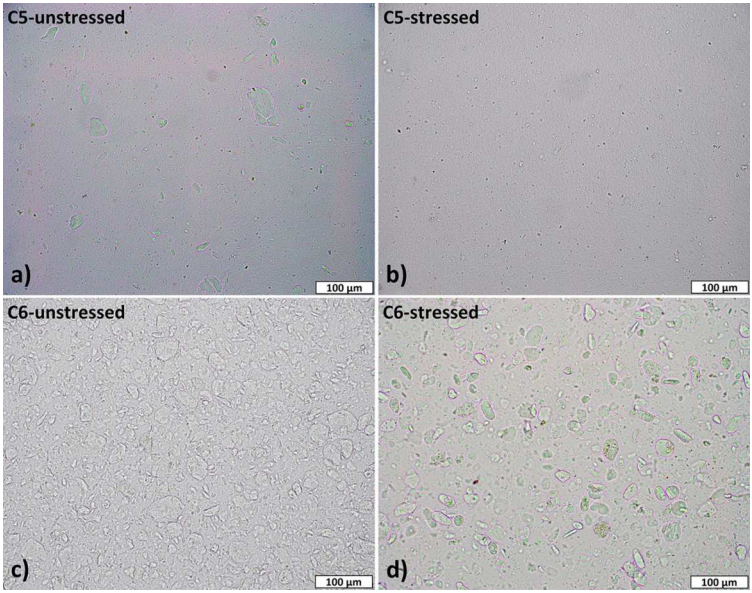

Fig. 5 Optical microscopic images of the calcium greases: **a**, **b** C5; **c**, **d** C6—left-side column are unstressed greases and right-side column are stressed greases (1000 s^{-1} for 22 h)

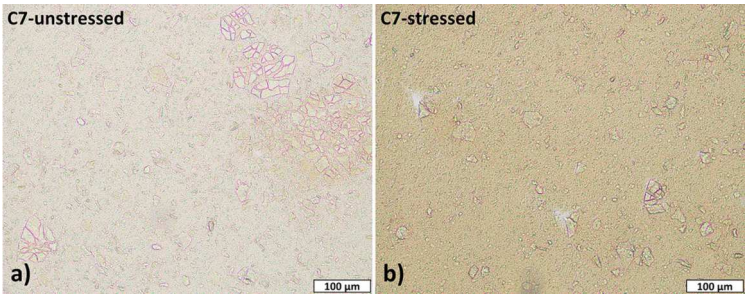

Fig. 6 Optical microscopic images of the polyurea grease (C7) **a** unstressed grease, **b** stressed grease (1000 s^{-1} for 22 h)

a higher shear-structural dependence (low values on flow index). After these lithium greases were highly stressed, lithium soap-based agglomerates were notably reduced, if not almost wholly destroyed.

Concerning calcium greases (Fig. 5), a similar behaviour to lithium greases was observed. Unstressed calcium greases showed uneven thickener agglomerates of different shapes and sizes. Calcium grease with the highest soap content (grease C6) showed a high density of more extensive calcium soap-based agglomerates. Just after stressing, calcium agglomerates' size was highly reduced. Then a comparison between optical images of both unstressed lithium (C1, C2) and calcium (C5, C6) greases was conducted. Both had different soap content and type of base oil (castor oil and PAO)

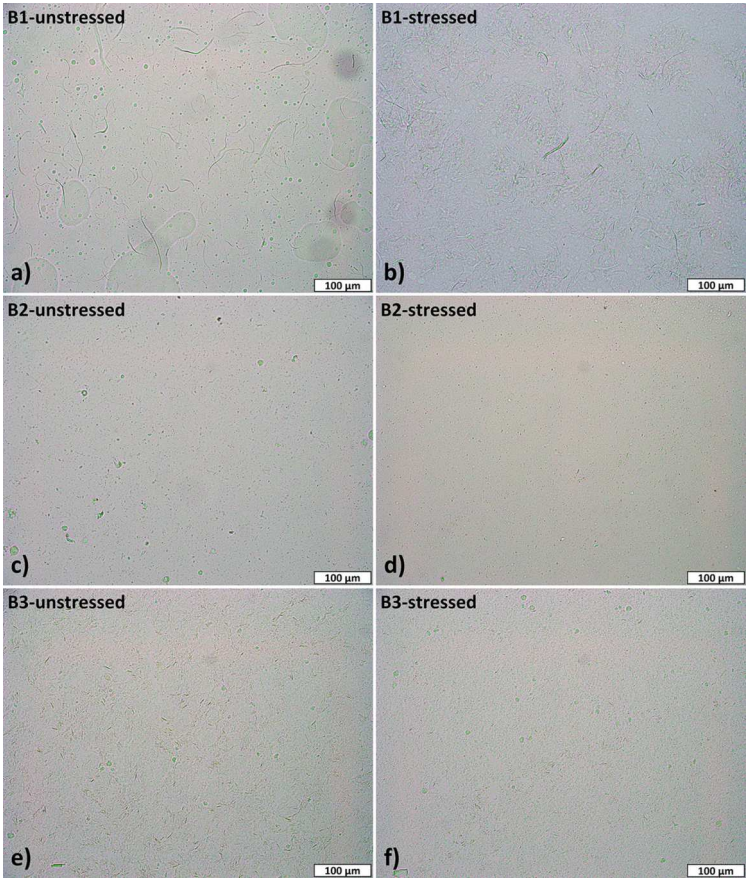

Fig. 7 Optical microscopic images of the pure biogenic greases: **a**, **b** B1; **c**, **d** B2; **e**, **f** B3—left-side column are unstressed greases and right-side column are stressed greases (1000 s^{-1} for 22 h)

with a kinematic viscosity of 240 mm^2/s. It shows that the size of metal soap-based agglomerates was mainly affected by the soap content and not the base oil type. Lithium or calcium greases with the lowest soap content were significantly more homogeneous in an idle state and showed fewer structural changes in the shear stress process.

The polyurea grease (Fig. 6) shows well-defined flakes of different sizes but are not more prominent than those observed for lithium or calcium greases. Unlike both stressed lithium and calcium greases, large agglomerates were kept for stressed polyurea grease, although with reduced and more homogeneous sizes than the unstressed polyurea grease.

Finally, the unstressed pure biogenic greases B1 to B3 studied (Fig. 7) did not present well-defined thickener agglomerates due to the thickener agent used. The cellulose fibres of grease B1 can be easily macroscopically recognised in the unstressed and stressed state. Contrarily to previous non-biogenic greases, the scattered cellulose fibres in the unstressed grease appeared closer after stress. Tiny spots were appreciated in biogenic greases B2 and B3, and their macroscopical structures appear much more homogeneous

after stressing. The particle arrangement looks very homogeneous after the stress, and only a few smaller and shapeless agglomerates are still present.

3.3 Expended Energy to Achieve the Liquid-Like Behaviour

Figures 8 and 9 show the required mechanical work during the oscillation test to achieve a liquid-like behaviour once the grease was stressed at a specific shear rate. Discontinuous lines show the tendency of the measured values, which a logarithm model may conveniently represent except for grease C2 in Fig. 9a. It displays as a function of the shear rate applied at which the greases studied were degraded on the previous rotational test performed. Although the initially examined shear rate range was from 0.1 to 1000 s^{-1}, a non-completely grease degraded structure was reached with lower shear rates than 100 s^{-1} at the test conditions, i.e. it was not reached a steady-state behaviour in all cases. Moreover, biogenic greases B1 and B2 did not provide valuable results at high shear rates due to significant fracture and expulsion phenomena up to 10 s^{-1}. Therefore, only data

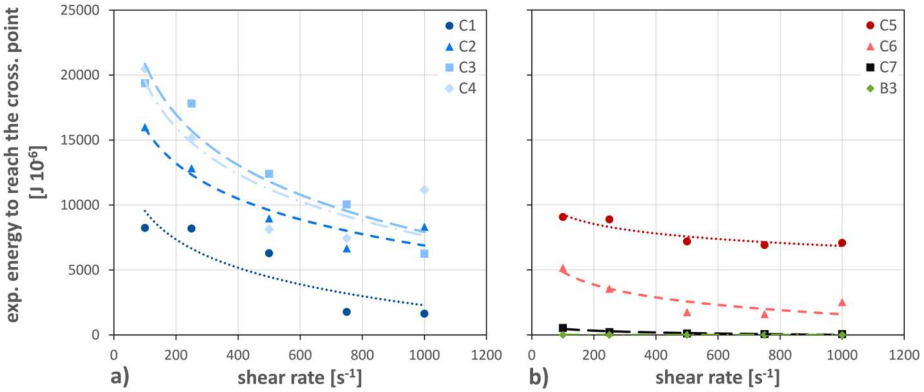

Fig. 8 Expended energy to reach the crossing point at 40 °C for **a** lithium greases and **b** other greases. Logarithm curve fittings are shown by a discontinuous line

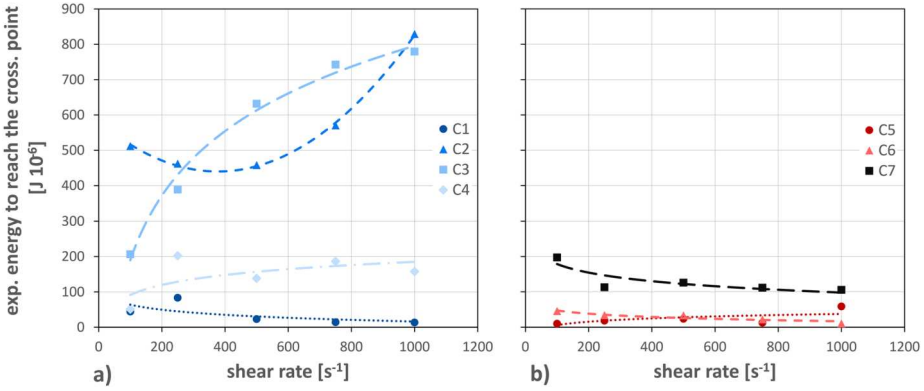

Fig. 9 Expended energy to reach the crossing point at 80 °C for **a** lithium greases and **b** other greases. Logarithm curve fittings (C1, C3, C4, C5, C6, C7) and polynomial curve fitting (C2) are shown by a discontinuous line

obtained from reproducible tests at higher shear rates than 100 s^{-1} were considered in the current study; the steady-state conditions were reached in all plotted cases after 22 h. According to Delgado et al. [6], it is worth mentioning that the shear-induced grease behaviour at these high shear rate ranges should be consistent with the physical degradation produced by the over rolling on the bulk grease close to the contact area.

Y-positions of these curves display the amount of expended energy to reach a specific structural degradation until the crossing point, i.e. the internal frictional energy involved within the grease degradation process starts and keeps the flow process. Thus, the higher the expended energy to reach the crossing point, the higher the internal frictional energy is. The structural features of the greases affect the internal frictional energy (Fig. 3). Consequently, lithium and calcium greases with a spongy and entangled fibres-based structural skeleton showed higher internal friction energies than polyurea grease, which showed matted fibres with barely free-motion space among themselves. On the other hand, the expended energy-shear rate dependence is an indirect expression of the internal structural degradation rate, i.e. the grease wear. It is closely related to the agglomerates' pattern originating from the shear conditions and observed by optical microscopy (Figs. 4, 5, 6, 7).

At 40 °C (Fig. 8), the higher the applied shear rate was, the lower the expended energy reached the crossing point between G′ and G″, regardless of the evaluated greases. It suggested a lower internal frictional energy to achieve the liquid-like behaviour as much stressed the lubricating grease was, i.e. as much degraded the structural pattern of the grease was. It is noteworthy that lithium, calcium and polyurea showed significant differences in the expended energy to reach the crossing point, despite being NLGI grade 2. In general, the degradation of the bulk structural skeleton of lithium greases showed a strong dependence on the shear rate applied. However, biogenic, polyurea and calcium greases, which showed fewer differences in the structural patterns between unstressed and stressed greases, hardly displayed any variation of the expended energy within the shear rate range studied. Therefore, the type of structural pattern highly affects the internal frictional energy involved in the grease degradation process to start and keep the flow process even more than the thickener content and the oil viscosity. Thus, Li-soap-based greases developed a high internal frictional energy within the structural rearrangement process to start to flow because their internal network is based on larger fibres forming a well-entangled structural skeleton (Fig. 3) [6]. Moreover, they also showed a higher internal wear rate than other greases studied.

On the other hand, greases with the highest thickener contents tested: C1 (16.1 wt%), C6 (22.8 wt%) and C7 (19.6 wt%), required less energy to flow than their grease counterpart with lower thickener content. Thus, lithium greases C3 (13 wt%) and C4 (9.5 wt%) showed the highest expended energies to reach the crossing point. In addition, Li grease C3, produced with the lowest oil viscosity (48 mm^2/s), implied the highest expended energy to start to flow and the highest internal structural degradation rate within the shear rate studied. As previously pointed out by Delgado et al. [1], the oil viscosity induced differences in the structural skeleton network of lithium grease, such as the lower oil viscosity is, the larger affected the structural skeleton by the shear rate. Contrarily, biogenic (B3) and polyurea (C7) greases developed a more intensive structural degradation, affecting their internal grease wear within the studied shear rate range. In addition, it is worth mentioning that the use of castor oil (greases C1 and C5) attenuates the expended energy-shear rate dependence of its grease group because of the molecular attraction between the hydroxyl groups present in both the 12-hydroxystearate of the thickener and the ricinoleic fatty acid in castor oil. Therefore, a suitable interaction between thickener and base oil is helpful to preserve the internal structural degradation within the shear rate applied.

At 80 °C (Fig. 9), the amount of expended energy to reach a specific structural degradation until the crossing point drastically decreased compared to 40 °C. It could be a consequence of, on the one hand, a decrease in the internal binding forces due to the external input of thermal energy; on the other hand, the viscosity reduction caused by temperature increase facilitated the bleeding oil. Only the lubricating grease C7, which showed the highest dropping point, was relatively unaffected within this temperature range. Moreover, the expended energy-shear rate dependence showed a completely different behaviour for lithium greases C2–C4 than at 40 °C. They all displayed increased expended energy to reach the crossing point with the shear rate applied, which evidence a different structural degradation process for lithium greases manufactured with mineral or synthetic oil. It appears as if the introduction of thermal energy stimulated a structural rebuilding process. We think that a total change in the grease structure occurred with temperature due to the separation of the components (thickener and base oil); it is highly affected by the base oil selected. This phenomenon was distinct in the lithium grease manufactured with PAO with the lowest oil viscosity (C3). Only the lithium greases manufactured with castor oil (C1) and the calcium and polyurea greases (C5–C7) displayed an almost similar behaviour with the applied shear rate, although less pronounced than at 40 °C.

Nevertheless, these remarkable results at 80 °C should be considered cautiously because this notable reduction in the internal frictional energy with temperature may facilitate leakage from the gap at high shear rates. Moreover, the grease wear process emphasised that it is almost constant

over the shear rate for nearly all the greases shown (less slope of the curves than 40 °C). Therefore, it is worth pointing out that temperature drastically affected the expended energy-shear rate dependence of Li grease, mainly when PAO was used, and not to the calcium and polyurea greases.

Unfortunately, the biogenic grease reacted more sensitively to rising temperature and became too soft when mechanically stressed at 80 °C, even though it appeared pretty solid at rest (at room temperature). Since measurements at 80 °C hardly provided any relevant results, they are not shown below.

3.4 Ratio of Expended Energies

Follow with the analysis of the energetical approach to structural degradation of lubricating greases; it is interesting to relate the mechanical energy involved within the grease degradation process to start and keep the flow process (W_{CP}), with the mechanical energy involved in the structural degradation achieved along with the viscous flow transient test at a specific shear rate (W_R). Thus, R_{tee} allows a holistic interpretation of the expended mechanical energy involved in the structural degradation that occurred in the stressed grease (Eq. 8).

$$R_{tee} = \frac{W_{CP}}{W_R}, \tag{8}$$

with

R_{tee} = Ratio of the total expended energy.

W_{CP} = Mechanical work until the crossing point at the oscillation test [J].

W_R = Mechanical work supplied from the viscous flow transient test [J].

As commented above, the higher the shear rate is, much mechanical energy was put into the grease to destroy the structure skeleton during the viscous flow transient test. Consequently, it was easier to reach the crossing point at the oscillation test. Thus, the larger the ratio of expended energies is, the less structural degradation occurred in the stressed grease. It means either more energy was required to reach the crossing point or less mechanical energy dissipated during the rotation test.

Figures 10 and 11 show the expended energies ratio versus the shear rate applied at 40 °C and 80 °C, respectively. In these figures, discontinuous lines show the tendency of the measured values, which power curves may conveniently represent. In these cases, the full shear rate range studied was from 0.1 to 1000 s^{-1} and considered to display the full shear rate range studied. As identified, the expended energies ratio drastically decreased within the shear rate range lower than 100 s^{-1}, regardless of the temperature level. After 100 s^{-1}, an asymptotic tendency appeared. This fact suggested that the maximum shear-induced structural degradation of greases reached around 100 s^{-1}. According to Delgado et al. [6], it is an asymptotic tendency of stress-growth behaviour for lithium greases.

At 40 °C (Fig. 10), lithium and calcium greases showed higher values of R_{tee} along the shear rate range studied than polyurea grease (C7) and biogenic greases (B3). The structural skeleton of lithium and calcium greases dissipated less mechanical energy during the rotation test than polyurea and biogenic greases. On the other hand, it reveals that lubricating greases with a higher thickener content led to lower values of R_{tee}, which means more structural

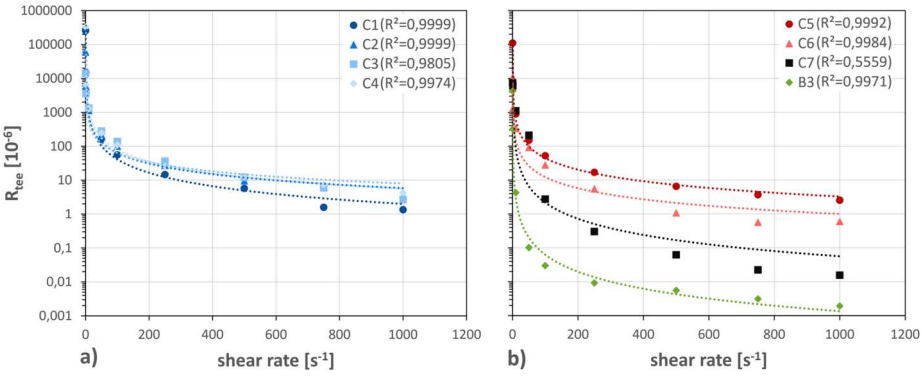

Fig. 10 Ratio of expended energies (R_{tee}) 40 °C for **a** lithium greases and **b** other greases. Power curve fittings are shown by a discontinuous line indicating each R-squared (R^2) in the legend

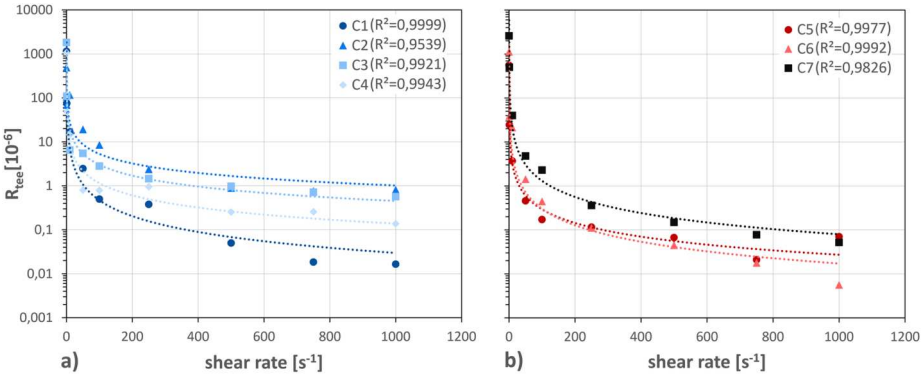

Fig. 11 Ratio of expended energies (R_{tee}) at 80 °C for **a** lithium greases and **b** other greases. Power curve fittings are shown by a discontinuous line indicating each R-squared (R^2) in the legend

degradation in the stressed grease. As commented above, R_{tee} allows a better interpretation of the expended mechanical energy involved in the structural degradation that occurred in the stressed grease. Thus, polyurea grease (C7) and the biogenic greases (B3), which exhibited similar variations of the expended energy to reach the liquid-like behaviour, are far apart in terms of their expended energy ratio. Such as, less structural degradation occurred in the stressed polyurea grease than in the stressed biogenic greases (B3). Therefore, biogenic greases (B3) expended the most mechanical energy to degrade their structural skeleton during the viscous flow transient test compared to the mechanical energy consumed to reach the liquid-like behaviour.

At 80 °C (Fig. 11), the expended energy ratio was substantially smaller than at 40 °C. It was linked with a significant reduction of the internal frictional energy to reach the liquid-like behaviour compared to the mechanical energy supplied into the lubricating greases during the viscous flow transient test. It is worth mentioning that lithium and calcium greases showed more significant differences in the expended energy ratio at 80 °C, with a drastic reduction for the calcium greases. However, the expended energy ratio of polyurea grease (C7) was hardly affected by temperature. It suggests that polyurea grease's structural skeleton better supports the shear-induced structural degradation within this temperature range studied than the other greases. Therefore, this energetical approach could be a suitable measurement of the mechanical stability of the lubricating greases according to the shear-induced structural changes.

4 Conclusion

This work highlights a better understanding of the influence of grease composition (thickener and base oil) on the macroscopically structural degradation of lubricating greases. In addition, it proposes a holistic interpretation of the expended energy involved in the internal structural degradation that occurred in the stressed grease. This expended energy, quantified as a mechanical work from the rheological test, measures the grease wear process, i.e. the shear-induced frictional energy inside the bulk grease.

Despite all traditional model greases studied being NLGI grade 2, they showed significant differences in the structural pattern of unstressed grease obtained by optical microscopy and the expended energy of the stressed greases to start the flow process. Numerous thickener-based agglomerates with different shapes and sizes were recognised in the unstressed sample. Furthermore, the size of these agglomerates depended on thickener content and base oil. Moreover, the type of thickener, which affects the microstructural skeleton, highly affects this internal frictional energy, even more than either thickener content or the base oil. It is worth pointing out that R_{tee} could be a suitable measurement of the expended mechanical energy by structural degradation of the lubricating greases according to the observed shear-induced structural changes. Thus, the larger the ratio of expended energies is, the less structural degradation occurred in the stressed grease. It means that either more internal friction energy is expended to start to flow (reach the crossing point) or

less mechanical energy is dissipated during the structural degradation of the stressed grease. Therefore, this work reveals that the structural skeleton of lithium and calcium greases dissipated less mechanical energy during the shearing process than polyurea and biogenic greases (B3). The stressed biogenic greases (B3) dissipated the highest amount of mechanical energy. In addition, it is noteworthy that lubricating greases with higher thickener content led to lower values of R_{tee}, which means more structural degradation in the stressed grease. On the other hand, the R_{tee} of polyurea grease was hardly affected by temperature, suggesting that the structural skeleton of polyurea grease better supports the shear-induced structural degradation within the temperature range studied than the other lubricating greases.

Author Contributions All authors contributed to the study conception and design. Material preparation, data collection and analysis were performed by Leif Ahme. The first draft of the manuscript was written by Leif Ahme, and all authors commented on previous versions of the manuscript. All authors read and approved the final manuscript.

Funding Open Access funding enabled and organized by Projekt DEAL. The authors did not receive support from any organisation for the submitted work. No funding was received to assist with the preparation of this manuscript. No funding was received for conducting this study. The authors declare that no funds, grants or other support were received during the preparation of this manuscript.

Declarations

Conflict of interest The authors have no relevant financial or non-financial interests to disclose. The authors have no competing interests to declare that are relevant to the content of this article. All authors certify that they have no affiliations with or involvement in any organisation or entity with any financial interest or non-financial interest in the subject matter or materials discussed in this manuscript. The authors have no financial or proprietary interests in any material discussed in this article.

References

1. Delgado, M.A., Valencia, C., Sánchez, M.C., Franco, J.M., Gallegos, C.: Influence of soap concentration and oil viscosity on the rheology and microstructure of lubricating greases. Ind. Eng. Chem. Res. (2006). https://doi.org/10.1021/ie050826f
2. Paszkowski, M.: Assessment of the effect of temperature, shear rate and thickener content on the thixotropy of lithium lubricating greases. Proceed. Instit. Mechan. Eng. Part J J. Eng. Tribol. (2013). https://doi.org/10.1177/1350650112460950
3. Sánchez, R., Valencia, C., Franco, J.M.: Rheological and tribological characterization of a new acylated chitosan-based biodegradable lubricating grease: a comparative study with traditional lithium and calcium greases. Tribol. Trans. (2014). https://doi.org/10.1080/10402004.2014.880541
4. Zhou, Y.: On the mechanical ageing of lubricating greases, University of Twente (2018)
5. Rezasoltani, A., Khonsari, M.M.: On the correlation between mechanical degradation of lubricating grease and entropy. Tribol. Lett. (2014). https://doi.org/10.1007/s11249-014-0399-8
6. Delgado, M.A., Secouard, S., Valencia, C., Franco, J.M.: On the steady-state flow and yielding behaviour of lubricating greases. Fluids (2019). https://doi.org/10.3390/fluids4010006
7. Delgado, M.A., Sánchez, M.C., Valencia, C., Franco, J.M., Gallegos, C.: Relationship among microstructure, rheology and processing of a lithium lubricating grease. Chem. Eng. Res. Des. (2005). https://doi.org/10.1205/cherd.04311
8. Delgado, M.A., Franco, J.M., Kuhn, E.: Effect of rheological behaviour of lithium greases on the friction process. Indus. Lubricat. Tribol. **60**, 37–45 (2008)
9. Kuhn, E.: Correlation between system entropy and structural changes in lubricating grease. Lubricants (2015). https://doi.org/10.3390/lubricants3020332
10. Kuhn, E.: Application of a thermodynamic concept for the analysis of structural degradation of soap thickened lubricating greases. Lubricants (2018). https://doi.org/10.3390/lubricants6010007
11. Abdel-Aal, H.A.: Thermodynamic Modeling of Wear. In: Wang, Q.J., Chung, Y.-W. (eds.) Encyclopedia of Tribology, pp. 3622–3636. Springer, US, Boston, MA (2013)
12. Roman, C., Valencia, C., Franco, J.M.: AFM and SEM assessment of lubricating grease microstructures: influence of sample preparation protocol, frictional working conditions and composition. Tribol. Lett. (2016). https://doi.org/10.1007/s11249-016-0710-y
13. Paszkowski, M., Olsztyńska-Janus, S.: Grease thixotropy: evaluation of grease microstructure change due to shear and relaxation. Indus. Lubricat. Tribol. (2014). https://doi.org/10.1108/ILT-02-2012-0014
14. Bryant, M., Khonsari, M., Ling, F.: On the thermodynamics of degradation. Proceedings of The Royal Society A: Mathematical, Physical and Engineering Sciences (2008). https://doi.org/10.1098/rspa.2007.0371
15. Osara, J.A., Bryant, M.D.: Thermodynamics of grease degradation. Tribol. Int. (2019). https://doi.org/10.1016/j.triboint.2019.05.020
16. Acar, N., Kuhn, E., Franco, J.M.: Tribological and rheological characterization of new completely biogenic lubricating greases: a comparative experimental investigation. Lubricants (2018). https://doi.org/10.3390/lubricants6020045
17. Acar, N., Franco, J.M., Kuhn, E., Gonçalves, D.E.P., Seabra, J.H.O.: Tribological investigation on the friction and wear behaviors of biogenic lubricating greases in steel-steel contact. Appl. Sci. (2020). https://doi.org/10.3390/app10041477
18. Olympus Europa SE & CO. KG: OLYMPUS Stream Online-Help. Stream 2.2. OLYMPUS EUROPA SE & CO. KG, Hamburg (2016). Accessed 14 Oct. 2020
19. Kuhn, E.: Zur Tribologie der Schmierfette. Eine energetische Betrachtungsweise des Reibungs- und Verschleißprozesses, 2nd edn. expert Verlag, Renningen (2017)
20. Fricke, H., Frohne, H., Vaske, P.: Grundlagen der Elektrotechnik. Elektrische Netzwerke, 17th edn. Teubner, Stuttgart (1982)

Terms and Conditions

Springer Nature journal content, brought to you courtesy of Springer Nature Customer Service Center GmbH (“Springer Nature”).

Springer Nature supports a reasonable amount of sharing of research papers by authors, subscribers and authorised users (“Users”), for small-scale personal, non-commercial use provided that all copyright, trade and service marks and other proprietary notices are maintained. By accessing, sharing, receiving or otherwise using the Springer Nature journal content you agree to these terms of use (“Terms”). For these purposes, Springer Nature considers academic use (by researchers and students) to be non-commercial.

These Terms are supplementary and will apply in addition to any applicable website terms and conditions, a relevant site licence or a personal subscription. These Terms will prevail over any conflict or ambiguity with regards to the relevant terms, a site licence or a personal subscription (to the extent of the conflict or ambiguity only). For Creative Commons-licensed articles, the terms of the Creative Commons license used will apply.

We collect and use personal data to provide access to the Springer Nature journal content. We may also use these personal data internally within ResearchGate and Springer Nature and as agreed share it, in an anonymised way, for purposes of tracking, analysis and reporting. We will not otherwise disclose your personal data outside the ResearchGate or the Springer Nature group of companies unless we have your permission as detailed in the Privacy Policy.

While Users may use the Springer Nature journal content for small scale, personal non-commercial use, it is important to note that Users may not:

1. use such content for the purpose of providing other users with access on a regular or large scale basis or as a means to circumvent access control;
2. use such content where to do so would be considered a criminal or statutory offence in any jurisdiction, or gives rise to civil liability, or is otherwise unlawful;
3. falsely or misleadingly imply or suggest endorsement, approval , sponsorship, or association unless explicitly agreed to by Springer Nature in writing;
4. use bots or other automated methods to access the content or redirect messages
5. override any security feature or exclusionary protocol; or
6. share the content in order to create substitute for Springer Nature products or services or a systematic database of Springer Nature journal content.

In line with the restriction against commercial use, Springer Nature does not permit the creation of a product or service that creates revenue, royalties, rent or income from our content or its inclusion as part of a paid for service or for other commercial gain. Springer Nature journal content cannot be used for inter-library loans and librarians may not upload Springer Nature journal content on a large scale into their, or any other, institutional repository.

These terms of use are reviewed regularly and may be amended at any time. Springer Nature is not obligated to publish any information or content on this website and may remove it or features or functionality at our sole discretion, at any time with or without notice. Springer Nature may revoke this licence to you at any time and remove access to any copies of the Springer Nature journal content which have been saved.

To the fullest extent permitted by law, Springer Nature makes no warranties, representations or guarantees to Users, either express or implied with respect to the Springer nature journal content and all parties disclaim and waive any implied warranties or warranties imposed by law, including merchantability or fitness for any particular purpose.

Please note that these rights do not automatically extend to content, data or other material published by Springer Nature that may be licensed from third parties.

If you would like to use or distribute our Springer Nature journal content to a wider audience or on a regular basis or in any other manner not expressly permitted by these Terms, please contact Springer Nature at

onlineservice@springernature.com

A.2 An approach of the internal friction-dependent temperature changes for conventional and pure biogenic lubricating greases

Leif Ahme[1], Erik Kuhn[1], Miguel Ángel Delgado Canto[2]

[1]Department of Mechanical Engineering and Production Management, Hamburg University of Applied Sciences, Hamburg 20099, Germany

[2]Department of Chemical Engineering, Research in Product Technology and Chemical Processes (Pro2TecS), University of Huelva, Huelva 21071, Spain

Published in: Friction

Publishing company: Springer Nature

Editor-in-Chief: Jianbin Luo

Missing

Year: August 2023

DOI: 10.1007/s40544-023-0818-7

ISSN:2223-7690

E-ISSN:2223-7704

Impact Factor (2022): 6.8

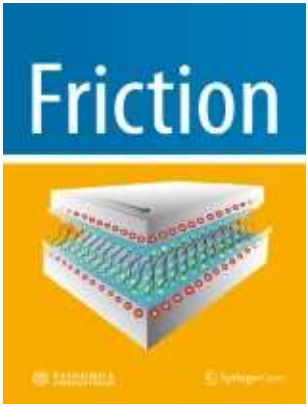

CiteScore (2022): 10.9

JCR Category	Rank
Engineering (Mechanical Engineering)	31/631
Materials Science (Surfaces, Coatings and Films)	13/131

Friction **12**(4): 780–795 (2024)
https://doi.org/10.1007/s40544-023-0818-7
ISSN 2223-7690
CN 10-1237/TH
RESEARCH ARTICLE

An approach of the internal friction-dependent temperature changes for conventional and pure biogenic lubricating greases

Leif AHME[1,*], Erik KUHN[1], Miguel Ángel DELGADO[2]

[1] *Department of Mechanical Engineering and Production Management, Hamburg University of Applied Sciences, Hamburg 20099, Germany*

[2] *Department of Chemical Engineering, Research in Product Technology and Chemical Processes (Pro2TecS), University of Huelva, Huelva 21071, Spain*

Received: 17 December 2022 / Revised: 25 May 2023 / Accepted: 27 August 2023

Abstract: This work investigated the temperature changes inside the bulk of lubricating greases under controlled high-shear stress conditions (250–500 s^{-1}). For this purpose, a newly developed temperature-measuring cell called Calidus was successfully tested. The temperature changes (ΔT) have been related to the greases' components (thickener, base oil-type, and composition) and the structural degradation of the lubricating greases. Furthermore, a theoretical approach was proposed for calculating the internal temperature change of lubricating greases during shear stress. All greases showed an internal temperature profile characterised by a sudden rise in ΔT within the first 4 h from starting the test and subsequent ΔT decay until it reaches the steady state value. Furthermore, it was found that greases C1 and C5, formulated with lithium and calcium soap, respectively, with different soap content (16.1 wt% and 9.7 wt%, respectively), but the same base castor oil, showed the highest value of the maximum ΔT, c.a. 3.2 K, and the most drastic drop of ΔT. These greases showed both the highest specific densities and heat capacities. In addition, they showed the lowest ratio of expended energies (R_{tee}), which means more structural degradation in the stressed grease. On the contrary, the grease C3, with 13 wt% of Li-soap but the lowest base oil's viscosity, showed the lowest maximum ΔT and the temperature profile was characterised by a moderate variation of ΔT along the test. The biogenic grease B3 developed a low-temperature change in the group of pure bio-genic greases close to grease C3.

Keywords: shear-induced structural degradation; rheology; temperature measurements; lubricating greases density; lubricating greases specific heat capacities

1 Introduction

The primary function of lubricants is to reduce friction and wear [1]. In addition, cleaning, sealing, and cooling functions used to be assigned to lubricants in different degrees depending on whether they are lubricating oils or greases. Lubricating greases consist of base oil and a thickener, among other additives. It is a colloidal suspension where the thickener forms a three-dimensional (3D) structure (gel-like) inside the base oil, adding a significant viscoelastic characteristic [2]. Lubricating greases generally consist of 65 wt%–95 wt% base oil (mineral oil, synthetic oil, or vegetable oil), 5 wt%–35 wt% thickener, and 0–10 wt% additives [1]. They are used when applying lubricating oils is technically or economically disadvantageous or impossible [3]. Lubricating greases are mainly used in ball bearings under mixed friction conditions. Different researchers [4–7] have investigated the tribological and rheological behaviour of lubricating greases with different approaches.

An ongoing problem in tribology is the behaviour of grease under lubrication conditions, or in other words, the effect of viscoelasticity on the friction

* Corresponding author: Leif AHME, E-mail: leif.ahme@haw-hamburg.de

Nomenclature

c_{pi}	Sample specific heat capacity (J/(g·K))	T_0	Starting temperature value (K)
M_d	Measured Torque (N·m)	T_i	Measured temperature value (K)
m_i	Sample mass (g)	U_1-U_2	Change in the internal energy of a closed system (J)
n	Rotational velocity (min^{-1})	V_i	Sample volume (cm^3)
NLGI	National Lubricating Grease Institute	W_{12}	Amount of thermodynamic work done by the system (J)
PAO	Poly-alpha-olefin	ΔT	Temperature change (K)
Q_{12}	Quantity of energy supplied to the system as heat (J)	ρ_i	Sample specific density (g/cm^3)
R_{tee}	Ratio of the total expended energy		
R_Z	Average surface roughness		

process. One way to clarify this problem is to determine the rheological properties of lubricating greases. Lubricating greases are exposed to structural degradation due to frictional stress, which can be divided into mechanical and chemical degradation. Delgado et al. [8] and Kuhn [9] have already attempted to analyse the lubricating grease-based friction process by rheological measurements. Kuhn [10] described that friction could be understood as the input (storage) and output (loss) of energy in the tribo-system, and wear may be related to the dissipation of this energy. Other researchers [7, 10–14] have used a thermodynamic approach to describe grease structural degradation better. In this regard, Bryant et al. [14] defined the generalised thermodynamic and degradation forces ratio as the term "degradation coefficient" for the first time. The calculation was based on the entropy concept and the degradation process instead of process variables. Rezasoltani and Khonsari [6] characterised the structural degradation of greases by showing that the shearing process breaks down the grease structure and leads to heat production. Entropy is generated during the heat transformation caused by the structural degradation process. From a thermodynamic point of view, Rezasoltani and Khonsari [6] and Osara and Bryant [12] described the degradation coefficient as a correlation of the entropy generation rate with mechanical degradation. Nevertheless, most of these studies focus on the numerical treatment of heat generation due to the mechanical degradation of greases. Kuhn [15] studied the specific entropy transport using different temperature values, such as the maximum friction energy temperature and the fixed temperature chamber. For further investigations according to Kuhn's model, it is helpful to know how greases behave regarding the temperature in the grease film.

It is known that temperature highly influences the viscosity and viscoelasticity of greases [16]. Various works on temperature investigations have different approaches, but in most cases, the heat is transferred externally into the system [13, 17–20]. For lithium lubricating greases, Delgado et al. [17] determined a critical temperature of 110 °C in their investigations, at which the viscoelastic behaviour of Li-greases drastically decayed. Pan et al. [18] concluded that after short thermal ageing at 120 °C for 2–24 h of lubricating greases, the high interconnections of the network microstructure and, in particular, the strength of the fibrous structure decrease. In addition, they pointed out that the interpretation of its chemical composition did not cause the variation in the lubrication performances after that short heat treatment but by its physical entanglement strength. With the help of a homemade Couette ageing machine, Zhou et al. [20] have developed a master curve for grease ageing. They showed the influence of temperature and shear on the mechanical ageing of lubricating greases with a fibrous-based structural skeleton. They observed that an increase in temperature accelerated the shear degradation. Rezasoltani and Khonsari [13] have developed a model examining greases at different shear rates and temperatures. This model uses the expressed entropy generation to predict the reduction of grease consistency subjected to mechanical shear.

They restricted themselves to temperatures of 25–45 °C to prevent chemical degradation or evaporation of the base oil. Thus, mechanical degradation is the dominant degradation process in the mentioned model. Only Osara and Bryant [19] studied differentiated temperature measurements to perform a pure heat analysis to evaluate the thermal entropy generation. They combine the fundamental thermal energy and thermodynamics with the degradation entropy generation theorem. For this purpose, they used the results of their study [12], in which they carried out unique temperature measurements by a motorised paint mixer (stirrer) and three thermocouples mounted at different points within the mixing vessel to record the temperature under shearing conditions.

The primary purpose of this work was to investigate the temperature changes inside the bulk of lubricating grease under controlled shear stress conditions (mechanical energy) at room temperature. This investigation focused solely on lubricating greases, not lubricating pairings, since in a mixed regimen, the friction energy is attributable to both the solid and the fluid friction. For this reason, rheometer measurements were chosen to provide accurate information on the fluid friction behaviour of greases. A standard rotational rheometer-measuring cell and a newly developed temperature-measuring cell called Calidus were used. Calidus device makes it possible to determine the temperature profile within the measuring gap. In addition, the basic design of Calidus helps to better isolate the internal temperature measurements from the geometry concerning heat conduction. The obtained results should provide information about the temperatures in the lubricating grease and later be used in a calculation model. In addition, the temperature change was related to the greases' components (thickener, base oil-type, and composition), and a comparison was made with the structural degradation of the lubricating greases. This work does not consider other influences, such as physic–chemical interactions among components. It allows the quantification of dissipation energy, converted via mechanical energy into thermal energy, and a gradient of intrinsic energy.

2 Materials and experimental methods

2.1 Materials

In this experimental study, ten different grease samples were tested, differing in their composition. They were kindly supplied by Fuchs Europe Schmierstoffe (Mannheim, Germany) and Fuchs Lubritech (Kaiserslautern, Germany). They can be grouped into two groups: On one hand, conventional greases based on lithium soap, calcium soap, and polyurea; on the other hand, newly developed, pure biogenic greases. The composition of the different lubricating greases analysed, and their basic properties are listed in Tables 1 and 2, respectively.

Samples C1–C7 are model lubricating greases with conventional thickeners. These greases were prepared to combine with different types of thickeners and types and viscosities of base oils, according to the study by Delgado et al. [21], as these parameters significantly influence the microstructural skeleton and the rheological behaviour. All of them have an NLGI grade 2, which is why the soap concentration of the greases varies. Although the soap concentration changes the consistency of the greases, its influence

Table 1 Composition and primary technical data of conventional lubricating grease samples studied.

Lubricating greases	NLGI-grade	Thickener type	Thickener concentration (%)	Base oil	Base oil viscosity at 40 °C (mm^2/s)	Dropping point (°C)
C1	2	Lithium-12-hydroxystearate	16.1	Castor oil	240	~190.111
C2	2	Lithium-12-hydroxystearate	10.6	PAO	240	~210.497
C3	2	Lithium-12-hydroxystearate	13	PAO	48	~208.479
C4	2	Lithium-12-hydroxystearate	9.5	Mineral oil	240	~206.493
C5	2	Calcium-12-hydroxystearate	9.7	Castor oil	240	~142.055
C6	2	Calcium-12-hydroxystearate	22.8	PAO	240	~150.872
C7	2	Polyurea	19.6	PAO	240	~296.913

Table 2 Composition and primary technical data of biogenic lubricating grease samples studied.

Lubricating greases	NLGI-grade	Thickener type	Thickener concentration (%)	Base oil	Base oil concentration (%)	Base oil viscosity at 40 °C (mm^2/s)	Dropping point (°C)
B1	1	Cellulose	1.5	Glycerine Glyceryl-monooleate	88.5 10	227.4 120.1	<≈100?
B2	0-1	Polyhydroxy butyrate Ethylcellulose	5.3 7.7	MCT oil Castor oil HOSO	55 22 10	14.7 258.3 46.2	≈80
B3	00	Beeswax Glycerol monostearate Cetyl alcohol	7 5 2	HOSO Castor oil	50 36	46.2 258.3	≈45

on the rheological behaviour is proportional and can be controlled [21]. Samples B1–B3 are biogenic lubricating greases previously tested as part of the TriBioGen research project by Acar et al. [22, 23]. In all cases, no additives were added deliberately to exclude other possible effects on the temperature behaviour.

2.2 Methods

2.2.1 Determination of the density and the specific heat capacities

The specific densities were determined both experimentally and theoretically. However, the specific heat capacities were determined experimentally only because theoretical values could not be sourced for all greases.

The specific densities were experimentally obtained using a PNR 10 penetrometer crucible (Petrotest, Germany) with a defined volume of 3,178 mm^3 and a precision balance, model 1602 MP8 (Sartorius, Germany). All samples were tempered with the penetrometer crucible in an F3 S circulating thermostat water bath (Haake, Germany) at 20, 40, and 80 °C for 15 min. After heating, the crucible was drawn off evenly and afterwards, immediately, the weight of the filled crucible was determined. The specific heat capacities were determined using a differential scanning calorimeter (DSC), model DSC 204 F1 (Netzsch, Germany), under a nitrogen atmosphere. Nitrogen flow was maintained at 20 mL/min. Grease samples (16.9–20.9 mg) were placed in closed aluminium crucibles and heated from –40 °C to max. 300 °C, at a heating rate of 10 K/min. At least three repeats of each test were obtained on fresh samples, and the data shown have statistically significant values, i.e. they did not exceed a significance level of 0.05 on the Student's t-test and had a 95% confidence interval. The specific values were determined by applying the standard protocol described by DIN 51007 [24]. For this purpose, an equation in which the heating rate and the weight of the sample are significant was applied to three measurements performed in the same way (baseline, sapphire, and sample) [25]. A sapphire from a DSC standard set from Netzsch, with a diameter of 4 mm and a height of 0.5 mm, was used for the measurements.

2.2.2 Rheological measurements

To investigate the temperature change inside the bulk of grease, stress-growth rheological tests were performed under controlled shear rate conditions using a smooth cone-plate geometry of 50 mm diameter, coupled to a controlled-stress rheometer model MCR 302 (Anton Paar, Austria). The measuring device was supplemented with an environmental control chamber (bonnet) to prevent external influences such as heat loss due to draughts or other environmental influences. According to the ISO 3219-2 standard, a cone angle of 1° was used. The gap resulting from the measuring system was always 0.103 mm. Shear test conditions of greases on the rheometer may deviate considerably from actual operating conditions but still provide a practical measure of the shear-induced frictional energy of the grease under shear stress. As Kuhn [2] and Delgado et al. [26] pointed out, adverse phenoms such as wall slip and leakage may be produced during rotational tests, significantly affecting the rheological results.

Thus, a cone-plate geometry was selected because it lets uniform shear conditions in the entire conical gap. Furthermore, a small sample size is required, allowing for better temperature measurement.

The experimental procedure with rheometers was organised in two consecutive steps (Fig. 1). The torque, rotational speed, and temperature were recorded every 15 s during the rheological measurements (5,320 points were recorded). It was done to quantify how much energy was introduced into the tested grease volume and how the internal frictional energy evolved along the test. In addition, it enables a statement about the temperature behaviour of the lubricating greases and the mechanical stress following the measurements.

In the first test step, the sample was stressed with a short linear shear rate ramp from 0 to the maximum values of 250 and 500 s^{-1} for 600 s. These shear rates selected in this series of tests were based on DIN 51810-1 [27]. In order to avoid material leakage in the measuring gap, it was decided not to use shear rates higher than 500 s^{-1}. The short linear shear rate ramp of 600 s was deliberately chosen to avoid possible leakage effects due to a sudden high shear rate. The temperature change in the bulk grease was recorded directly at the start of the measurement. In the second phase, the sample was stressed at a constant shear rate (250/500 s^{-1}) for 79,200 s to record both a long period of temperature change and, simultaneously, to induce structural changes in the lubricating greases under liquid friction-liked conditions. Three replicates were performed on fresh samples for each grease. Afterwards, a mean value was calculated for all three outcomes.

2.2.3 *Temperature measurements*

Different temperature environments can be simulated during the rheological tests, and the reference temperature can be kept constant or dynamic. However, the behaviour differs at a given temperature than under real conditions, i.e., non-constant temperature conditions. As an innovation in this research work, internal temperature measurements within the bulk grease were recorded during the structural degradation behaviour of greases, which was investigated in rheological tests. It allows the quantification of dissipation energy, converted via mechanical energy into thermal energy and a gradient of intrinsic energy.

This work chose two different approaches to record the temperature values during the stress-growth test. Firstly, a standard plate Peltier temperature control system (PTD) from Anton Paar (Fig. 2) was used. In this configuration, the temperature sensor was

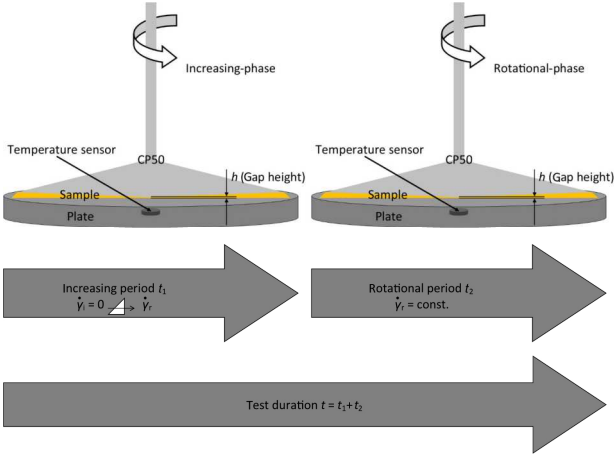

Fig. 1 Schematic illustration of the experimental procedure.

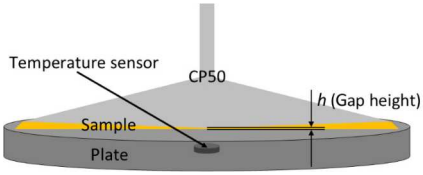

Fig. 2 Schematic of standard plate PTD with the temperature sensor.

located in the centre and just below the bottom plate, recording the average temperature of the grease sample. The PTD measuring cell from Anton Paar has been thoroughly tested in various tests concerning its temperature behaviour. Before the first measurements, the temperature measuring cell was calibrated according to the Anton Paar standard procedure.

Secondly, a new measuring cell, called Calidus, was developed for such purposes, which is installed in an Anton Paar MCR302 rheometer (Fig. 3). Calidus is a modular measuring cell in which different modules can be coupled using a thread system. The temperature module consists of a thermoplastic base plate on which two temperature sensors are mounted (in the centre and slightly off-centre). The Calidus measuring system was also tested and calibrated in advance with a customised test set-up.

Each configuration was supplemented with an Anton Paar environmental control chamber (bonnet) and a PT-100 sensor to record the room temperature during all measurements. This chamber encapsulates

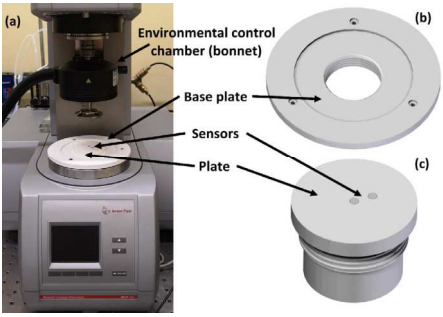

Fig. 3 (a) Calidus coupled to the rheometer; (b) schematic of Calidus base plate; and (c) schematic of Calidus plate with two sensors.

the environment around the sample, minimising heat loss and achieving a more accurate resolution for the temperature measurements.

3 Results and discussion

3.1 Density and the specific heat capacities of lubricating greases studied

The density and the specific heat capacities of the respective greases were required to determine an approachable theoretical temperature curve of the lubricating greases. The density was needed to determine the grease mass considering the respective volume, and the specific heat capacities were needed for the energetic theoretical approach.

Due to the complexity of experimentally measuring the specific densities of such highly viscous materials, theoretical values were determined by Eq. (1) to validate the experimental values.

$$\rho_{\text{grease}} = \rho_{\text{thickener}} \cdot \text{percentage}_{\text{thickener}} + \rho_{\text{baseoil}} \cdot \text{percentage}_{\text{baseoil}} \quad (1)$$

The specific densities of each grease's components required for this purpose can be found in Table 3.

Table 4 shows the theoretical and experimental specific densities and the specific heat capacities of all lubricating greases tested. As can be appreciated, the experimental results agree with the theoretical ones. All experimental values are within a variation range of minus 5% of the theoretical specific density values, except for grease C7 below 10%. Thus, experimental values of specific density were preferred for the following calculations.

It is worth mentioning that the grease's specific densities mainly depend on the base oil's specific density. Thus, conventional greases C1 and C5 have the highest specific density values due to the castor oil used. They are followed in order by grease C4, with mineral oil, and the other greases with PAO (C2, C3, C6, and C7). On the other hand, calcium soap has the highest specific density values among the thickeners, followed by lithium soap and polyurea. The grease with the polyurea-based thickener (1.33 g/cm^3), C7, only falls somewhat out of order since the combination with the PAO base oil (0.85 g/cm^3) ensures

Table 3 Specific densities at 20 °C of the different grease components.

Ingredient	Specific density (g/cm³) at 20 °C	Ingredient	Specific density (g/cm³) at 20 °C
Lithium 12-hydroxystearate	1.03 [28]	Glyceryl monooleate	0.94 [29]
Calcium 12-hydroxystearate	1.08 [30]	Polyhydroxybutyrate	1.22 [31]
Urea	1.33 [32]	Ethyl cellulose	1.14 [33]
Castor oil	0.97 [34]	Beeswax	0.97 [35]
PAO	0.85 [36]	HOSO	0.92 [37]
Mineral oil	0.90 [36]	MTC oil	0.96 [38]
Cellulose	1.50 [39]	Glycerol monostearate	1.03 [40]
Glycerol	1.26 [41]	Cetyl alcohol	0.82 [42]

Table 4 Specific densities (experimentally and theoretically) and specific heat capacity at 20 °C of the different greases used.

Lubricating grease	Experimental specific density (g/cm³)	Theoretical specific density (g/cm³)	Specific heat capacity (J/(g·K))
C1	0.9357	0.9780	2.106
C2	0.8126	0.8691	1.948
C3	0.8299	0.8734	2.000
C4	0.8639	0.9124	1.847
C5	0.9481	0.9789	2.206
C6	0.8609	0.9024	2.063
C7	0.8498	0.9441	1.997
B1	1.2109	1.2318	2.245
B2	0.9643	0.9849	2.012
B3	0.9205	0.9414	2.144

a comparatively lower density. In addition, it was found that the specific heat capacities of conventional greases studied were related to their specific density values, such as the higher the specific density was, the higher the heat capacity. Concerning the bio-greases, a similar picture appears, at least about the specific densities. Grease B3, with glycerine and glyceryl monooleate, showed the highest specific density. The grease-specific densities mainly depend on the base oil's specific density; however, the order of the specific heat capacities differs. The grease with the lowest density (B3) is placed between the grease with the highest density (B1) and the medium density (B2). Figure 4 shows an overview of the results obtained.

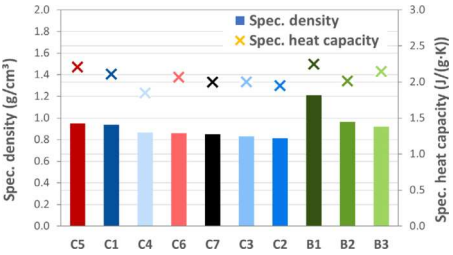

Fig. 4 Comparison of the specific density and the specific heat capacity at a temperature of 20 °C of all investigated lubricating greases.

3.2 Internal temperature changes profile under controlled shear stress conditions

Ahme et al. [43] pointed out that macroscopic structural degradation occurs in lubricating grease during shearing. Such an increase in the grease's internal temperature may be detected. This research analysed temperature changes inside the bulk of lubricating greases under controlled shear stress conditions at 250 and 500 s^{-1}. Slight differences were observed in grease temperature profiles at 250 s^{-1} compared to 500 s^{-1}.

The temperature values at 250 s^{-1} were c.a. 1/3 smaller than those at 500 s^{-1}; maximum temperature change values between 1.2 and 1.8 K were appreciated for 250 s^{-1} and 1.4–3.2 K for 500 s^{-1}. Thus, for the sake of simplicity, data at 250 s^{-1} were not plotted. Figure 5 shows the shear stress curve and grease temperature within the gap for the lithium grease (C4), which was measured using the standard PTD cell for 22 h (red and light blue, respectively); the room temperature (dark blue) along the test was included. An environmental control chamber (bonnet) was used to mitigate the external heat dissipation.

Figure 5 shows the grease's internal temperature and the internal friction energy during the shearing process. It is essential to realise that the temperature variation within the gap was unaffected by oscillations in the room temperature, as it was kept constant during the entire measurement period. The temperature of stressed grease C4 sharply increased until 25.5 °C within the first hour at 500 s^{-1}. Then, the temperature slightly decreased with time until a steady temperature was reached, c.a. 2 °C higher than room temperature. It is worth pointing out that the maximum temperature was reached around 1.5 h after the stress overshoot was surpassed due to the low heat transfer rate within the so viscous sample [44].

Before comparing the temperature profiles of the group of lubricating greases studied, adjusting the temperature changes (ΔT) in each test was necessary. For this purpose, it considered a temperature offset in each test. It was mandatory because the starting grease temperature was neither at room temperature nor the same in the different tests. Therefore, a reference state was necessary to counterbalance the temperature deviations and compare suitable temperature changes along each test. Thus, and considering room temperatures were always the same, the starting temperature value (T_0) was always subtracted from all other measured temperature values (T_i) in each test, according to Eq. (2):

$$\Delta T_i = T_i - T_0 \qquad i = 1,\ldots,5{,}320 \qquad (2)$$

The temperature changes (ΔT) determined experimentally at a shear rate of 500 s^{-1} with the standard PTD measuring cell are shown in Figs. 6–8. Figure 6 summarises all conventional greases (lithium, calcium, and polyurea) studied, while Fig. 8 shows the pure biogenic greases. The grease C6 is missing in Fig. 6 because it showed a high shear rate fracture phenomenon, and no reproducible data were obtained. Three fresh samples were measured for each grease; the corresponding average values are shown in Fig. 6.

As can be observed in Fig. 6, the temperature change profiles present the next evolution: A sudden rise in temperature change caused by the solid internal friction due to a high structural consistency of the lubricating grease and a more or less smooth drop until reaching a stationary value of the ΔT, once the grease structural degradation reached a steady

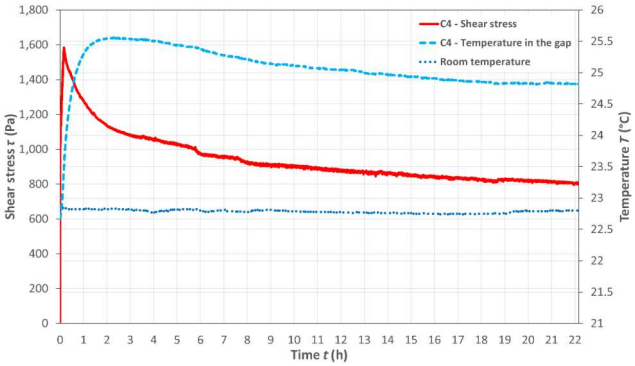

Fig. 5 Experimental room temperature, shear stress, and temperature profile of lithium grease C4, with the standard PTD measuring cell at a shear rate of 500 s^{-1}.

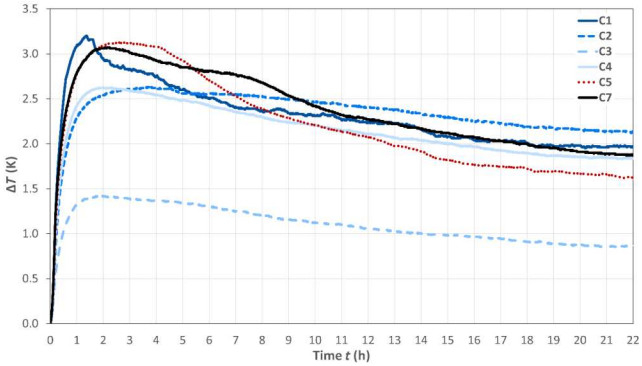

Fig. 6 Experimental temperature profile of conventional lubricating greases, with the standard PTD measuring cell at a shear rate of 500 s^{-1}.

state. All conventional greases reached their maximum temperature change within the first 4 h (240 min), being the limit time values of 72 and 240 min for greases C1 and C2, respectively. Grease C1 showed the highest value of the maximum ΔT among all conventional greases, c.a. 3.2 K, while grease C3 showed the lowest temperature change, c.a. 1.4 K. It is noticeable that greases C2 and C3, formulated with PAO and lithium soap, developed a similar temperature change profile, characterized by a moderate increase until the maximum ΔT value, followed by a smooth decay till a steady temperature change was reached. Much higher temperature changes were detected for grease C2 than C3, probably due to its base oil's higher viscosity, which hampers heat dissipation with the environment. Furthermore, the grease C1 showed the sharpest increase at the beginning of the test, after which the curve roughly dropped to a slowly decreasing course after eight hours. The highly entangled structural skeleton achieved by the highest lithium soap content [21] might bring the highest internal friction during the shearing process, which led to this drastic temperature increase in the bulk grease. Despite greases C2 and C4 being formulated with different base oils, they showed similar temperature change profiles. Both had similar lithium soap content and the same base oil's kinematic viscosity. In general, it can be said that lithium greases, except for C1, showed a softer temperature variation along the test. Calcium grease C5 shows the second sudden rise in temperature change and a steep decay until the steady value of ΔT is reached. Moreover, this grease suffered the highest temperature variation once the maximum temperature reached 1.5 K. While polyurea grease (C7) showed a temperature change profile similar to lithium grease with the highest soap content (C1).

In addition, it can be stated that if one looks at the individual composition of these lubricating greases, the ones with castor base oil showed a substantial increase in internal temperature change and then a strong decay. Therefore, the main component of the lubricating grease, i.e., the base oil, decisively determines its properties. Furthermore, it was appreciated that the grease's specific densities and heat capacities might be involved in the internal temperature change once the maximum value was reached. Thus, greases with castor oil (greases C1 and C5), which has both the highest specific densities and heat capacities, showed a substantial increase. They then showed a strong decay of internal ΔT. The combination of polyurea with a PAO (grease C7) also showed these characteristics of internal thermal behaviour, despite its lower values of specific density and heat capacity. In contrast, the greases with a lithium thickener and a PAO (greases C2 and C3) or mineral oil (grease C4), which has lower specific densities and heat capacities, showed a lower increase in internal temperature change and a smooth drop of the ΔT until the steady value was reached. Finally, it

is worth pointing out that grease C6, with the highest soap content, showed the highest temperature change, c.a. 4.56 K. After that, grease C6 was rejected from the measured geometry due to the fracture phenomenon at this high shear rate, and no reproducible data could be shown. In fact, according to Ahme et al. [44], this agglomerate-based calcium grease structure was highly affected by the stressing conditions tested.

These temperature change profiles have been related to the expended energy on structural degradation of lubricating grease during the shearing process published by Ahme et al. [44] (Fig. 7). It was appreciated that the larger the ratio of expended energies (R_{tee}) is, the lower the temperature changes (ΔT) are. In other words, samples that showed the lowest structural degradation in the stressed greases (C2, C3, and C4) developed the lowest temperature changes. Contrarily, the greases (C1, C5, and C7) with the lowest R_{tee} values, which means more structural degradation in the stressed grease [44], had the highest temperature change along the test. It was evidenced by the highest maximum ΔT and the steepest drops until reaching the steady value of ΔT. Therefore, a direct relationship was found between structural degradation (inverse of R_{tee}) and the temperature changes in the stressed grease. It is worth pointing out that base oil viscosity played a crucial role in the dissipation of this internal temperature increase. Thus, although the grease C3 had a similar R_{tee} value to greases C4 or C2, it showed a temperature change c.a. 52% lower than these greases.

Concerning pure biogenic greases studied (Fig. 8), biogenic greases B2 and B3 showed a similar temperature change profile to the conventional greases

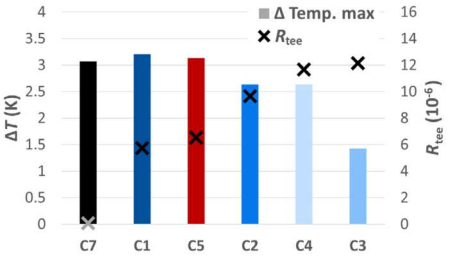

Fig. 7 Comparison of the maximum ΔT values with the ratio of expended energies (R_{tee}).

studied, characterized by a moderate increase until the maximum ΔT value, followed by a smooth decay till a steady temperature change was reached. Thus, greases B2 and B3 reached the maximum ΔT at 300 and 102 min, respectively. It is noteworthy that grease B2 showed the most remarkable temperature change in the group of pure biogenic greases, obtaining the highest ΔT, c.a. 3.2 K, while grease B3 was the lowest, c.a. 1.6 K. On the other hand, the grease B1 developed an atypical course of ΔT profile. It means this grease did not reach a maximum temperature value within the test period; the temperature increases linearly to 2.6 K after 22 h. It could be because the thickener consists of cellulose fibers, which are quite strong and do not end up breaking, but instead, move and rub against each other. This phenomenon produces a continuous temperature increase due to significant internal friction.

In contrast to the analysed conventional greases, there is no discernible trend in the specific thermal capacities. Therefore, it can be concluded that the thickener types used in this work react to tribological stress with different heat development regarding typical friction and wear mechanisms.

3.3 Temperature measurements using Calidus cell

The Calidus measuring cell comprised two sensors to measure a temperature difference within the bulk of grease with a plate–plate measuring system (see Fig. 3). A cone–plate measuring system was used, for which the shear rate was the same in the entire measuring gap. Due to this condition, the sensor's temperature differed slightly (between 0.1 to 0.2 K), which was within the range of measurement accuracy. Therefore, an average value was calculated from both temperature sensors.

It should be mentioned that some differences in roughness were appreciated with the surfaces in each temperature-measuring cell. The surface in the conventional PTD cell was titanium (Rz = 5.417), and a polylactide-based polyester in the Calidus cell (Rz = 27.704). These differences hardly affected most of the shear stress profiles measured at such a high shear rate with the prototype of the new Calidus temperature measuring cell in relation to the conventional PTD cell. Unfortunately, the shear stress fell to 0 after

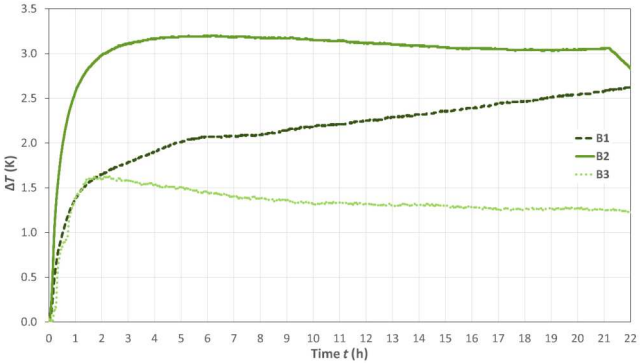

Fig. 8 Experimental temperature profile of the pure biogenic lubricating greases, with the standard PTD measuring cell at a shear rate of 500 s^{-1}.

about 2 h due to some greases leaking out of the measuring gap. Therefore, the surface of the Calidus measuring cell had higher surface roughness, which may promote the fracture and the ejection of the sample from the gap at a high shear rate [26, 45].

Taking into account the previous results published by Ahme et al. [44], the type of structural pattern related to the type of thickener higher affects the internal frictional energy involved in the grease degradation process than both the thickener content and the oil viscosity. Consequently, only the optimal data for the selected lithium-(C2), calcium-(C5), polyurethane-(C7), and pure bionic-(B2) greases were considered to analyse the results with the newly developed Calidus temperature measuring cell. Figure 9 shows the experimental temperature changes of these selected greases during 22 h at a shear rate of 500 s^{-1} using both temperature-measuring cells. The newly developed Calidus temperature measuring cell results are represented with a dotted line and those of the conventional PTD cell with a solid line.

As can be appreciated in Fig. 9, the temperature profiles obtained by both devices are essentially similar, only differ more significantly in the case of grease C5. The temperature changes measured by either method are affected by the extremely high viscosity of these greases. The Calidus device has different mass inertia of the measuring cell material, and the sensors installed have different thermal conductivities concerning their inertia due to the better installation position (see Fig. 3). Consequently, the temperature-change values determined with Calidus are higher than those of the PTD measuring cell. Moreover, the maximum ΔT values were detected faster with the Calidus cell. It leads to the conclusion that the Calidus-based temperature measurement was more thorough since it was placed almost touching the grease and not just below the bottom plate like the PTD device. Thus, the conventional PTD configuration led to the average temperature of the grease bulk, while the Calidus cell showed the local temperature inside the gap. In summary, the new Calidus measuring cell delivers accurate results regarding temperature values, which are close to those of the PTD measuring cell. By further developing the surface roughness of the Calidus measuring cell, it will be qualified for reliable rheological measurements in the future.

3.4 Theoretical approach to a temperature determination

A theoretical approach to the grease temperature within the measuring gap was made in this work. This approach is understood as a theoretical temperature determination and is not intended to represent a model. Instead, it should compare the experimental observations and the theoretical predictions and help validate the results obtained.

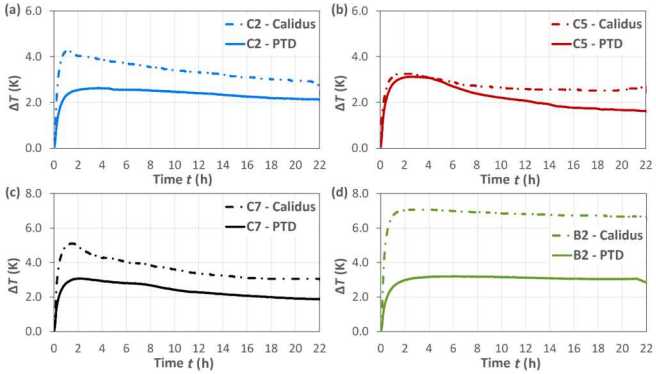

Fig. 9 Comparison of the temperature measuring cell–Calidus and Anton Paar PTD–with the selected lubricating greases (a) C2; (b) C5; (c) C7; and (d) B2 concerning the experimental ΔT profile.

Although it was mainly based on the 1st Law of Thermodynamics, the heat transfer rate into the grease was not considered:

$$Q_{12} + W_{12} = U_1 - U_2 \tag{3}$$

with

Q_{12} = quantity of energy supplied to the system as heat (J);

W_{12} = amount of thermodynamic work done by the system (J);

$U_1 - U_2$ = change in the internal energy of a closed system (J).

This approach assumed that the system did not exchange heat with the environment. The exchange of thermal energy with the environment cannot be prevented entirely, although an environmental control chamber (bonnet) was used. Therefore, it was defined as

$$Q_{12} = 0 \tag{3.1}$$

Thus, it was stated that

$$W_{12} = U_1 - U_2 = m_i \cdot c_i \cdot (T_1 - T_2) \tag{3.2}$$

with

Q_{12} = quantity of energy supplied to the system as heat (J);

W_{12} = amount of thermodynamic work done by the system (J);

$U_1 - U_2$ = change in the internal energy of a closed system (J);

m_i = sample mass (g);

c_{pi} = sample specific heat capacity (J/(g·K));

$(T_1 - T_2)$ = sample temperature change (K).

Rearranging according to T results in

$$\Delta T = \frac{W_{12}}{m_i \cdot c_{pi}} = (\mathrm{K}) \tag{3.3}$$

where

$$m_i = \rho_i \cdot v_i = (\mathrm{g}) \tag{3.4}$$

and

$$W_{12} = W_R = \int_0^{15} \frac{M_d \cdot n \cdot 2\pi}{60} \mathrm{d}t = \frac{M_d \cdot n \cdot \pi}{2} = (\mathrm{J}) \tag{3.5}$$

While using Eq. (3.3), it is then possible to easily determine the respective theoretical temperature change value for each measuring point of the investigation. Of course, the theoretically determined temperature curves should not prove the experimentally determined temperature curves but rather help to evaluate the results better. Thus, Fig. 10 shows the experimental data of selected greases obtained by the standard PTD cell (solid line) and the Calidus cell (dashed line) at a shear rate of 500 s^{-1} for 22 h and the theoretical values calculated by Eq. (3.3) (dashed line).

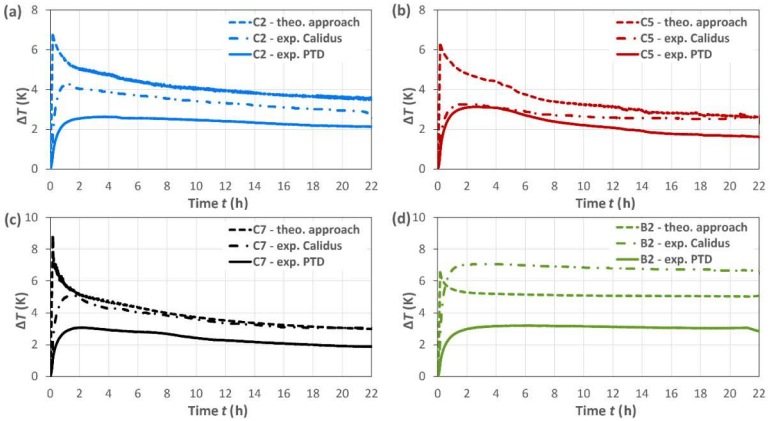

Fig. 10 Comparison of the rheometer measuring Cell–Calidus and Anton Paar PTD–with the use of lubricating greases (a) C2; (b) C5; (c) C7; and (d) B2 concerning the experimental ΔT profile and the theoretical approach curve.

It should be emphasised that the values determined with the theoretical approach were consistently higher than the experimentally determined values. Only in the case of the pure biogenic grease B2, the Calidus measurement curve is above the theoretical prediction. The theoretical approach strictly followed the shear stress curve, meaning that the grease heat transfer rate was irrelevant in most of the shearing time in the experimental data. However, more significant deviations were mainly observed at the beginning of the test, i.e., the greases showed the most significant deviations up to about 1.5 h between the experimental and theoretical data. It was expected since the extremely low grease thermal conductivity and high viscosity of all greases studied (NLGI grade 2). Nevertheless, from 6 h onwards, this simple theoretical approach describes a similar temperature change profile to the two experimentally determined ones, again except for the organic grease B2. In addition, the determined temperature values of Calidus are closer to the theoretical prediction.

4 Conclusions

This work has evidenced a relationship between the structural degradation and the temperature changes associated with the stressed grease at a high shear rate for several conventional model greases. They all belong to NLGI grade 2 and a group of newly developed pure biogenic greases (with lower NLGI grade). All greases showed an internal temperature profile characterized by a sudden rise in ΔT, caused by the strong internal friction due to a high structural consistency of the lubricating grease. A subsequent ΔT decay followed it until it reached the steady state value. In addition, based on the knowledge gained in this work, a new measuring system called Calidus has been developed. Finally, a straightforward theoretical approach was proposed for calculating the temperature change of stressed greases.

The examined conventional model greases showed significant differences in the temperature profiles-the grease C1, with a thickener content of 16.1 wt%, heated up the most (3.2 K) and showed a drastic drop of ΔT. The grease C5, with a content of 9.7 wt% and the same base oil, was slightly below this and on par with the grease C7, with a content of 19.6 wt% and poly-alpha-olefin (PAO) as base oil. It means that it is not the absolute concentration of the thickener that is decisive for the internal frictional heating but the type of thickener and the base oil. These three greases showed both the highest specific densities and heat capacities, which evidenced that the specific thermal capacity of these greases may be involved in the

temperature change profile. Thus, grease C5, with the more significant decay of ΔT, had the highest specific thermal capacity, followed by greases C1 and C7. In contrast, grease C4, with the lowest value of specific thermal capacity, showed a smooth drop of the ΔT until the steady value was reached.

On the other hand, a direct relationship was found between structural degradation (inverse of R_{tee}) and the temperature changes in the stressed greases. Thus, the larger the ratio of expended energies (R_{tee}), the lowest the temperature change (ΔT). Therefore, samples that showed the lowest structural degradation in the stressed grease (C2, C3, and C4) developed the lowest temperature changes. Contrarily, the greases (C1, C5, C7) with the lowest R_{tee} values had the highest maximum ΔT and the steepest drops until reaching the steady value of ΔT. It is worth pointing out that base oil viscosity played a crucial role in the dissipation of this internal temperature increase. Thus, the grease C3, with 13 wt% of Li-soap but the lowest base oil's viscosity, despite having a similar R_{tee} value than greases C4 or C2, showed a temperature change c.a. 52% lower than these greases. In addition, grease C3 showed the lowest maximum ΔT, and the temperature profile was characterized by a moderate variation of ΔT along the test.

Regarding the measurements with Calidus, it can be stated that the measurements with this newly developed measuring cell are more precise, as the mass inertia of the measuring cell material (Calidus: polylactide, PTD: titanium) is lower, and therefore, the temperature values are reached faster. At the same time, the sensors used with Calidus have a better installation position and are thus located directly at the measuring gap. Nevertheless, it should be mentioned that the surface finish should be optimised for future measurements. In addition, Calidus's experimental data correlated much better with the theoretical approach. The theoretically determined temperature values were consistently higher than the experimentally determined ones. It is plausible because $Q_{12} = 0$ was assumed in the calculation. If future investigations make it possible to determine a theoretical value for Q_{12}, this could bring the theoretical model closer to reality. Subsequently, with a more extensive base of experimental results, which also considers the heat transfer rate within the grease, the theoretical model could be further developed to determine temperature values as input variables without experimental temperature measurements.

Declaration of competing interest

The authors have no competing interests to declare that are relevant to the content of this article.

Electronic Supplementary Material: Supplementary material of an image with a thermal imaging camera, and further diagrams of the experimental temperature changes are available in the online version of this article at https://doi.org/10.1007/s40544-023-0818-7.

References

[1] Dresel W, Heckler R P. Lubricating Grease. In: *Lubricants and Lubrication, 2nd Ed*. Mang T, Dresel W, Eds. Weinheim: Wiley-VCH, 2007: 603–646.

[2] Kuhn E. *Zur Tribologie der Schmierfette: Eine energetische Betrachtungsweise des Reibungs- und Verschleißprozesses*, 2nd ed. Renningen: expert Verlag, 2017 (in German).

[3] Bartz W J. *Schmierfette: Zusammensetzung, Eigenschaften, Prüfung und Anwendung*. Renningen-Malmsheim: expert-Verl., 2000 (in German).

[4] Paszkowski M. Assessment of the effect of temperature, shear rate and thickener content on the thixot-ropy of lithium

lubricating greases. *Proc Inst Mech Eng Part J* **227**(3): 209–219 (2013)

[5] Sánchez R, Valencia C, Franco J M. Rheological and tribological characteriza-tion of a new acylated chitosan–based biodegradable lubricating grease: A compara-tive study with traditional lithium and calcium greases. *Tribol Trans* **57**(3): 445–454 (2014)

[6] Rezasoltani A, Khonsari M M. On the correlation between mechanical degrada-tion of lubricating grease and entropy. *Tribol Lett* **56**(2): 197–204 (2014)

[7] Zhou Y. On the mechanical ageing of lubricating greases. Ph.D. Thesis. Beijing (China): University of Twente, 2018.

[8] Delgado M A, Franco J M, Kuhn E. Effect of rheological behaviour of lithium greases on the friction process. *Ind Lubr Tribol* **60**(1): 37–45 (2008)

[9] Kuhn E. Correlation between system entropy and structural changes in lubricating grease. *Lubricants* **3**(2): 332–345 (2015)

[10] Kuhn E. Application of a thermodynamic concept for the analysis of structural degradation of soap thickened lubricating greases. *Lubricants* **6**(1): 7 (2018)

[11] Kuhn E. Experimental grease investigations from an energy point of view. *Ind Lubr Tribol* **51**(5): 246–251 (1999)

[12] Osara J, Bryant M. Thermodynamics of grease degradation. *Tribol Int* **137**: 433–445 (2019)

[13] Rezasoltani A, Khonsari M. An engineering model to estimate consistency reduction of lubricating grease sub-jected to mechanical degradation under shear. *Tribol Int* **103**: 465–474 (2016)

[14] Bryant M, Khonsari M, Ling F. On the thermodynamics of degradation. *Proc R Soc A* **464**: 2001–2014 (2008)

[15] Kuhn E. Tribological stress of lubricating greases in the light of system entropy. *Lubricants* **4**(4): 37 (2016)

[16] Adhvaryu A, Sung C, Erhan S Z. Fatty acids and antioxidant effects on grease microstructures. *Ind Crops Prod* **21**(3): 285–291 (2004)

[17] Delgado M, Valencia C, Sánchez M C, Franco J, Gallegos C. Fatty acids and antioxidant effects on grease microstructures. *Tribol Lett* **23**: 47–54 (2006)

[18] Pan J, Yanhai C, Yang J. Effect of Heat treatment on lubricating properties of lithium lubricating grease. *RSC Adv* **5**: 58686–58693 (2015)

[19] Osara J, Bryant M. A temperature-only system degradation analysis based on thermal entropy and the degradation-entropy generation methodology. *Int J Heat Mass Transfer* **158**: 120051 (2020)

[20] Zhou Y, Bosman R, Lugt P. A master curve for the shear degradation of lubricating greases with a fibrous structure. *Tribol Trans* **62**: 1–21 (2018)

[21] Delgado M A, Valencia C, Sánchez M C, Franco J M, Gallegos C. Influence of soap concentration and oil viscosity on the rheology and microstructure of lubricating greases. *Ind Eng Chem Res* **45**(6): 1902–1910 (2006)

[22] Acar N, Kuhn E, Franco J M. Tribological and rheological characterization of new completely biogenic lubricating greases: A comparative experimental investigation. *Lubricants* **6**(2): 45 (2018)

[23] Acar N, Franco J M, Kuhn E, Gonçalves D E P, Seabra J H O. Tribological investigation on the friction and wear behaviors of biogenic lubricating greases in steel–steel contact. *Appl Sci* **10**(4): 1477 (2020)

[24] NETZSCH-Gerätebau GmbH, Precise determination of the specific heat capacity by means of DSC on https://www.netzsch-thermal-analysis.com/en/contract-testing/tips-tricks/dsc/precise-determination-of-the-specific-heat-by-means-of-dsc/, 2022.

[25] NETZSCH-Gerätebau GmbH, Specific heat capacity (cp), on https://www.netzsch-thermal-analysis.com/en/contract-testing/glossary/specific-heat-capacity-cp/, 2022.

[26] Delgado M A, Secouard S, Valencia C, Franco J M. On the steady-state flow and yielding behaviour of lubricating greases. *Fluids* **4**(1): 1477 (2019)

[27] Deutsches Institut für Normung. DIN 51810 *Prüfung von Schmierstoffen-Prüfung der rheologischen Eigenschaften von Schmierfetten: Teil 1: Bestimmung der Scherviskosität mit dem Rotationsviskosimeter und dem Messsystem Kegel/Platte.* Beuth, 2017 (in German), on https://www.beuth.de/de/norm/din-51810-1/269916043.

[28] European Chemicals Agency, Lithium stearate: Density on: https://echa.europa.eu/es/registration-dossier/-/registered-dossier/22040/4/5, 2022.

[29] PubChem, Glyceryl monooleate: Density, on https://pubchem.ncbi.nlm.nih.gov/compound/Glyceryl-monooleate#section=Solubility, 2022.

[30] European Chemicals Agency, fatty acids, tallow, calcium salts: density, on https://echa.europa.eu/es/registration-dossier/-/registered-dossier/5720/4/5, 2022.

[31] Polymer Properties Database, Polyhydroxybutyrate: Density, on https://polymerdatabase.com/polymers/poly3-hydroxybutyrate.html, 2022.

[32] European Chemicals Agency, Urea: Density, on https://echa.europa.eu/de/registration-dossier/-/registered-dossier/16152/4/5, 2022.

[33] Chemical Book, Ethyl cellulose: Density, on https://www.chemicalbook.com/ChemicalProductProperty_EN_CB6165620.htm, 2022.

[34] European Chemicals Agency, Castor oil: Density, on https://echa.europa.eu/de/registration-dossier/-/registered-dossier/14599/4/5, 2022.

[35] Tinto W F, Elufioye T O, Roach J. Chapter 22-Waxes. In: *Pharmacognosy*. Badal S, Delgoda R, Eds. Boston: Academic Press, 2017: 443–455.
[36] OKS Spezialschmierstoffe GmbH, oils with high-performance additives for reliable lubrication: properties of base oils, on https://www.oks-germany.com/en/tribology/types-of-lubricants/oils/, 2022.
[37] AMD Special Oil LLC, *S*unflower Oil, High Oleic RBDW: Density, on https://www.amdoilsales.com/products/ho-sunflower/, 2022.
[38] Kraft Chemical, Safety Data Sheet MTC oil: Density, on https://greenfield.com/wp-content/uploads/2018/11/MCT-Oil-SDS.pdf, 2022.
[39] PubChem, Cellulose: Density, on https://pubchem.ncbi.nlm.nih.gov/compound/CELLULOSE, 2022.
[40] Wikipedia, Glycerol monostearate: Density, on https://en.wikipedia.org/wiki/Glycerol_monostearate, 2022.
[41] PubChem, Glycerol: Density, on https://pubchem.ncbi.nlm.nih.gov/compound/Glycerol#section=Density, 2022.
[42] PubChem, 1-Hexadecanol (Cetyl alcohol): Density, on https://pubchem.ncbi.nlm.nih.gov/compound/1-Hexadecanol#section=Density, 2022.
[43] Ahme L, Kuhn E, Delgado Canto M Á. Experimental study on the expended energy on structural degradation of lubricating greases. *Tribol lett* **70**(3): 81(2022)
[44] Wu L, Tan Q. A study of cooling system in a grease-lubricated precision spindle. *Adv Mech Eng* **8**(8): 1687814016665296 (2016)
[45] Balan C, Franco J M. Influence of the geometry on the transient and steady flow of lubricating greases. *Tribol Trans* **44**(1): 53–58 (2001)

Leif AHME. He completed his Bachelor of Engineering degree in 2015 and earned his Master of Science degree in 2017, both in Mechanical Engineering from Hamburg University of Applied Sciences in Hamburg, Germany. Subsequently, he embarked as a Ph.D. candidate in collaboration with the Tribology Research Center of the Hamburg University of Applied Sciences and the University of Huelva. His research expertise centres on the field of Tribology, explicitly focusing on the intricate study of structural degradation in lubricating greases.

Erik KUHN. He reached his Dr.-Ing. degree in 1987 at Otto von Guericke University in Magdeburg, Germany. Since 1991, he has been a full Professor at Hamburg University of Applied Sciences (HAW) and head of the Tribology Research Center. His research area is Tribology of lubricating greases, and he is the author of a book with the same title. Prof. KUHN is the organizer of the annual Armold Tross Colloquium.

Miguel Ángel DELGADO. He received his M.Eng. (2000) and Ph.D. (2005) degrees in Chemical Engineering from the University of Huelva, Spain. He joined the Centre for Research in Product Technology and Chemical Processes (Pro2TecS) in 2011. His current position is as a Professor at the Department of Chemical Engineering at the same institution. His research areas cover the manufacture and rheological and microstructural characterization of bio-thickener-based lubricating greases and vegetable oils. Nowadays, he is very involved in electro-active control of the friction process.

Electronic Supplementary Material

An approach of the internal friction-dependent temperature changes for conventional and pure biogenic lubricating greases

Leif AHME[1,*], **Erik KUHN**[1], **Miguel Ángel DELGADO**[2]

[1] *Department of Mechanical Engineering and Production Management, Hamburg University of Applied Sciences, Hamburg 20099, Germany*

[2] *Department of Chemical Engineering, University of Huelva, Huelva 21071, Spain*

Supporting information to https://doi.org/10.1007/s40544-023-0818-7

Various images with a thermal imaging camera confirmed that the measuring device (Anton Paar Rheometer MCR 302 with Peltier temperature control system (PTD) measuring cell) did not cause any relevant heat input into the grease system. Figure S1 shows one of these images from the thermal imaging camera, which demonstrated this.

Fig. S1 Thermal image of rheometer MCR 302 during operation.

Figures S2 and S3 show the experimental temperature changes (ΔT) at a shear rate of 250 s^{-1} with the standard PTD measuring cell. All the conventional greases investigated (lithium, calcium, and polyurea greases) are summarised in Fig. S2, while Fig. S3 shows the pure biogenic greases. Three fresh samples were measured for each grease, and the corresponding average values were shown.

Figure S4 shows the experimental shear stress and temperature curve of the pure biogenic lubricating grease B1, with the standard PTD measuring cell at a shear rate of 500 s^{-1}. Again, a somewhat atypical behaviour for a lubricating grease can be seen—as the shear stress curve rises after the growing stress period. Accordingly, the temperature also increases with a growing stress period.

* Corresponding author: Leif AHME, E-mail: leif.ahme@haw-hamburg.de

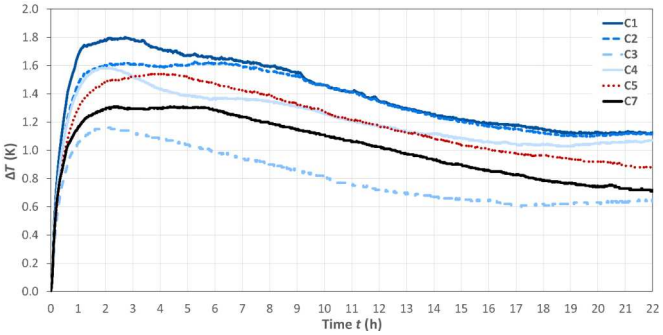

Fig. S2 Experimental temperature profile of conventional lubricating greases, with the standard PTD measuring cell at a shear rate of 250 s^{-1}.

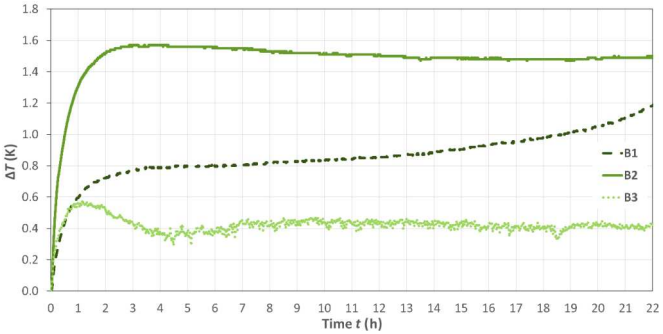

Fig. S3 Experimental temperature profile of the pure biogenic lubricating greases, with the standard PTD measuring cell at a shear rate of 250 s^{-1}.

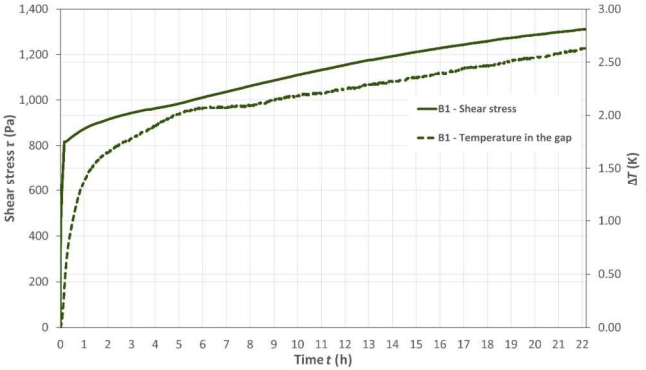

Fig. S4 Experimental shear stress and temperature profile of the pure biogenic lubricating greases B1, with the standard PTD measuring cell at a shear rate of 500 s^{-1}.

A.3 On the Optical Assessment of the Structural Degradation of Rheologically Stressed Lubricating Greases

Leif Ahme[1], Erik Kuhn[1], Miguel Ángel Delgado Canto[2]

[1]Hamburg University of Applied Sciences, Department of Mechanical Engineering and Production Management, Hamburg, Germany

[2]University of Huelva, Department of Chemical Engineering, Huelva, Spain

Published in: Tribology International

Publishing company: Elsevier

Editors: B. Bou-Saïd, H. Liang, W. M. Liu

Volume 187, Article 108771

Year: September 2023

DOI: 10.1016/j.triboint.2023.108771

ISSN: 0301-679X

E-ISSN: 1879-2464

Impact Factor (2022): 6.2

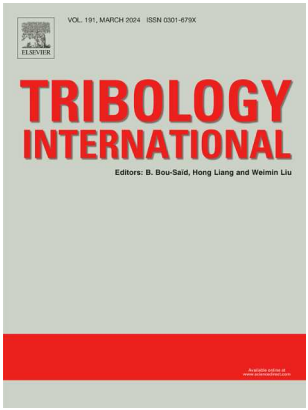

CiteScore (2022): 10.4

JCR Category	Rank
Engineering (Mechanical Engineering)	36/631
Engineering (Mechanics of Materials)	26/391
Materials Science (Surfaces, Coatings and Films)	15/131
Physics and Astronomy (Surfaces and Interfaces)	9/55

A Scientific publications in this thesis

Debido a restricciones relativas a derechos de autor, el artículo “On the Optical Assessment of the Structural Degradation of Rheologically Stressed Lubricating Greases” ha sido retirado de la tesis. En sustitución del mismo ofrecemos la siguiente información: referencia bibliográfica, enlace a la revista y resumen.

- Ahme, L., Kuhn, E., & Delgado Canto, M. Á. (2023). On the Optical Assessment of the Structural Degradation of Rheologically Stressed Lubricating Greases. In Tribology International (Vol. 187, p. 108771). Elsevier BV. https://doi.org/10.1016/j.triboint.2023.108771

Enlace al texto completo: https://doi.org/10.1016/j.triboint.2023.108771

RESUMEN:

This work explores optical measurements' potential to better understand structural degradation due to the internal friction process of lubricating greases. The samples have been examined as closely as possible to their original state due to the specimen preparation protocol. Eleven model lubricating greases were evaluated for these purposes. Image analysis of transmitted light microscope, SEM and AFM measurements were used to evaluate the grease microstructure under stressed and unperturbed conditions. The results showed that the type of thickener could significantly influence the internal frictional energy due to the structural degradation of the lubricating grease. Thus, the structural skeletons of lithium and calcium greases can dissipate less mechanical energy during a shearing process than polyurea grease or isolated pure biogenic greases.